

STRUCTURE AND FUNCTION OF BENM, A TRANSCRIPTIONAL ACTIVATOR
FROM *ACINETOBACTER* SP. STRAIN ADP1

by

TODD JON CLARK

(Under the Direction of Ellen L. Neidle)

ABSTRACT

BenM and CatM, members of the LysR-family of transcriptional regulators, activate the expression of the *ben* and *cat* genes needed for benzoate degradation by the bacterium *Acinetobacter* sp. Strain ADP1. These two proteins, which are similar in sequence and function, regulate more than a dozen chromosomal genes organized in multiple operons. Both BenM and CatM respond to the metabolite *cis,cis*-muconate. BenM, but not CatM, additionally responds to the effector benzoate. As described in this dissertation, BenM and CatM were purified to homogeneity and shown to regulate the expression of two genes, *benP* and *benK*, that form an operon adjacent to the *benM* gene. BenP and BenK, a putative outer membrane porin and an inner membrane permease, respectively, were predicted to contribute to aromatic compound catabolism in ADP1. The BenM and CatM regulators were equally important in *benPK* expression. Furthermore, although BenM activates the *benABCDE* genes in response to benzoate, only *cis,cis*-muconate was able to increase *benPK* expression. To characterize the interactions of BenM with the two distinct effectors, tryptophan fluorescence methods were used. BenM was able to bind to benzoate and to *cis,cis*-muconate, and the affinity for each effector was determined. Benzoate and *cis,cis*-muconate competed for the same BenM binding site. However, the conformation changes in BenM caused by benzoate were distinct from those caused by *cis,cis*-muconate. From these results, a model was proposed to account for BenM's ability to activate *benA* transcription synergistically in response to both compounds. High-level activation of *benA* transcription may require a tetramer of BenM to which two monomers bind benzoate and two bind *cis,cis*-muconate. The structure of this tetramer would be distinct from those bound only to a single type of effector. To better understand these structural differences, a truncated version of BenM was purified and crystallized. X-ray diffraction methods (done in collaboration with Dr. Cory Momany) were used to solve the structure of the BenM effector-binding domain to a resolution of 2.0Å. This study describes the first structural characterization of a protein from an important subclass of LysR-type regulators that controls the catabolism of natural aromatic compounds and pollutants by diverse bacteria.

INDEX WORDS: *Acinetobacter* sp. Strain ADP1, BenM, CatM, LysR-type transcriptional regulator, *cis,cis*-Muconate, Benzoate, Effector binding, β -Ketoadipate pathway, Aromatic compound degradation, Crystal structure

STRUCTURE AND FUNCTION OF BENM, A TRANSCRIPTIONAL ACTIVATOR
FROM *ACINETOBACTER* SP. STRAIN ADP1

by

TODD JON CLARK

B.S., The University of Wisconsin - La Crosse, 1995

A Dissertation Submitted to the Graduate Faculty of The University of Georgia in Partial
Fulfillment of the Requirements for the Degree

DOCTOR OF PHILOSOPHY

ATHENS, GEORGIA

2002

© 2002

TODD JON CLARK

All Rights Reserved.

STRUCTURE AND FUNCTION OF BENM, A TRANSCRIPTIONAL ACTIVATOR
FROM *ACINETOBACTER* SP. STRAIN ADP1

by

TODD JON CLARK

Approved:

Major Professor: Ellen Neidle

Committee: Cory Momany
Anna Karls
Timothy Hoover
Robert Maier

Electronic Version Approved:

Maureen Grasso
Dean of the Graduate School
The University of Georgia
December 2002

DEDICATION

To my wife Kimberly-

Thank you for your love, patience, and unwavering support that allowed me to realize and achieve this goal. You were, and always will be my inspiration. From the bottom of my heart, this work is dedicated to you.

"Once you learn to quit, it becomes a habit. Adversity is the first path to truth.

Prosperity is a great teacher; adversity is better."

-Vince Lombardi

ACKNOWLEDGEMENTS

I would like to thank Ellen Neidle for exercising "extreme" patience with my development as a scientist. She inherited the thankless, and often times difficult task of motivating me towards the completion of this goal. Her guidance, although not always acknowledged in the past, is most sincerely and appreciably acknowledged now. I would like to thank Cory Momany for tirelessly guiding me through numerous protein purification and crystallization sessions. Thanks to Anna Karls for always making time to listen. I am grateful to Robert Phillips for his guidance with tryptophan fluorescence experiments. I would like to thank Anne Summers for her advice with protein-binding experiments. To my committee members (past and present), Tim Hoover, Rob Maier, Mark Schell, Frank Gherardini, Anne Summers, Larry Shimkets, and Mike Adams, thanks for all your help and advice over the years. I wish to thank Lauren Collier-Hyams for her encouragement, friendship, and support in helping me start and finish this work. Thanks to my labmates, Matt Eby, Drew Reams, Sandra Haddad, and Becky Bundy for sharing everything from their lab space and equipment, to their time and friendship. Thanks go out to Andrea de Oliviera, Jarrat Jordan, and Adriana Olczak for their friendship and all their help in times of desperation. Thanks to "The Gang" for all of the memories. "High-fives" to the local Cheesehead chapter for many memorable football games. Finally, I want to thank my family for their love, patience, and support over the years. I'm happy to say that my career as a student is finally over.

TABLE OF CONTENTS

	Page
ACKNOWLEDGEMENTS	vii
CHAPTER	
1 INTRODUCTION AND LITERATURE REVIEW	1
Purpose of the study	1
Fine-tuned regulation of genes necessary for benzoate degradation.....	5
Intracellular CCM levels affect CatM-regulated gene expression	6
BenM-mediated synergistic activation of <i>benABCDE</i> expression in response to CCM and benzoate	7
BenM- and CatM-mediated transcriptional repression	8
LTTR structure and function.....	12
The structure of CysB.....	20
The structure of OxyR.....	30
The structure of BenM	36
References	37
2 THE <i>BENPK</i> OPERON, PROPOSED TO PLAY A ROLE IN TRANSPORT, IS PART OF A REGULON FOR BENZOATE CATABOLISM IN <i>ACINETOBACTER</i> SP. STRAIN ADP1	49
Abstract	50
Introduction	51

	Methods	55
	Results	63
	Discussion	82
	References	87
3	CHARACTERIZATION OF THE EFFECTOR-BINDING PROPERTIES OF BENM USING FLUORESCENCE EMISSION SPECTROSCOPY	93
	Abstract	94
	Introduction	95
	Methods	97
	Results	101
	Discussion	121
	References	133
4	CRYSTALLIZATION AND STRUCTURAL DETERMINATION OF THE EFFECTOR-BINDING DOMAIN OF BENM	138
	Abstract	139
	Introduction	140
	Methods	147
	Results	150
	Discussion	165
	References	187
5	CONCLUSIONS	196

CHAPTER 1

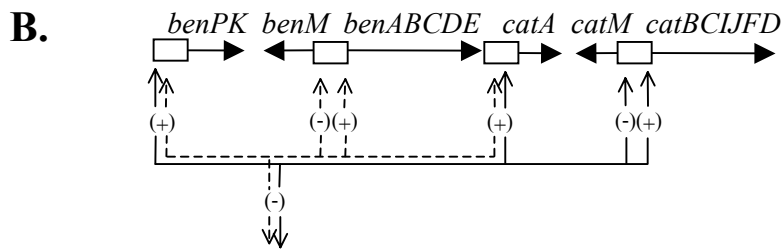
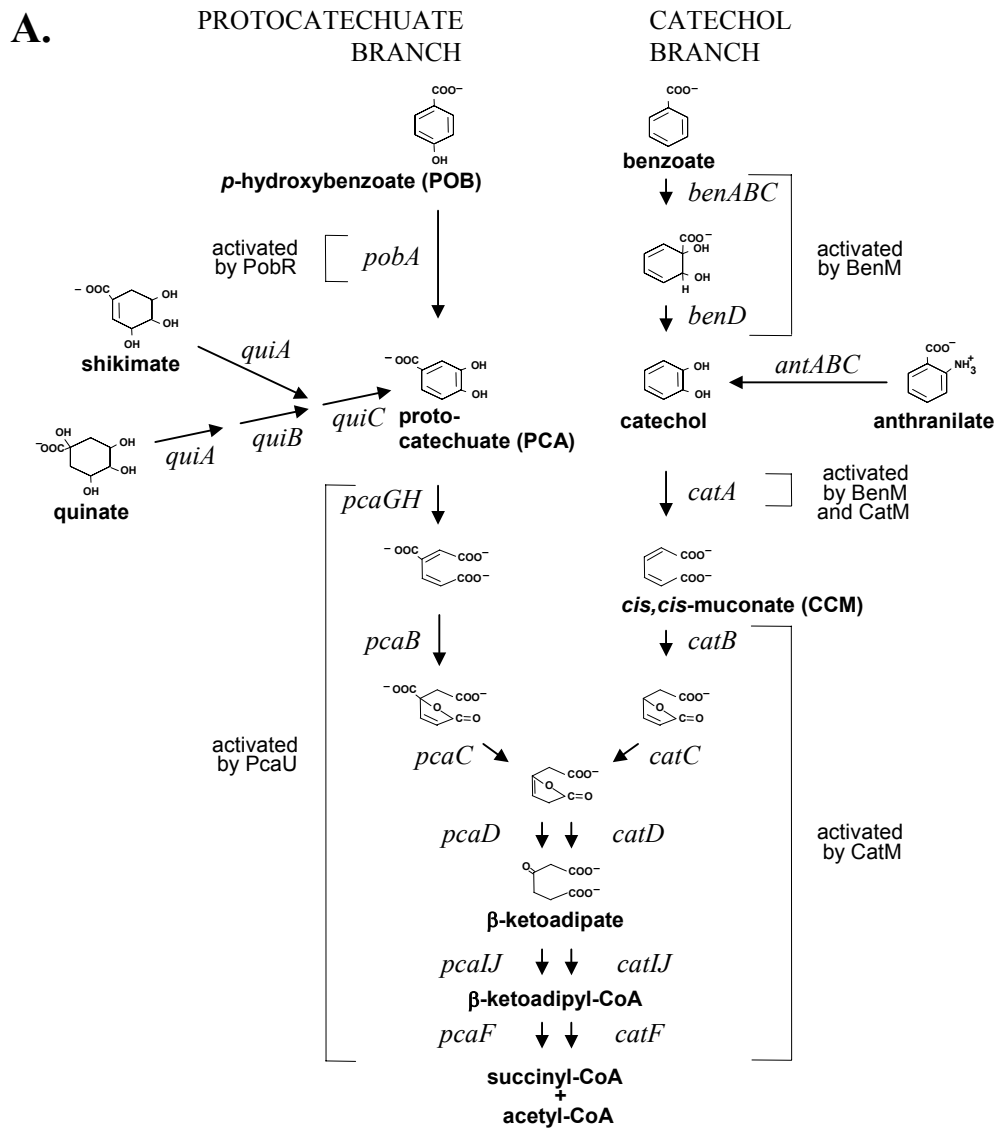
INTRODUCTION AND LITERATURE REVIEW

PURPOSE OF THE STUDY

Microbial pathways for the degradation of aromatic compounds have served as model systems for the study of enzymes, evolution, transcription, and other complex physiological processes (Averhoff *et al.*, 1992; McFall *et al.*, 1998; Ornston & Neidle, 1991; Srere, 1987; Young *et al.*, 2001). Recently, the emphasis in studies of aromatic compound catabolism has shifted towards prospective bioremediation applications (Diaz & Prieto, 2000; Hanson *et al.*, 1997; Harayama, 1997; Timmis & Pieper, 1999). Such potential applications are based on the structural similarity of many problematic pollutants to naturally occurring aromatic compounds that are readily biodegradable (Gibson & Subramanian, 1984; Reineke & Knackmuss, 1988). In order to facilitate the successful implementation of bioremediation approaches, a firm understanding of the metabolic and genetic regulatory mechanisms governing the natural catabolic pathways is necessary (Diaz and Prieto, 2000; Timmis and Pieper, 1999).

This study focuses on understanding the complex regulatory circuit controlling the degradation of benzoate and similar naturally occurring aromatic compounds by the bacterium *Acinetobacter* sp. strain ADP1. In this bacterium, aromatic compounds are degraded via one of two biochemically analogous branches of the β -ketoacid pathway referred to as the catechol and protocatechuate branches (Fig. 1.1A) (Fewson, 1991). The

Fig. 1.1. Diagram of the β -ketoacid pathway in *Acinetobacter* sp. strain ADP1 (A). The brackets indicate genes whose expression is controlled by the indicated transcriptional regulators. The relative position and transcriptional directions are depicted for the genes that encode the catechol branch (B) and the protocatechuate branch (C) (not drawn to scale). The dashed and solid lines indicate promoters that are significantly, positively (+) or negatively (-) regulated by BenM or CatM, respectively.



genes encoding these pathways are organized into two supraoperonic clusters on the ADP1 chromosome (Fig. 1.1B and C) (Gralton *et al.*, 1997). The *ben* and *cat* genes encode the necessary metabolic, transport, and regulatory proteins for the degradation of benzoate via the catechol branch of the pathway (Fig.1.1B). Among these genes are *benM* and *catM*, which encode two LysR-type transcriptional regulators (LTTRs) that represent the key regulators of benzoate degradation.

BenM and CatM are highly similar in sequence and function, and yet they serve distinct roles in regulating the genes for benzoate degradation. Due to their many similarities, and slight but significant differences, BenM and CatM are excellent models for comparative studies to investigate LTTR structure and function in relation to effector response. As described in Chapter 2 of this dissertation, both proteins were purified and subsequently shown to regulate the expression of a new set of transport genes, *benPK*. Because these genes were included in the BenM/CatM regulon, it was inferred that their protein products, a putative porin and an inner membrane permease, contribute to aromatic compound catabolism in ADP1. CatM and BenM were equally important in regulating the expression of *benPK* in response to *cis,cis*-muconate (CCM). These studies of *benPK* gene expression were complemented by tryptophan fluorescence emission spectroscopy experiments that investigated differences between BenM and CatM effector response. It had previously been shown that BenM, but not CatM, could respond to benzoate as well as CCM (Collier *et al.*, 1998). These tryptophan fluorescence studies were used to monitor the affinity of BenM for either or both effector compounds. It appeared that CCM could cause a conformational change in BenM that

was different from that caused by interactions with benzoate. This observation allowed the development of a regulatory model (presented in Chapter 3) to explain the recent demonstration that BenM responds to both compounds synergistically to activate *benA* transcription (Bundy *et al.*, 2002). In an additional set of experiments, a truncated version of BenM containing the effector-binding domain was purified and crystallized for direct structural determinations. As described in Chapter 4, the crystal structure of this protein was solved in collaboration with Dr. Cory Momany. The BenM effector-binding domain is the first structure to be solved of a transcriptional regulator involved directly in aromatic compound degradation.

FINE-TUNED REGULATION OF GENES NECESSARY FOR BENZOATE DEGRADATION

The *in vitro* studies described in this dissertation provide a structural framework for evaluating the complex transcriptional regulation of benzoate degradation. Previous studies done *in vivo* with wild-type and mutant *Acinetobacter* strains assessed the physiological significance of the effector responses of both BenM and CatM. Similarities and differences were revealed between these regulatory proteins. CatM responds to CCM to activate expression of *catA* and the *catBCIJFD* operon during growth on benzoate as a sole carbon source (Fig. 1.1A and B) (Romero-Arroyo *et al.*, 1995). BenM similarly responds to CCM to activate high-level expression of *catA* (Collier, *et al.*, 1998). In the absence of CatM, mutants grow on benzoate, albeit slowly, because BenM can activate low-level expression of the *catBCIJFD* operon (Gaines *et al.*, 1996; Neidle *et al.*, 1989).

BenM responds to benzoate and CCM to activate the expression of the *benABCDE* operon (Collier, *et al.*, 1998). In a mutant strain lacking BenM, CatM is unable to activate *benABCDE* expression to levels high enough to sustain growth on benzoate. However, using the mutant strain lacking BenM, spontaneous mutants were readily obtained following direct selection on growth medium containing benzoate as the sole carbon source. Several types of expected mutations allowing *benABCDE* expression were generated (Collier, 2000). These included one *benABCDE* promoter-region mutation that allowed higher than normal CatM-mediated expression in response to CCM. A different mutation increased the strength of the promoter and allowed high-level *benABCDE* expression in the absence of any transcriptional activator. One mutation altered the CatM protein and enabled it to activate high level *ben* gene expression in response to CCM (Collier, 2000).

INTRACELLULAR CCM LEVELS AFFECT CATM-REGULATED GENE EXPRESSION

Surprisingly, four mutations in *catB* caused sufficiently high BenM-independent expression of the *ben* genes to allow growth on benzoate. The *catB* gene encodes muconate cycloisomerase, an enzyme that catalyzes the conversion of CCM to muconolactone (Shanley *et al.*, 1986). Its substrate CCM, is enzymatically produced from catechol via the activity of catechol 1,2-dioxygenase, encoded by *catA* (Neidle & Ornston, 1986). Three of the four variant proteins were purified and shown to have reduced CatB activity in vitro.

One of my first projects upon entering the Neidle lab was to ascertain the physiological effects of the *catB* mutations on the expression of *benABCDE*, *catA* and *catB*. The *catB* mutants grown on benzoate showed decreased muconate cycloisomerase activity, and increased catechol 1,2-dioxygenase activity. My studies further showed that *benABCDE* expression in the mutants was comparable to that of wild-type cells. Based on these collective results, it was inferred that the *catB* mutations caused intracellular CCM to accumulate above normal levels during growth on benzoate. We were able to propose a model whereby CatM, responding to the CCM accumulation, increased *catA* activation resulting in higher catechol 1,2-dioxygenase activity. Higher CatA activity and lower CatB activity would result in the conversion of more catechol to CCM. The accumulation of intracellular CCM, at levels higher than normal could then enable CatM-mediated *benABCDE* expression to allow growth on benzoate as a sole carbon source. These results are summarized in a paper that I coauthored (Cosper *et al.*, 2000).

BENM-MEDIATED SYNERGISTIC ACTIVATION OF *BENABCDE* EXPRESSION IN RESPONSE TO CCM AND BENZOATE

The ability of CatM to activate *benABCDE* expression in response to CCM was later tested by in vitro transcription studies (Bundy, *et al.*, 2002). These studies demonstrated that in the presence of CCM, purified CatM could activate *benA* expression to levels similar to BenM in response to CCM. However, unlike BenM, CatM was unable to activate *benA* expression in response to benzoate. Further, the presence of both CCM and benzoate caused BenM to activate *benA* expression to levels higher than the sum of expression due to either compound alone. These studies demonstrated that BenM

causes a synergistic effect on transcription in the presence of both compounds. This result was consistent with previous *in vivo* studies that showed substantially increased *benA* expression *in vivo* in response to CCM and benzoate (Collier, *et al.*, 1998). The structural basis for the synergistic response of BenM to both CCM and benzoate was investigated further in studies described in this dissertation.

BENM- AND CATM-MEDIATED TRANSCRIPTIONAL REPRESSION

BenM and CatM not only serve as activators, but they can also repress gene expression. Like many LTTRs, BenM and CatM repress their own expression (Schell, 1993). Furthermore, both proteins have been shown to repress *benA* expression in the absence of effectors (Bundy, *et al.*, 2002). DNase I footprinting studies showed that tetrameric CatM or BenM bind to the *benA* region and protect an extended region from DNase I cleavage (Collier, 2000). Three BenM/CatM consensus sites are located within the protected region. Each site should bind a protein dimer of CatM or BenM. One of these sites directly overlaps the *benA* promoter region. In the absence of effectors, the regulatory proteins protect this region and presumably prevent RNA polymerase from binding.

Recent studies that I performed, suggest that BenM and CatM also repress the expression of genes involved in protocatechuate catabolism. This possible role for BenM and CatM was raised during investigations of multiple carbon source utilization. Nuclear magnetic resonance (NMR) studies demonstrated that ADP1 preferentially uses benzoate as a growth substrate when provided together with *p*-hydroxybenzoate (POB) (Gaines, *et al.*, 1996). This latter compound is a benzoate homolog that is degraded by the

protocatechuate branch of the β -ketoacid pathway. The NMR studies demonstrated that the inhibition of POB utilization was caused by CCM accumulation. The identification of CCM as the key regulatory effector raised the possible involvement of CatM and BenM in regulation.

I carried out *in vitro* studies to determine if CatM or BenM could interact with regions of DNA likely to influence *pobA* expression. POB is degraded to protocatechuate by the enzyme 4-hydroxybenzoate 3-hydroxylase, encoded by *pobA* (Hartnett *et al.*, 1990). Normally, the PobR transcriptional activator responds to POB to increase *pobA* expression (DiMarco *et al.*, 1993). However, during growth on benzoate, *pobA* is not expressed at high levels despite the addition of POB to the growth medium (Brzostowicz, 1997). To test whether BenM and CatM could directly repress *pobA* expression, I used both proteins in gel-shift assays. However, neither CatM nor BenM was able to bind to the *pobA* promoter region (discussed in Chapter 2).

Following the hydroxylation of POB by the PobA enzyme, subsequent catabolic steps are encoded by the *pca* genes (Fig. 1.1C). A computer-assisted search of the *pca* region identified a possible BenM/CatM binding site. LTTRs recognize a conserved DNA binding motif with the general consensus T-N₁₁-A (Schell, 1993). BenM and CatM bind the specific motif ATAC-N₇-GTAT (Collier, 2000; Romero-Arroyo, *et al.*, 1995). The putative BenM/CatM binding site was identified within *pcaU* (Fig. 1.2A and D), the gene encoding an activator of the *pcaIJFBDKCHG* operon necessary for the degradation of protocatechuate (Gerischer *et al.*, 1998; Hartnett *et al.*, 1990). Gel-shift assays demonstrated that both CatM and BenM were able to bind to this region (Fig.1.2C). Further, binding was enhanced by the presence of CCM (Fig. 1.2B).

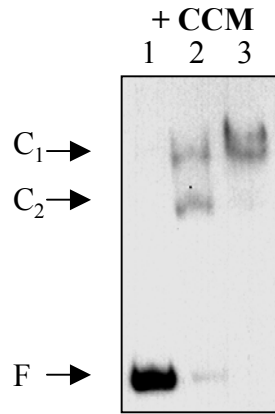
Fig. 1.2. Interactions of CatM at the *pcaU-I* regulatory region. A. Immediately downstream of the *pcaU* transcriptional start site is the sequence ATAT-N₁₁-GTAT, which matches a LysR-type binding consensus T-N₁₁-A. This sequence is shown aligned with other sequences proposed to bind CatM and/or BenM upstream of the promoters for the *ben* and *cat* genes. The results of gel-shift assays with CatM and a labeled *pcaU* DNA fragment are shown in the presence (B) and absence of CCM (C). Lane 1 in both panels shows the mobility of free DNA (F) in the absence of protein. The binding reactions contained 100 or 200 ng of CatM shown in lanes 2 and 3, respectively. Two shifted species of fragments labeled as C₁ and C₂, were generated presumably due to the formation of protein-DNA binding complexes. The recently identified *pcaU-I* regulatory sequences are indicated. The position of the PcaU binding site is underlined (Popp *et al.*, 2002). The numbers correspond to the DNA sequence (Genbank accession number L05770) such that 1 is the last position of the stop codon of the complementary sequence of *pcaU*. The proposed CatM/BenM binding site, indicated by the box, is shown relative to the 291 bp fragment amplified by PCR with the PCAUO/P primers and used in gel-shift assays.

A.

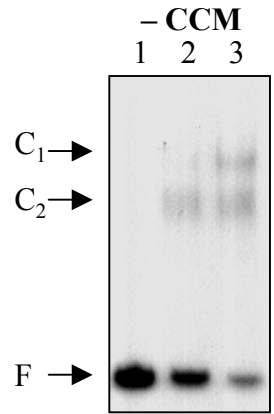
		T...11 nt...A			
<i>pcaU</i>	TCA	ATAT	GACAATC	GTAT	GTAGTAGC
<i>benP</i>	AAC	ATAT	CCTAAAG	GTAT	GAATATAT
<i>benA</i>	AAA	ATAC	TCCATAG	GTAT	TTTATTAT
<i>cata</i>	AGT	ATAC	CAAAAAA	GCAT	GAAAACAT
<i>catB</i>	TAT	ATAC	CTTTTTA	GTAT	GCAAAAAT

CatM/BenM binding site

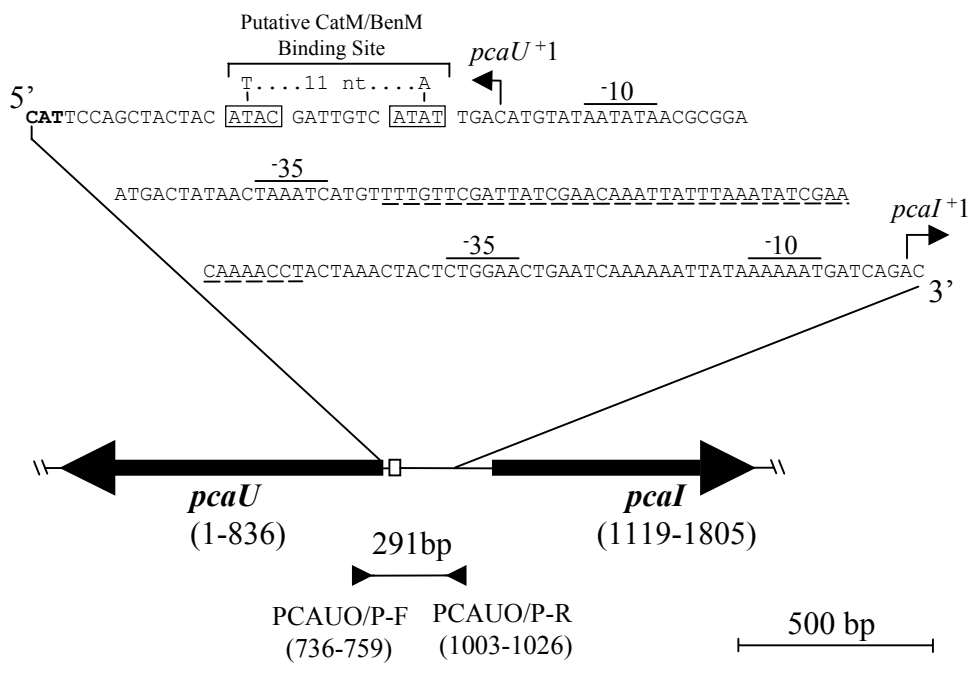
B.



C.



D.



In a paper that I coauthored, we proposed a model to explain how BenM/CatM-mediated repression at *pcaU* could affect *pobA* expression (Brzostowicz *et al.*, 2003). In ADP1, the *pcaK* gene codes for a membrane permease that has been demonstrated to facilitate POB uptake (D'Argenio *et al.*, 2001). PcaU activates expression of *pcaK* (Popp, *et al.*, 2002). Thus, repression of *pcaU* would result in the absence of *pcaK* expression. This might exclude POB transport into the cell, resulting in the inability of PobR to activate *pobA* expression. A similar model has been proposed to account for the preferential consumption of benzoate relative to POB in *Pseudomonas putida* PRS2000 (Nichols & Harwood, 1995).

Additional studies of *Acinetobacter* CatM and BenM mutants tested the significance of the repressive role of these LTTRs in carbon source preference. Mutants that could degrade benzoate in the absence of its normal activators no longer consumed benzoate prior to POB. Collectively the data indicate that CatM and BenM activate genes for benzoate degradation and repress genes for protocatechuate degradation.

LTTR STRUCTURE AND FUNCTION

It is interesting to note that the genes encoding the protocatechuate branch of the β -ketoacid pathway are activated by PobR and PcaU, members of the IclR/GylR family, while genes of the catechol branch are activated by LTTRs. The presence of two distinct classes of transcriptional regulators appears to facilitate cross-regulation between the two pathway branches. The simultaneous expression of the genes of both pathway branches could be deleterious by allowing enzymes to contact inhibitory substrate analogs. However, regardless of whether they repress or activate gene expression, CatM

and BenM can each recognize the same DNA binding sites and each responds to CCM as a co-effector metabolite.

BenM and CatM are 59% identical and 74% similar in amino acid sequence. Phylogenetic analysis shows that both BenM and CatM belong to a subfamily of well-characterized LTTRs that respond to CCM and halogenated-CCM (Fig. 1.3). In contrast, BenM, but not CatM, also responds to benzoate. However, BenM shows relatively little sequence similarity to NahR, an LTTR that responds to salicylate, a compound that differs in chemical structure from benzoate by a single hydroxyl group.

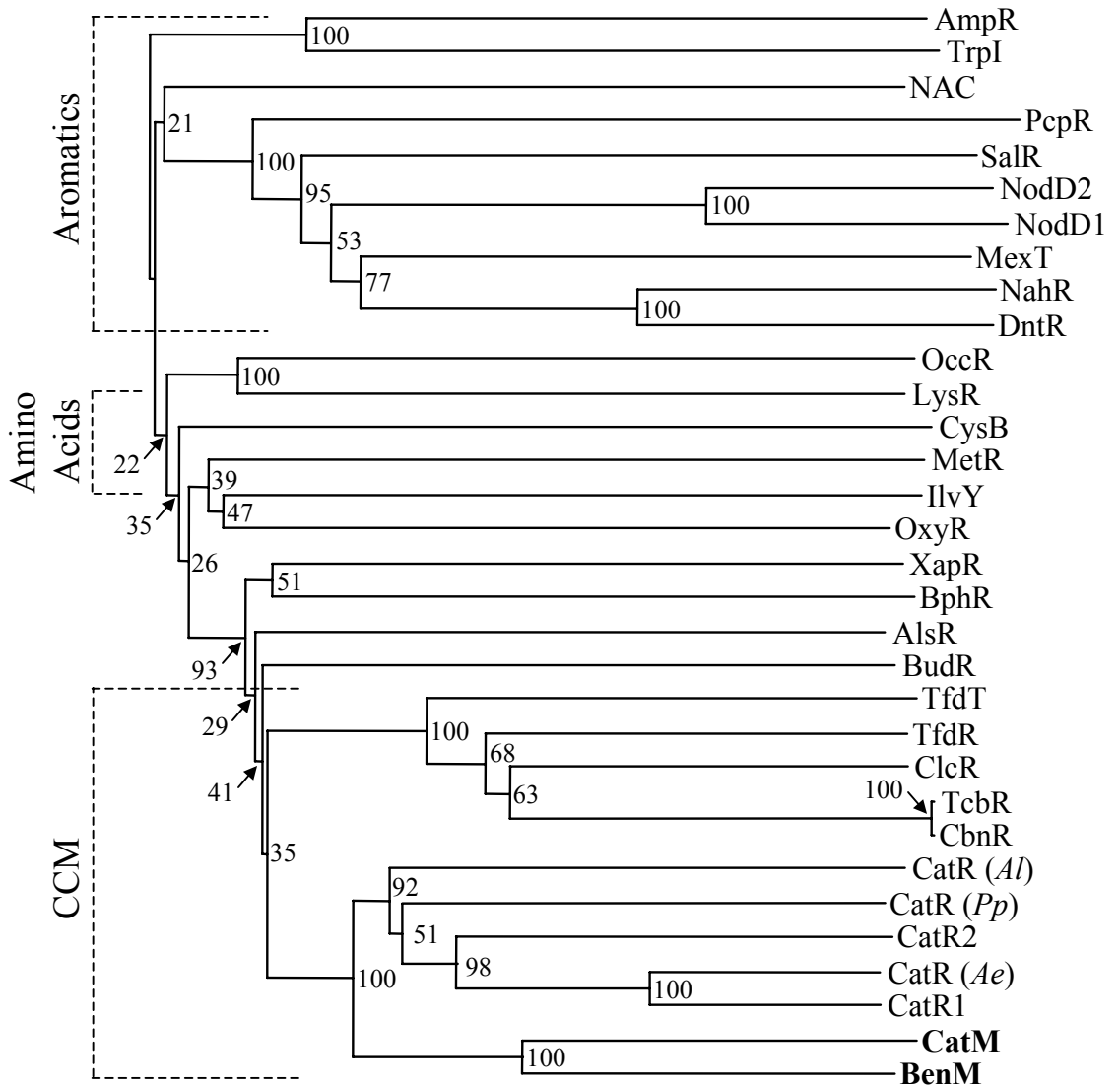
Little is known about the structural regions that allow LTTRs to bind and recognize effector compounds. In contrast, regions necessary for DNA binding and recognition have been well characterized. Mutational studies have identified the N-terminal domain of LTTRs, comprised of residues 1-66, as necessary for DNA binding and recognition (Schell, 1993). This region of LTTRs contains a classic helix-turn-helix (HTH) motif common to many DNA-binding proteins (Fig. 1.4) (Henikoff *et al.*, 1988). This motif is highly conserved between family members, displaying greater than 40% sequence identity between most members (Schell, 1993). The structure of this HTH region has never been directly confirmed. Nevertheless, mutational data indicate that the residues within this region are necessary for DNA binding and recognition (Jorgenson & Dandanell, 1999; Kullik *et al.*, 1995; Lochowska *et al.*, 2001).

This N-terminal region of the protein may also be involved in contacting RNA polymerase (RNAP). Mutational studies of RNAP indicate that most LTTRs act as Class I transcriptional activators (McFall, *et al.*, 1998; Shi & Bennett, 1994; Tao *et al.*, 1993). Activators of this class contact the C-terminal domain of the α subunit of RNAP

Fig. 1.3. Unrooted phylogenetic tree based on the amino acid sequences of the putative effector-binding domains of several LTTRs. The bootstrap values were calculated using the CLUSTALX software (Thompson *et al.*, 1997). The tree was constructed using the NJplot software (Perriere & Gouy, 1996). Bootstrap values are shown for each node out of 100 bootstrap resamplings (values below 50 are shown, but not significant). The scale bar represents the evolutionary distance between the proteins at 0.05 substitutions per residue position. The proteins used in the tree are listed along with the appropriate Genbank accession numbers (top to bottom): AmpR (P12529) from *Citrobacter freundii* (Lindquist *et al.*, 1989), TrpI (P11720) from *Pseudomonas aeruginosa* (Chang *et al.*, 1989), NAC (Q08597) from *Klebsiella aerogenes* (Schwacha & Bender, 1993), PcpR (P52679) from *Flavobacterium* sp. strain ATCC 39723 (Orser & Lange, 1994), SalR (Q9RBI3) from *Acinetobacter* sp. strain ADP1 (Jones *et al.*, 2000), NodD2 (P12233) from *Bradyrhizobium japonicum* (Applebaum *et al.*, 1988), NodD1 (P12232) from *Bradyrhizobium japonicum* (Applebaum, *et al.*, 1988), MexT (O87785) from *Pseudomonas aeruginosa* (Kohler *et al.*, 1999), NahR (P10183) from *Pseudomonas putida* (You *et al.*, 1988), DntR (Q8VUD7) from *Burkholderia cepacia* (Johnson *et al.*, 2000), OccR (Q00679) from *Agrobacterium tumefaciens* (Habeeb *et al.*, 1991), LysR (P03030) from *Escherichia coli* (Stragier & Patte, 1983), CysB (P45600) from *Klebsiella aerogenes* (Lynch *et al.*, 1994), MetR (P19797) from *Escherichia coli* (Maxon *et al.*, 1989), IlvY (P05827) from *Escherichia coli* (Wek & Hatfield, 1986), OxyR (P11721) from *Escherichia coli* (Christman *et al.*, 1989), XapR (P23841) from *Escherichia coli* (Seeger *et al.*, 1995), BphR (Q9L4R4) from *Alcaligenes eutrophus* (Mouz *et al.*, 1999), AlsR (Q04778) from *Bacillus subtilis* (Renna *et al.*, 1993), BudR (P52666) from

Klebsiella terrigena (Mayer *et al.*, 1995), TfdT (P42427) from *Alcaligenes eutrophus* (Leveau & van der Meer, 1996), TfdR (P10086) from *Alcaligenes eutrophus* (Matrubutham & Harker, 1994), ClcR (Q05840) from *Pseudomonas putida* (Coco *et al.*, 1993), TcbR (P27102) from *Pseudomonas* sp. strain P51 (van der Meer *et al.*, 1991), CbnR (Q9WXC7) from *Alcaligenes eutrophus* (Ogawa & Miyashita, 1999), CatR (*Al*) (O33945) from *Acinetobacter lwolfii* (Kim *et al.*, 1998), CatR (*Pp*) (P20667) from *Pseudomonas putida* (Rothmel *et al.*, 1990), CatR2 (AB035325) from *Burkholderia* sp strain TH2 (Suzuki *et al.*, 2002), CatR (*Ae*) (Q9EV43) from *Alcaligenes eutrophus* (Hinner *et al.*, 1998), CatR1 (AB035483) from *Burkholderia* sp strain TH2 (Suzuki, *et al.*, 2002), CatM (P07774) from *Acinetobacter* sp. strain ADP1 (Romero-Arroyo, *et al.*, 1995), BenM (O68014) from *Acinetobacter* sp. strain ADP1 (Collier, *et al.*, 1998).

Full-Length Protein



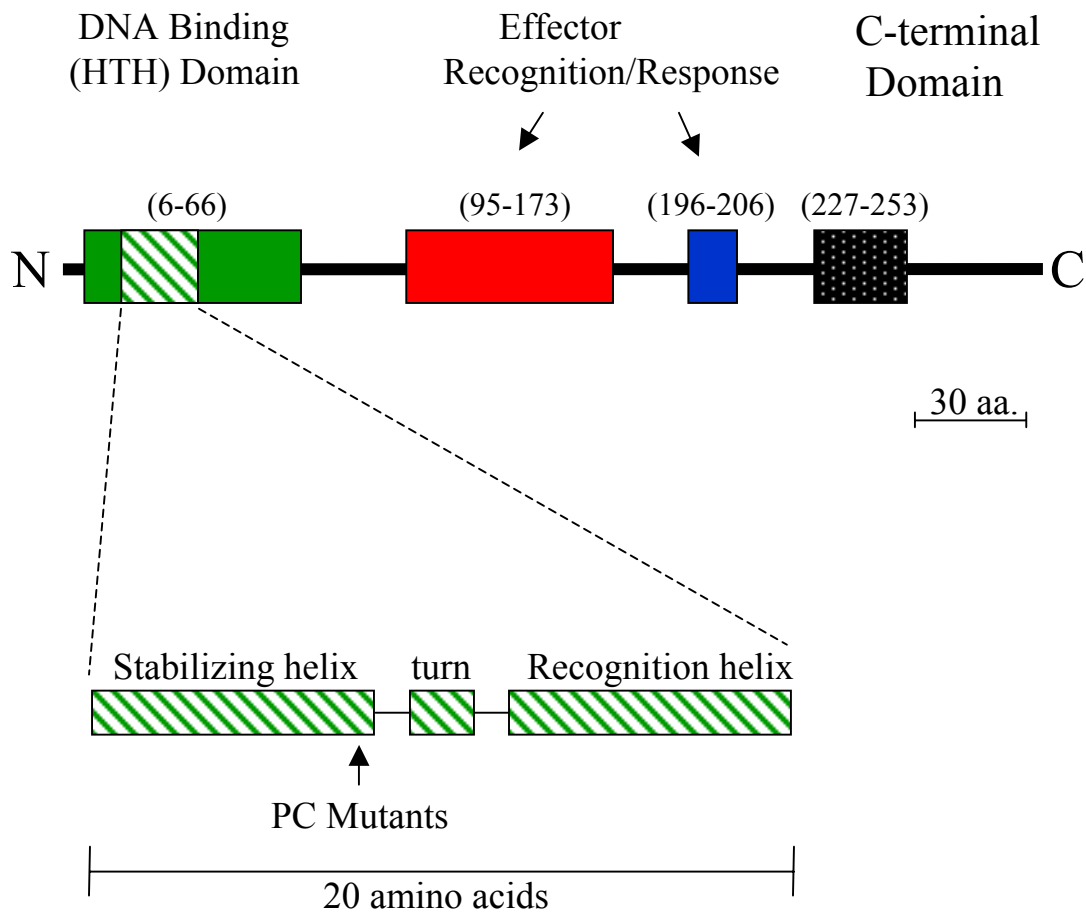
0.05

(Ishihama, 1993). Mutations have been generated in the LTTR genes *gcvA* (Jourdan & Stauffer, 1998), *xapR*, (Jorgenson and Dandanell, 1999), *cysB*, (Lochowska, *et al.*, 2001), and *occR* (Akakura & Winans, 2002) that result in variant proteins that can bind to DNA, but fail to activate transcription. These mutations, termed positive control mutations, all correspond to residues located at the end of the first helix, or stabilizing helix, of the HTH motif of the respective LTTRs (Fig. 1.4). The fact that these mutations correspond to residues located in the same region of the protein, suggests a significant role for this region in transcriptional activation. Direct contact between the HTH region of an LTTR with RNAP has not been demonstrated. Attempts to isolate mutations in *rpoA*, encoding the α -subunit of RNAP, that suppress LTTR positive control mutations have been unsuccessful to date (Jourdan and Stauffer, 1998).

The functional role of the C-terminal domain of LTTRs is poorly understood. Mutations resulting in residue changes in this region have been shown to affect a number of functions including protein multimerization, DNA-binding, and effector-binding (Fig. 1.4) (Schell, 1993). It has been proposed that the C-terminal region may come into contact with N-terminal domain, thus affecting DNA binding. This C-terminal region shows great variability between family members (Henikoff, *et al.*, 1988; Schell, 1993).

Mutational studies have identified residues within the central domain of LTTRs that are predicted to be involved in effector-binding and response (Fig. 1.4) (Schell, 1993). Most of the characterized mutations cause a constitutive, inducer-independent phenotype. Some cause a non-responsive phenotype while still retaining the ability to bind DNA. The recent structural characterization of the effector binding domains of two LTTRs, CysB and OxyR, provided new insight into effector recognition and binding.

Fig. 1.4. Model of the domain organization of a generic LTTR. Domains are color-coded according to function. The green areas correspond to residues that comprise the N-terminal DNA binding domain. Residues within this domain that correspond to a helix-turn-helix motif are indicated by the green-stripped lines, and shown in the blown-up diagram. The regions in red and blue indicate the central subdomains necessary for effector-binding. The black dotted region denotes the residues of the C-terminal domain. The relative location of positive control (PC) mutants on the putative stabilizing helix is indicated.



The primary sequence of the crystallized regions of CysB and OxyR show 19 and 24 % similarity, respectively to the comparable regions of BenM.

THE STRUCTURE OF CYSB

CysB controls the expression of genes necessary for cysteine biosynthesis in gram-negative bacteria (Kredich, 1996). The genes regulated by CysB, collectively referred to as the cysteine regulon, encode enzymes that allow for the uptake of sulfate and the conversion of serine to L-cysteine (Ostrowski *et al.*, 1987). The regulated expression of these genes is activated in response to the effector N-acetylserine (Lynch, *et al.*, 1994). The compounds sulfide and thiosulfate acting as anti-effectors and compete with N-acetylserine for binding to CysB when intracellular sulphur levels are high (Kredich, 1996; Ostrowski & Kredich, 1990).

A chymotryptic fragment of the CysB protein from *Klebsiella aerogenes* yielded the first three-dimensional structural information of an LTTR (Tyrrell *et al.*, 1997; Verschueren *et al.*, 1999). The CysB(88-324) fragment lacks only the first 87 N-terminal residues of the protein including the putative helix-turn-helix, DNA-binding motif. Removal of this region results in increased solubility of the protein fragment, compared to that of the full-length protein. Unable to bind DNA, CysB(88-324) does contain the functional effector-binding domain as demonstrated by its ability to bind N-acetylserine similar to the full-length protein (Tyrrell, *et al.*, 1997). However, in contrast to full-length CysB that exists as a tetramer, CysB(88-324) was shown to exist as a dimer in solution (Tyrrell, *et al.*, 1997).

The structure of CysB(88-324) was elucidated from X-ray data, at a resolution of 1.8Å, using a combination of multiple isomorphous replacement techniques and multi-crystal averaging (Tyrrell, *et al.*, 1997; Verschueren, *et al.*, 1999). The CysB(88-324) monomer has an overall ellipsoid shape with a structural core consisting of two α/β domains (I and II) connected by two short polypeptide strands (Fig 1.5A) (Tyrrell, *et al.*, 1997). Domain I is comprised of two regions of the protein chain corresponding to residues 88-162 and 270-292. Domain II consists of residues 166-265. The two domains are arranged in a side-by-side manner, collectively enclosing a large central cavity, approximately 6Å in diameter and 10Å deep. Mainly hydrophobic residues from both domains line the cavity surface (Tyrrell, *et al.*, 1997).

The CysB(88-324) dimer was shown to have an antiparallel arrangement of monomers such that domain I of one monomer interacted with domain II of the other monomer (Fig. 1.5B) (Tyrrell, *et al.*, 1997). The cavity openings of each monomer were brought together to form an internal channel through the middle of the structure. The channel formed was approximately 22 Å long and was partially covered by residues from each monomer. An α -helix present on each monomer is positioned in a manner that may allow it to block excess to the central channel of the dimer.

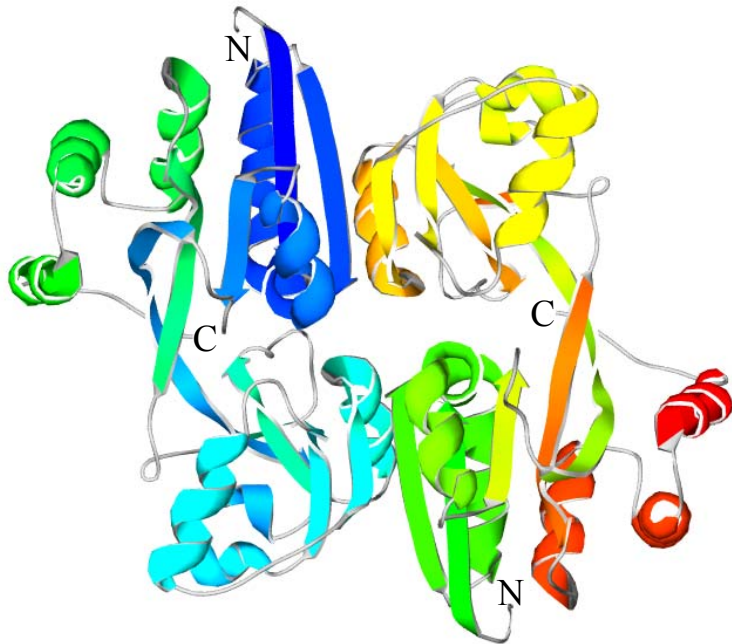
Although the binding site for N-acetylserine was not directly determined by the crystallization data, several strong lines of evidence support the notion that the interdomain cavity of CysB(88-324) does represent the effector-binding site. Firstly, a sulfate ion was found buried within the interdomain cavity of the protein along with several well-ordered water molecules (Tyrrell, *et al.*, 1997). The likely source of this sulfate ion is ammonium sulfate used in the initial protein purification, suggesting that

Fig. 1.5. Ribbon diagrams of the CysB(88-324) monomer (A) and dimer (B). Panel A shows the monomer colored according to the residues comprising the three domains of the protein. Residues 88-164 and 268-292 comprise domain I (colored red), domain II (blue) is made up of residues 165-267, and the C-terminal domain, made up of the remaining residues (293-324) is colored black. The location of residues corresponding to the mutations resulting inducer independent CysB are colored yellow. The presence of the sulfate ion is indicated. Panel B shows the dimer of CysB(88-324) colored according to secondary structure succession. The N and C-terminal ends of the protein are indicated in both panels. The figure was constructed using the Deep View Swiss-PdbViewer (Guex & Peitsch, 1997).

A.



B.



strong interactions hold the sulfate in place to allow retention through multiple purification and crystallization steps. Given the structural relatedness between sulfate and thiosulfate, it is possible that similar binding interactions could form between CysB and the anti-effector as with sulfate. Because thiosulfate competes with N-acetylserine for a common binding site, it would be consistent that the cavity would also represent the binding site for the effector.

The *cysB* mutations resulting in altered effector-binding and response correspond to residues located within or near the cavity. Three of the residues Thr149, Tyr164, and Trp166 line the inner surface of the cavity and form hydrogen bonding interactions with the sulfate ion. Mutations resulting in the substitutions T149M/P, Y164N, and W166R result in constitutive expression of the cysteine regulon as a consequence of inducer-independent CysB activation (Colyer & Kredich, 1996).

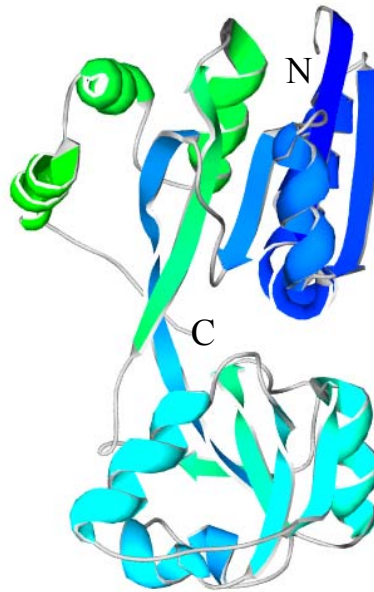
Fluorescence emission spectroscopy studies showed that N-acetylserine binding by CysB affected the wavelength spectrum corresponding to tryptophan fluorescence (Lynch, *et al.*, 1994). It was concluded that a tryptophan residue was located within close proximity of the N-acetylserine binding site. CysB contains only two tryptophan residues Trp89, the second residue of CysB(88-324) and Trp166.

The tertiary structure of CysB(88-324) is structurally similar to that of a family of periplasmic binding proteins in gram-negative bacteria that function as transporters, and in some cases chemotactic receptors for amino acid uptake systems (Fig. 1.6A and B) (Quioco & Ledvina, 1996). CysB most closely resembles a protein that binds to sulfate and the amino acids lysine, arginine, and ornithine (Oh & Kim, 1993). Members of this family that are similar to CysB(88-324) have a central cavity region that is enclosed by

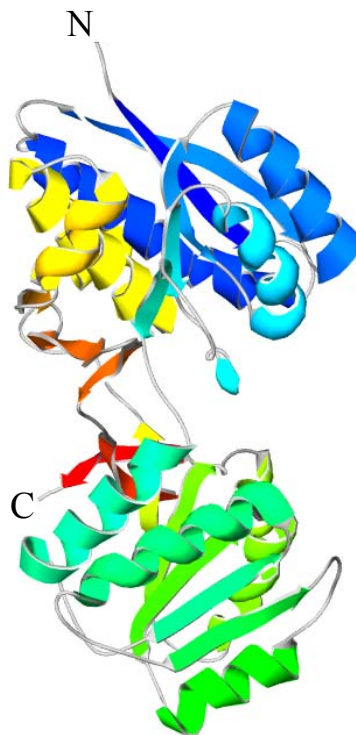
Fig. 1.6. Ribbon diagrams of the structure of the CysB(88-324) monomer and the Leucine/Isoleucine/Valine Periplasmic binding protein (L/I/V-PBP). The L/I/V-PBP protein is a member of a family of proteins that are structurally similar to CysB (Sack *et al.*, 1989).

A.

CysB(88-324) Monomer



B. Leucine/Isoleucine/Valine-periplasmic binding protein



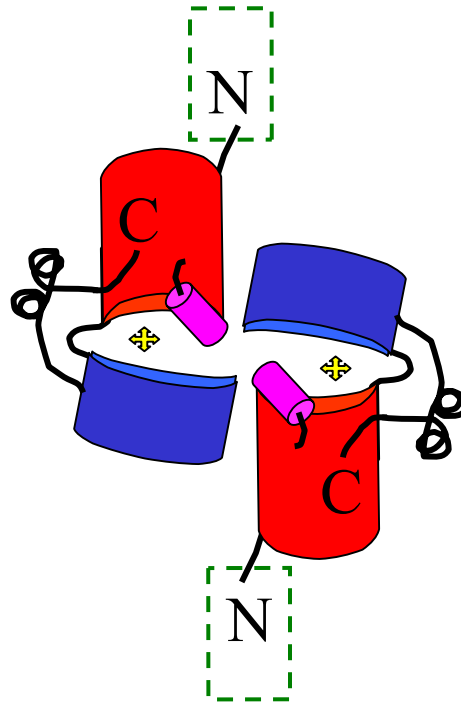
two α/β domains connected by short polypeptide strands. Substrates are bound within the cavity region of the protein causing the domains to contract, engulfing the molecule via a mechanism resembling a venus fly-trap plant (Quiocho and Ledvina, 1996). Enclosure of the effector in this manner may allow precise protein-ligand interactions that enable the protein to bind substrates selectively (Miller *et al.*, 1980).

One interesting question to arise from the crystal structure of CysB(88-324) is how the N-terminal DNA-binding domain of CysB affects tetramerization in the full-length protein. The crystal structure showed that protein crystals were composed of dimers of CysB(88-324), while full-length CysB exists as a tetramer. Mutational analysis of other LTTRs has consistently implicated the C-terminal region of the proteins as being critical for protein oligomerization and the N-terminal region as necessary for DNA-binding (Schell, 1993). Interestingly, recent mutational analysis showed that methodical deletion of the last 30 residues of the C-terminus of CysB resulted in a phenotype suggesting altered DNA-binding (Lochowska, *et al.*, 2001). These results suggest an interaction between the C- and N- terminal domains of CysB.

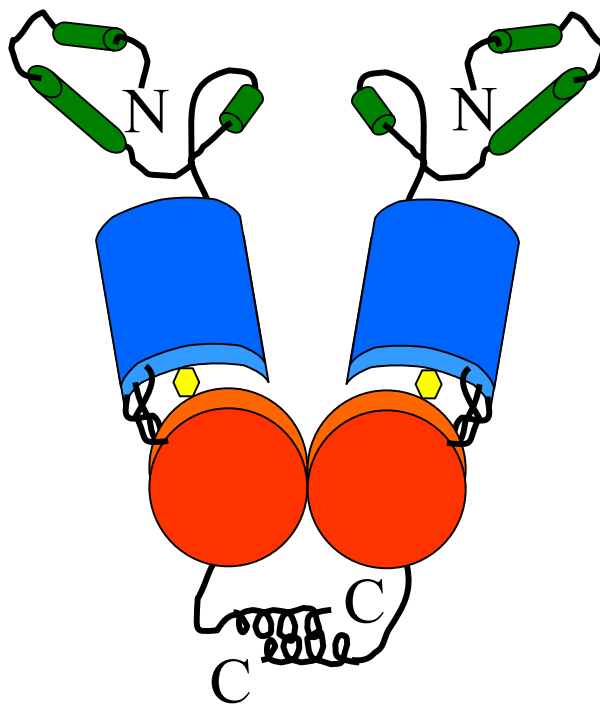
The mechanism by which CysB binds to DNA is unclear. The antiparallel arrangement of the CysB(88-324) monomers would presumably place the DNA-binding domains of each monomer at opposite ends of the dimer (Fig. 1.7A). This would be in contrast to the well-characterized *lac* repressor protein, in which the DNA-binding domains of two monomers interact together at the same end of the monomers (Fig. 1.7B) (Friedman *et al.*, 1995). Like the *lac* repressor, it has been suggested that the helix-turn-helix regions of LTTR dimers interact together to bind DNA (Kullik, *et al.*, 1995; Lochowska, *et al.*, 2001). However a full-length LTTR crystal structure will be

Fig. 1.7. Diagram depicting the general domain organization of a CysB(88-324) dimer (A) compared to a dimer of the full-length *lac* repressor (B). In panel A, domains I and II are represented by the red and blue cylinders, respectively. A sulfate ion is represented as a yellow star. The green box indicates the relative position of the N-terminal DNA binding domain. Panel B is a representation of a dimer of the *lac* repressor. Domains necessary for effector binding are colored red and blue. The yellow hexagon represents the effector isopropyl- β -D-thiogalactoside (IPTG). The DNA binding domain containing the helix-turn-helix motif is represented by the green cylinders.

A.



B.



necessary to determine the structure and location of the DNA-binding domain relative to the effector binding domain. The formation of diffracting crystals of full-length CysB has recently been reported (Verschuere *et al.*, 2001), which should provide clues about how CysB binds DNA.

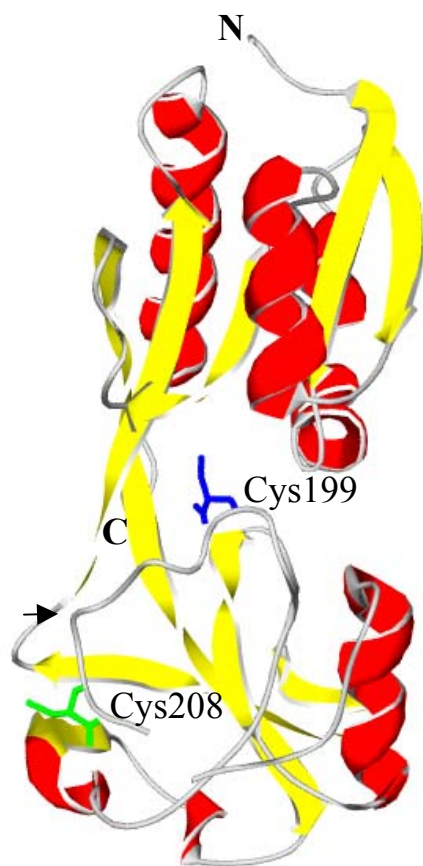
THE STRUCTURE OF OXYR

The OxyR regulator controls the expression of genes required for oxidative stress protection in *Escherichia coli* and *Salmonella typhimurium* (Christman *et al.*, 1985). OxyR positively activates gene expression in response to the presence of reactive oxygen species like hydrogen peroxide, superoxide anions, and hydroxyl radicals. Under normal and stressed growth conditions, OxyR also acts as a repressor of its own expression (Storz & Altuvia, 1994). Mutational studies have determined that OxyR responds to the oxidation of an intramolecular disulfide bond (Zheng *et al.*, 1998). Residue Cys199, which represents the active site residue of OxyR, is reduced under normal cellular conditions (Kullik *et al.*, 1995). The presence of reactive oxygen species results in the formation of a disulfide bond between Cys199 and Cys208 (Zheng, *et al.*, 1998). The disulfide bond causes conformational changes to occur within OxyR that result in altered DNA-binding contacts (Aslund *et al.*, 1999).

Recently, the crystal structures of the oxidized and reduced forms of the OxyR regulatory domain (residues 80-305) were solved to a resolution of 2.3 Å and 2.7 Å, respectively (Choi *et al.*, 2001). Both forms of the protein have a structural organization closely resembling that of CysB(88-324). Like CysB(88-324), the OxyR regulatory

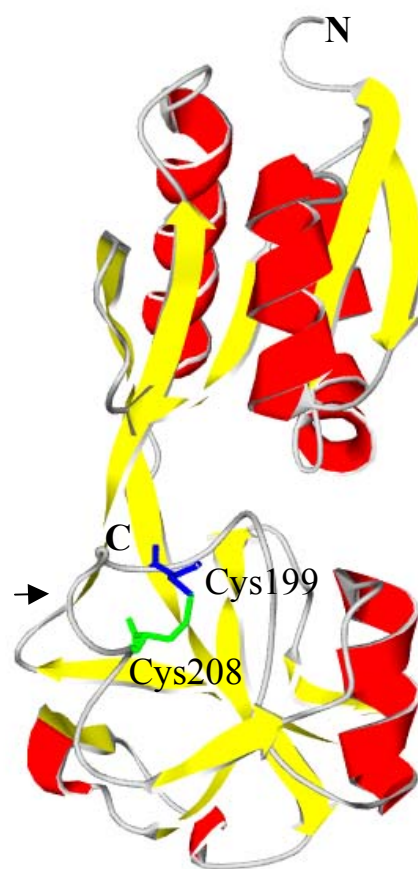
Fig. 1.8. Ribbon diagram showing the structure of a reduced (A) and oxidized (B) monomer of OxyR. The structures are colored according to secondary structure with α -helices in red and β -strands in yellow. Residues Cys199 and Cys208 that form the redox sensitive disulfide bond are colored in blue and green, respectively. The figure was constructed using the Deep View Swiss-PdbViewer software.

A.



Reduced

B.



Oxidized

domain monomer is comprised of two α/β domains connected by two β -strands that enclose an interdomain cleft approximately 8 Å in diameter (Fig. 1.8A and B). Similarly, the OxyR regulatory domain dimer is composed of monomers arranged anti-parallel to one another. This alignment, like that of the CysB(88-324) dimer, positions the cleft openings of each monomer towards one another (Fig.1.9A and B).

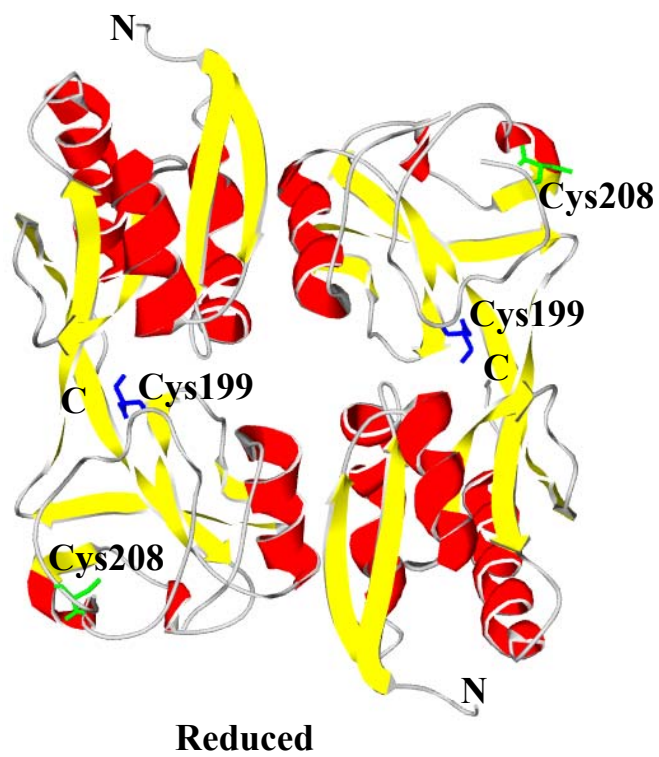
Under reducing conditions, Cys199, the redox sensor of OxyR, is located within the cleft. The sidechain of Cys199 is pointed toward the center of the pocket and forms stabilizing hydrogen bond interactions with several of the residues lining the pocket surface. Cys208, the complementing cysteine residue of the disulfide bond is situated within domain II of the protein, approximately 17 Å away from Cys199.

During oxidizing conditions, the disulfide bond formation results in pronounced conformational changes in domain II of the monomers. A loop region comprised of the residues between Cys199 and Cys208 protrudes out from domain II (Fig. 1.8B, indicated by black arrow). This region, predicted to be highly flexible in the reduced form, forms stabilized interactions along the outer surface of the oxidized protein. Previous studies suggested that this region of the protein could form contacts with RNA polymerase (Kullik, *et al.*, 1995). Mutational studies showed that residue His198 at the base of this loop region, forms interactions with RNA polymerase. Disulfide bond formation causes dramatic changes around this loop region that may play a key role in transcriptional activation in response to oxidizing conditions.

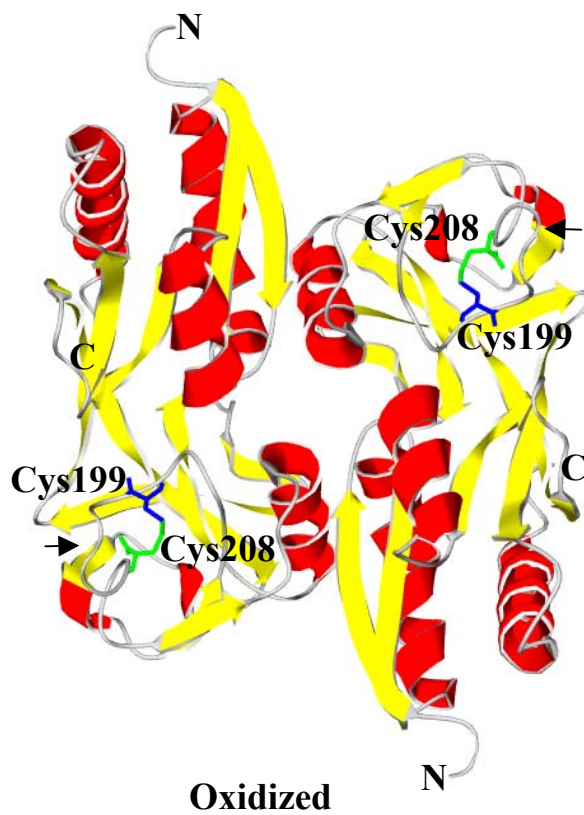
Additional conformational changes in domain II caused changes in the overall dimeric structure of the protein. Formation of the disulfide bond caused the interactions

Fig. 1.9. Ribbon diagram showing the structure of a reduced (A) and oxidized (B) dimer of OxyR. The structures are colored according to secondary structure with α -helices in red and β -strands in yellow. Residues Cys199 and Cys208 that form the redox sensitive disulfide bond are colored in blue and green, respectively. The black arrows denote areas within each monomer that undergo conformational changes. The figure was constructed using the Deep View Swiss-PdbViewer software.

A.



B.



between the monomers to change (Fig. 1.9A and B). Under reduced conditions, the monomers are aligned side-by-side along the long axis of the dimer.

Upon oxidation of the disulfide bond, the subunits rotate approximately 30 ° compared to the reduced forms. This significant structural change is predicted to influence the formation of tetramers between two sets of dimers. Such dramatic conformational changes are predicted to be necessary to alter DNA-binding interactions, although no structural data yet supports this notion.

THE STRUCTURE OF BENM

Since the removal of the N-terminal regions of CysB and OxyR had proven successful for structural studies, a similar approach was used with BenM. As described here, the structure of the BenM effector-binding domain was solved (Chapter 4). These structural studies revealed that despite limited sequence identity among corresponding regions of CysB, OxyR, and BenM, the three LysR-type transcriptional regulators share common structural features that allow transcription to be regulated in response to physiological changes. In the case of BenM, structural changes appear to underlie the previously observed ability to activate transcription synergistically in response to two different effectors (Chapter 3). Collectively, the studies described in this dissertation clarify the complex role of an important protein in *Acinetobacter* sp. strain ADP1 that may be representative of one of the largest classes of prokaryotic transcriptional regulators.

REFERENCES

- Akakura, R. & Winans, S. C. (2002).** Constitutive mutations of the OccR regulatory protein affect DNA bending in response to metabolites released from plant tumors. *J. Biol. Chem.* **277**, 5866-5874.
- Applebaum, E. R., Thompson, D. V., Idler, K. & Chartrain, N. (1988).** *Rhizobium japonicum* USDA 191 has two *nodD* genes that differ in primary structure and function. *J. Bacteriol.* **170**, 12-20.
- Aslund, F., Zheng, M., Beckwith, J. & Storz, G. (1999).** Regulation of the OxyR transcription factor by hydrogen peroxide and the cellular thiol-disulfide status. *Proc. Natl. Acad. Sci.* **96**, 6161-6165.
- Averhoff, B., Gregg-Jollu, L., Elsemore, D. & Ornston, L. N. (1992).** Genetic analysis of supraoperonic clustering by use of natural transformation in *Acinetobacter calcoaceticus*. *J. Bact* **174**, 200-204.
- Brzostowicz, P. C. (1997).** Carbon-source dependent expression of the *pobA* gene needed for 4-hydroxybenzoate degradation in *Acinetobacter* species Strain ADP1. M.S. Thesis. In *Department of Microbiology*. Athens, GA: University of Georgia.
- Brzostowicz, P. C., Reams, A. B., Clark, T. J. & Neidle, E. L. (2003).** Transcriptional cross-regulation of the catechol and protocatechuate branches of the β -ketoacid pathway contributes to carbon-source dependent expression of the *Acinetobacter* sp. strain ADP1 *pobA* gene. *Appl. Environ. Microbiol.* **In Press**.
- Bundy, B. M., Collier, L. S., Hoover, T. A. & Neidle, E. L. (2002).** Synergistic transcriptional activation by one regulatory protein in response to two metabolites. *Proc. Natl. Acad. Sci.* **99**, 7693-7698.

- Chang, M., Hadero, A. & Crawford, I. P. (1989).** Sequence of the *Pseudomonas aeruginosa trpI* activator gene and relatedness of *trpI* to other procaryotic regulatory genes. *J. Bacteriol.* **171**, 172-183.
- Choi, H., Kim, S., Mukhopadhyay, P., Cho, S., Woo, J., Storz, G. & Ryu, S. (2001).** Structural basis of the redox switch in the OxyR transcription factor. *Cell* **105**, 103-113.
- Christman, M. F., Morgan, R. W., Jacobson, F. S. & Ames, B. N. (1985).** Positive control of a regulon for defenses against oxidative and some heat-shock proteins in *Salmonella typhimurium*. *Cell* **41**, 753-762.
- Christman, M. F., Storz, G. & Ames, B. N. (1989).** OxyR, a positive regulator of hydrogen peroxide-inducible genes in *Escherichia coli* and *Salmonella typhimurium*, is homologous to a family of bacterial regulatory proteins. *Proc. Natl. Acad. Sci.* **86**, 3484-3488.
- Coco, W. M., Rothmel, R. K., Henikoff, S. & Chakrabarty, A. M. (1993).** Nucleotide sequence and initial functional characterization of the *clcR* gene encoding a LysR family activator of the *clcABD* chlorocatechol operon in *Pseudomonas putida*. *J. Bacteriol.* **175**, 417-427.
- Collier, L. S. (2000).** Transcriptional regulation of benzoate degradation by BenM and CatM in *Acinetobacter* sp. Strain ADP1. Ph.D. Thesis. In *Department of Microbiology*. Athens, GA: University of Georgia.
- Collier, L. S., Gaines, G. L., III & Neidle, E. L. (1998).** Regulation of benzoate degradation in *Acinetobacter* sp. strain ADP1 by BenM, a LysR-type transcriptional activator. *J. Bacteriol.* **180**, 2493-2501.

- Colyer, T. E. & Kredich, N. M. (1996).** In vitro characterization of constitutive CysB proteins from *Salmonella typhimurium*. *Mol. Microbiol.* **21**, 247-246.
- Cosper, N. J., Collier, L. S., Clark, T. J., Scott, R. A. & Neidle, E. L. (2000).** Mutations in *catB*, the gene encoding muconate cycloisomerase, activate transcription of the distal *ben* genes and contribute to a complex regulatory circuit in *Acinetobacter* sp. Strain ADP1. *J Bacteriol* **182**, 7044-7052.
- D'Argenio, D. A., Segura, A., Coco, W. M., Bunz, P. V. & Ornston, L. N. (2001).** The physiological contribution of *Acinetobacter* PcaK, transport system that acts upon protocatechuate, can be masked by overlapping specificity of VanK. *J. Bacteriol.* **181**, 3505-3515.
- Diaz, E. & Prieto, M. A. (2000).** Bacterial promoters triggering biodegradation of aromatic pollutants. *Curr. Opin. Biotechnol.* **11**, 467-75.
- DiMarco, A. A., Averhoff, B. & Ornston, L. N. (1993).** Identification of the transcriptional activator *pobR* and characterization of its role in the expression of *pobA*, the structural gene for *p*-hydroxybenzoate hydroxylase in *Acinetobacter calcoaceticus*. *J. Bacteriol.* **175**, 4499-4506.
- Fewson, C. A. (1991).** Metabolism of aromatic compounds by *Acinetobacter*. In *The Biology of Acinetobacter*, pp. 351-390. Edited by K. J. Towner, E. Bergogne-Berezin & C. A. Fewson. New York: Plenum Press.
- Friedman, A. M., Fischman, T. O. & Steitz, T. A. (1995).** Crystal structure of *lac* repressor core tetramer and its implications for DNA looping. *Science* **268**, 1721-1727.

- Gaines, G. L., III, Smith, L. & Neidle, E. L. (1996).** Novel nuclear magnetic resonance spectroscopy methods demonstrate preferential carbon source utilization by *Acinetobacter calcoaceticus*. *J. Bacteriol.* **178**, 6833-6841.
- Gerischer, U., Segura, A. & Ornston, L. N. (1998).** PcaU, a transcriptional activator of genes for protocatechuate utilization in *Acinetobacter*. *J. Bacteriol.* **180**, 1512-24.
- Gibson, D. T. & Subramanian, V. (1984).** Microbial degradation of aromatic hydrocarbons. In *Microbial degradation of organic compounds*, pp. 181-252. Edited by D. T. Gibson. New York: Marcel Dekker, Inc.
- Gralton, E. M., Campbell, A. L. & Neidle, E. L. (1997).** Directed introduction of DNA cleavage sites to produce a high-resolution genetic and physical map of the *Acinetobacter* sp. strain ADP1 (BD413UE) chromosome. *Microbiol. U.K.* **143**, 1345-1357.
- Guex, N. & Peitsch, M. C. (1997).** SWISS-MODEL and Swiss-PdbViewer: An environment for comparative protein modeling. *Electrophoresis* **18**, 2714-2723.
- Habeeb, L. F., Wang, L. & Winans, S. C. (1991).** Transcription of the octopine catabolism operon of the *Agrobacterium* tumor-inducing plasmid pTiA6 is activated by a LysR-type regulatory protein. *Mol. Plant Microbe Interact.* **4**, 379-385.
- Hanson, K. G., Nigam, A., Kapadia, M. & Desai, A. J. (1997).** Bioremediation of crude oil contamination with *Acinetobacter* sp. A3. *Curr. Microbiol.* **35**, 191-193.
- Harayama, S. (1997).** Polycyclic aromatic hydrocarbon bioremediation design. *Curr. Opin. in Biotech.* **8**, 268-273.
- Hartnett, C., Neidle, E. L., Ngai, K.-L. & Ornston, L. N. (1990).** DNA sequences of genes encoding *Acinetobacter calcoaceticus* protocatechuate 3,4-dioxygenase: Evidence

indicating shuffling of genes and of DNA sequences within genes during their evolutionary divergence. *J. Bacteriol.* **172**, 956-966.

Hartnett, G. B., Averhoff, B. & Ornston, L. N. (1990). Selection of *Acinetobacter calcoaceticus* mutants deficient in the p-Hydroxybenzoate hydroxylase gene (*pobA*), a member of a supraoperonic cluster. *J. Bacteriol.* **172**, 6160-6161.

Henikoff, S., Haughn, G. W., Calvo, J. M. & Wallace, J. C. (1988). A large family of bacterial activator proteins. *Proc. Natl. Acad. Sci.* **85**, 6602-6606.

Hinner, I. S., Lohmann, M. & Schloemann, M. (1998). Characterization of gene clusters coding for enzymes of catechol catabolism in *Ralstonia eutropha* 335: *catA*, *R*, *B*, *C1*, and *D1*. . Submitted to the EMBL/GenBank/DDBJ databases.

Ishihama, A. (1993). Protein-protein communication within the transcriptional apparatus. *J. Bacteriol.* **175**, 2483-2489.

Johnson, G. R., Jain, R. K. & Spain, J. C. (2000). Properties of the trihydroxytoluene oxygenase from *Burkholderia cepacia* R34: an extradiol dioxygenase from the 2,4-dinitrotoluene pathway. *Arch. Microbiol.* **173**, 86-90.

Jones, R. M., Pagmantidis, V. & Williams, P. A. (2000). *sal* Genes determining the catabolism of salicylate esters are part of a supraoperonic cluster of catabolic genes in *Acinetobacter* sp. Strain ADP1. *J. Bacteriol.* **182**, 2018-2025.

Jorgenson, C. & Dandanell, G. (1999). Isolation and characterization of mutations in the *Escherichia coli* regulatory protein XapR. *J. Bacteriol.* **181**, 4397-4403.

Jourdan, A. D. & Stauffer, G. V. (1998). Mutational analysis of the transcriptional regulator GcvA: amino acids important for activation, repression, and DNA binding. *J. Bacteriol.* **180**, 4865-4871.

- Kim, S. I., Leem, S.-H., Choi, J.-S. & Ha, K.-S. (1998).** Organization and transcriptional characterization of the *catI* gene cluster in *Acinetobacter lwoffii* K24. *Biochem. Biophys. Res. Commun.* **243**, 289-294.
- Kohler, T., Epp, S. F., Kocjancic Curty, L. & Pechere, J. C. (1999).** Characterization of MexT, the regulator of the MexE-MexF-OprN multidrug efflux system of *Pseudomonas aeruginosa*. *J. Bacteriol.* **181**, 6300-6305.
- Kredich, N. M. (1996).** Biosynthesis of cysteine. In *Escherichia coli and Salmonella typhimurium: Cellular and Molecular Biology*, pp. 514-523. Edited by F. C. Neidhardt, R. Curtiss, III., J. L. Ingraham, E. C. C. Lin, K. B. Low, B. Magasanik, W. S. Reznikoff, M. Riley, M. Schaechter & H. E. Umbarger. Washington D. C.: American Society for Microbiology.
- Kullik, I., Stevens, J., Toledano, M. B. & Storz, G. (1995).** Mutational analysis of the redox-sensitive transcriptional regulator OxyR: Residues important for DNA binding and multimerization. *J. Bacteriol.* **177**, 1285-1291.
- Kullik, I., Toledano, M. B., Tartaglia, L. A. & Storz, G. (1995).** Mutational analysis of the redox-sensitive transcriptional regulator OxyR: regions important for oxidation and transcriptional activation. *J. Bacteriol.* **177**, 1275-1284.
- Leveau, J. H. & van der Meer, J. R. (1996).** The *tfdR* gene product can successfully take over the role of the insertion element-inactivated TfdT protein as a transcriptional activator of the *tfdCDEF* gene cluster, which encodes chlorocatechol degradation in *Ralstonia eutropha* JMP134(pJP4). *J. Bacteriol.* **178**, 6824-6832.

- Lindquist, S., Lindberg, F. & Normark, S. (1989).** Binding of the *Citrobacter freundii* AmpR regulator to a single DNA site provides both autoregulation and activation of the inducible *ampC* beta-lactamase gene. *J. Bacteriol.* **171**, 3746-3753.
- Lochowska, A., Iwanicka-Nowicka, R., Plochocka, D. & Hryniewicz, M. M. (2001).** Functional dissection of the LysR-type CysB transcriptional regulator. *J. Biol. Chem.* **276**, 2098-2107.
- Lynch, A. S., Tyrrell, R., Smerdon, S. J., Briggs, G. S. & Wilkinson, A. J. (1994).** Characterization of the CysB protein of *Klebsiella aerogenes*: direct evidence that *N*-acetylserine rather than *O*-acetylserine serves as the inducer of the cysteine regulon. *Biochem. J.* **299**, 129-136.
- Matrubutham, U. & Harker, A. R. (1994).** Analysis of duplicated gene sequences associated with *tfdR* and *tfdS* in *Alcaligenes eutrophus* JMP134. *J. Bacteriol.* **176**, 2348-2353.
- Maxon, M. E., Redfield, B., Cai, X. Y., Shoeman, R., Fujita, K., Fisher, W., Stauffer, G., Weissbach, H. & Brot, N. (1989).** Regulation of methionine synthesis in *Escherichia coli*: effect of the MetR protein on the expression of the *metE* and *metR* genes. *Proc. Natl. Acad. Sci.* **86**.
- Mayer, D., Schlensog, V. & Bock, A. (1995).** Identification of the transcriptional activator controlling the butanediol fermentation pathway in *Klebsiella terrigena*. *J. Bacteriol.* **177**, 5261-69.
- McFall, S. M., Chugani, S. A. & Chakrabarty, A. M. (1998).** Transcriptional activation of the catechol and chlorocatechol operons: variations on a theme. *Gene* **223**, 257-67.

- Miller, D. M., Olson, J. S. & Quioco, F. A. (1980).** The mechanism of sugar binding to the periplasmic receptor for galactose chemotaxis and transport in *Escherichia coli*. *J. Biol. Chem.* **225**, 2465-2471.
- Mouz, S., Merlin, C., Springael, D. & Toussaint, A. (1999).** A GntR-like negative regulator of the biphenyl degradation genes of the transposon Tn4371. *Mol. Gen. Genet.* **262**, 790-799.
- Neidle, E. L., Hartnett, C. & Ornston, L. N. (1989).** Characterization of *Acinetobacter calcoaceticus* *catM*, a repressor gene homologous in sequence to transcriptional activator genes. *J. Bacteriol.* **171**, 5410-5421.
- Neidle, E. L. & Ornston, L. N. (1986).** Cloning and expression of the *Acinetobacter calcoaceticus* catechol 1,2-dioxygenase structural gene *catA* in *Escherichia coli*. *J. Bacteriol.* **165**, 557-563.
- Nichols, N. N. & Harwood, C. S. (1995).** Repression of 4-hydroxybenzoate transport and degradation by benzoate: a new layer of regulatory control in the *Pseudomonas putida* β -ketoadipate pathway. *J. Bacteriol.* **177**, 7033-7040.
- Ogawa, N. & Miyashita, K. (1999).** The chlorocatechol-catabolic transposon Tn5707 of *Alcaligenes eutrophus* NH9, carrying a gene cluster highly homologous to that in the 1,2,4-trichlorobenzene-degrading bacterium *Pseudomonas* sp. Strain P51, confers the ability to grow on 3-chlorobenzoate. *Appl. Environ. Microbiol.* **65**, 724-731.
- Oh, B. H. & Kim, S. H. (1993).** Three dimensional structure of the periplasmic lysine/arginine/ornithine binding protein with and without ligand. *J. Biol. Chem.* **268**, 11348-11355.

- Ornston, L. N. & Neidle, E. L. (1991).** Evolution of genes for the β -ketoacid pathway in *Acinetobacter calcoaceticus*. In *The biology of Acinetobacter*, pp. 201-237. Edited by K. J. Towner, E. Bergogne-Berezin & C. A. Fewson. New York: Plenum Press.
- Orser, C. S. & Lange, C. C. (1994).** Molecular analysis of pentachlorophenol degradation. *Biodegradation* **5**, 277-88.
- Ostrowski, J., Jagura-Burdzy, G. & Kredich, N. M. (1987).** DNA sequences of the *cysB* region of *Salmonella typhimurium* and *Escherichia coli*. *J. Biol. Chem.* **262**, 5999-6005.
- Ostrowski, J. & Kredich, N. M. (1990).** In vitro interactions of CysB protein with the *cysJH* promoter of *Salmonella typhimurium*: inhibitory effects of sulfide. *J. Bacteriol.* **172**, 779-785.
- Perriere, G. & Gouy, M. (1996).** WWW-Query: An on-line retrieval system for biological sequence banks. *Biochimie* **78**, 364-369.
- Popp, R., Kohl, T., Patz, P., Trautwein, G. & Gerischer, U. (2002).** Differential DNA binding of transcriptional regulator PcaU from *Acinetobacter* sp Strain ADP1. *J. Bacteriol.* **184**, 1988-1997.
- Quioco, F. A. & Ledvina, P. S. (1996).** Atomic structure and specificity of bacterial periplasmic receptors for active transport and chemotaxis - variation of common themes. *Mol. Microbiol.* **20**, 17-25.
- Reineke, W. & Knackmuss, H.-J. (1988).** Microbial degradation of haloaromatics. *Ann. Rev. Microbiol.* **42**, 263-287.

- Renna, M. C., Najimudin, N., Winik, L. R. & Zahler, S. A. (1993).** Regulation of the *Bacillus subtilis alsS*, *alsD*, and *alsR* genes involved in post-exponential-phase production of acetoin. *J. Bacteriol.* **175**, 3863-3875.
- Romero-Arroyo, C. E., Schell, M. A., Gaines III, G. L. & Neidle, E. L. (1995).** *catM* encodes a LysR-type transcriptional activator regulating catechol degradation in *Acinetobacter calcoaceticus*. *J. Bacteriol.* **177**, 5891-5898.
- Rothmel, R. K., Aldrich, T. L., Houghton, J. E., Coco, W. M., Ornston, L. N. & Chakrabarty, A. M. (1990).** Nucleotide sequencing and characterization of *Pseudomonas putida catR*: a positive regulator of the *catBC* operon is a member of the LysR family. *J. Bacteriol.* **172**, 922-931.
- Sack, J. S., Saper, M. A. & Quicho, F. A. (1989).** Periplasmic binding protein structure and function. Refined X-ray structures of the leucine/isoleucine/valine-binding protein and its complex with leucine. *J. Mol. Biol.* **206**, 171-191.
- Schell, M. A. (1993).** Molecular biology of the LysR family of transcriptional regulators. *Annu. Rev. Microbiol.* **47**, 597-626.
- Schwacha, A. & Bender, R. A. (1993).** The *nac* (nitrogen assimilation control) gene from *Klebsiella aerogenes*. *J. Bacteriol.* **175**, 2107-2115.
- Seeger, C., Poulsen, C. & Dandanell, G. (1995).** Identification and characterization of genes (*xapA*, *xapB*, and *xapR*) involved in xanthosine catabolism in *Escherichia coli*. *J. Bacteriol.* **177**, 5506-5516.
- Shanley, M. S., Neidle, E. L., Parales, R. E. & Ornston, L. N. (1986).** Cloning and expression of *Acinetobacter calcoaceticus catBCDE* genes in *Pseudomonas putida* and *Escherichia coli*. *J. Bacteriol.* **165**, 557-563.

- Shi, X. & Bennett, G. N. (1994).** Effects of *rpoA* and *cysB* mutations on acid induction of biodegradative arginine decarboxylase in *Escherichia coli*. *J. Bacteriol.* **176**, 7017-7023.
- Srere, P. A. (1987).** Complexes of sequential metabolic enzymes. *Ann. Rev. Biochem.* **56**, 89-124.
- Storz, G. & Altuvia, S. (1994).** OxyR regulon. *Methods Enzymol.* **234**, 217-223.
- Stragier, P. & Patte, J. C. (1983).** Regulation of diaminopimelate decarboxylase synthesis in *Escherichia coli* III. Nucleotide sequence and regulation of the *lysR* gene. *J. Mol. Biol.* **168**, 333-350.
- Suzuki, K., Ichimura, A., Ogawa, N., Hasebe, A. & Miyashita, K. (2002).** Differential expression of two catechol 1,2-dioxygenases in *Burkholderia* sp. Strain TH2. *J. Bacteriol.* **184**, 5805-5809.
- Tao, K., Fujita, N. & Ishihama, A. (1993).** Involvement of the RNA polymerase alpha subunit C-terminal region in co-operative interaction and transcriptional activation with OxyR protein. *Mol. Microbiol.* **7**, 859-864.
- Thompson, J. D., Gibson, T. J., Plewniak, F., Jeanmougin, F. & Higgins, D. G. (1997).** The CLUSTAL_X windows interface: flexible strategies for multiple sequence alignment aided by quality analysis tools. *Nucleic Acids Res* **25**, 4876-4882.
- Timmis, K. N. & Pieper, D. H. (1999).** Bacteria designed for bioremediation. *Trends Biotechnol.* **17**, 201-204.
- Tyrrell, R., Verschueren, K. H. G., Dobson, E. J., Murshudov, G. N., Abby, C. & Wilkinson, A. J. (1997).** The structure of the cofactor-binding fragment of the LysR

family member, CysB: a familiar fold with a surprising subunit arrangement. *Structure* **5**, 1017-1032.

van der Meer, J. R., Frijters, A. C. J., Leveau, J. H. J., Eggen, R. I. L., Zehnder, A. J. B. & de Vos, W. M. (1991). Characterization of the *Pseudomonas* sp. strain P51 gene *tcbR*, a LysR-type transcriptional activator of the *tcbCDEF* chlorocatechol oxidative operon, and analysis of the regulatory region. *J. Bacteriol.* **173**, 3700-3708.

Verschueren, K. H. G., Addy, C., Dobson, E. J. & Wilkinson, A. J. (2001). Crystallization of full-length CysB of *Klebsiella aerogenes*, a LysR-type transcriptional regulator. *Acta Cryst.* **D57**, 260-262.

Verschueren, K. H. G., Tyrrell, R., Murshudov, G. N., Dobson, E. J. & Wilkinson, A. J. (1999). Solution of the structure of the cofactor-binding fragment of CysB: a struggle against non-isomorphism. *Acta Cryst.* **D55**, 369-378.

Wek, R. C. & Hatfield, G. W. (1986). Nucleotide sequence and in vivo expression of the *ilvY* and *ilvC* genes in *Escherichia coli* K12. Transcription from divergent overlapping promoters. *J. Biol. Chem.* **261**, 2441-2450.

You, I. S., Ghosal, D. & Gunsalus, I. C. (1988). Nucleotide sequence of plasmid NAH7 gene *nahR* and DNA binding of the *nahR* product. *J. Bacteriol.* **170**, 5409-5415.

Young, D. M., Parke, D., D'Argenio, D. A., Smith, M. A. & Ornston, L. N. (2001). Evolution of a catabolic pathway. *ASM News* **67**, 362-369.

Zheng, M., Aslund, F. & Storz, G. (1998). Activation of the OxyR transcription factor by reversible disulfide bond formation. *Science* **279**, 1718-1721.

CHAPTER 2

THE *BENPK* OPERON, PROPOSED TO PLAY A ROLE IN TRANSPORT, IS PART
OF A REGULON FOR BENZOATE CATABOLISM IN *ACINETOBACTER* SP.

STRAIN ADP1¹

¹Clark, T. J., C. Momany, and E. L. Neidle. 2002. *Microbiology*. 148:1213-1223.
Reprinted here with permission of the publisher, 5/9/02.

ABSTRACT

BenM and CatM are distinct, but similar, LysR-type transcriptional regulators of the soil bacterium *Acinetobacter* sp. strain ADP1. Together, the two regulators control the expression of at least 14 genes involved in the degradation of aromatic compounds via the catechol branch of the β -keto adipate pathway. In these studies, BenM and CatM were each purified to homogeneity to test the possibility that they regulate the expression of two additional genes, *benP* and *benK*, that are adjacent to *benM* on the chromosome. Each regulator bound to a DNA fragment containing the *benP* promoter region. Additional transcriptional studies suggested that *benP* and *-K* are co-transcribed as an operon, and a site of transcription initiation was identified. Alignment of this initiation site with those of several CatM- and BenM-regulated genes revealed common regulatory motifs. Mutants lacking both CatM and BenM failed to activate *benP* transcription. The ability of each protein to regulate gene expression was inferred from strains lacking either CatM or BenM that were still capable of increasing *benP* expression in response to *cis,cis*-muconate. This compound has previously been shown to induce all enzymes of the catechol branch of the β -keto adipate pathway through a complex transcriptional circuit involving CatM and BenM. Thus, the regulated expression of the *benPK* operon in concert with other genes of the regulon is consistent with the model that BenP, a putative outer-membrane porin, and BenK, an inner-membrane permease, transport aromatic compounds in strain ADP1.

INTRODUCTION

The adjacent *benP* and *benK* genes of the Gram-negative soil bacterium *Acinetobacter* sp. strain ADP1 are in a chromosomal region associated with aromatic compound degradation. A wide variety of aromatic compounds can serve as carbon and energy sources for ADP1 and are degraded through the β -keto adipate pathway. This multi-step catabolic route feeds into the tricarboxylic acid cycle and is encoded by genes that are grouped together in large supraoperonic clusters (Harwood & Parales, 1996; Young *et al.*, 2001). The location and sequence of *benP* and *-K* suggest that they participate in the uptake of compounds, such as benzoate, that are subsequently converted to catechol, a key metabolite of the β -keto adipate pathway. BenK, an inner-membrane permease, plays a role in the cellular entry of benzoate and other aromatic compounds, although it is not essential for growth on benzoate as a sole carbon source (Collier *et al.*, 1997). As described in this report, we tested the effect of inactivating *benP*, which encodes a putative outer-membrane porin. Moreover, the expression of *benP* and *-K* was investigated to determine whether transcriptional regulation of these genes is coordinated with that of other genes of the associated pathway.

Upstream of *benP* are genes involved in the degradation of alkyl salicylates (*salA*, *-R*, *-E*, *-D*) and the degradation of alkanoate esters of benzyl alcohols (*areA*, *-B*, *-C*, *-R*) (Jones *et al.*, 1999; Jones *et al.*, 2000; Jones & Williams, 2001). The SalE and AreABC enzymes convert various aromatic compounds to salicylate (2-hydroxybenzoate) or benzoate. Salicylate is the substrate of SalA, a hydroxylase that mediates the production of catechol. Genes for the degradation of catechol and those that enable benzoate to be converted to catechol are immediately downstream of *benK* (Fig.

2.1) (Collier *et al.*, 1998). Thus, *benP* and *benK* are sandwiched between genes that help funnel a wide array of aromatic compounds into catechol, the substrate of a ring-cleaving dioxygenase (Fig. 2.1). This genetic arrangement may reflect the participation of BenP and BenK in aromatic compound transport.

BenK is required for wild-type rates of benzoate uptake and for the unimpaired use of benzoate or benzaldehyde as a sole carbon source. In addition, the expression of a chromosomal *benK::lacZ* fusion increases in response to *cis,cis*-muconate (CCM), an inducer that regulates all genes known to participate in catechol degradation (Collier, *et al.*, 1997). CCM, which is produced from catechol ring cleavage, interacts with CatM, a LysR-type transcriptional regulator, to activate expression of the *catA* gene and the *catBCIJFD* operon (Fig. 2.1) (Romero-Arroyo *et al.*, 1995). One goal of the current studies was to determine whether CatM is responsible for the CCM-inducibility of *benK* expression. A second LysR-type transcriptional regulator, BenM, activates expression of the *benABCDE* operon needed for the conversion of benzoate to catechol (Collier, *et al.*, 1998). This regulator, encoded by a gene adjacent to *benK*, is similar to CatM in sequence and in its ability to respond to CCM and activate *catA* expression. Therefore, a possible role for BenM in *benK* expression was also investigated.

The function and expression of *benP* have not previously been investigated. Porin-like genes similar to *benP* have been identified near several genetic regions involved in bacterial aromatic compound degradation (Cowles *et al.*, 2000; Segura *et al.*, 1999). For example, *phaK*, essential for the assimilation of phenylacetic acid in a *Pseudomonas putida* strain, appears to encode a specific-channel forming protein (Olivera *et al.*, 1998). The presence of genes likely to encode porins in different

Fig. 2.1. Benzoate degradation in ADP1. The Ben and Cat enzymes (a) are encoded by genes and operons in a 21 kbp chromosomal region that is not drawn to scale (b). Arrows below genes indicate their relative transcriptional orientation. The BenM and CatM regulators control expression of their own genes and activate transcription from the promoters of the *benABCDE* operon (P_{bA}), *catA* (P_{cA}), and the *catBCIJFD* operon (P_{cB}). Regulation of the *benPK* promoter (P_{bP}) was investigated in these studies. In an alignment of the promoter regions (c), known or proposed binding sequences for the regulatory proteins are boxed, and transcriptional start sites are underlined (+1). Identities in three (:) or four (|) of the aligned sequences are indicated. Arrows (*A and *B) indicate the sites of *benP* transcription initiation that would generate primer-extension products of the size shown by corresponding arrows in Figs. 2.3 and 2.4.

catabolic regions suggests that protein channels can facilitate the entry of aromatic compounds into Gram-negative bacteria. In ADP1, the location of the *benP* gene immediately upstream of *benK* suggested that both might be co-expressed. It also seemed likely that CatM and/or BenM would control gene expression. To test these possibilities, RT-PCR and primer extension methods were used to study the transcriptional regulation of *benP* and *benK*. In addition, the CatM and BenM proteins were purified to enable further investigation of their roles in regulating the β -ketoadipate pathway for aromatic compound dissimilation.

METHODS

Strains and growth conditions

Descriptions of strains and plasmids used in this study are listed in table 2.1. *Acinetobacter* strains are derivatives of *Acinetobacter* sp. ADP1, originally designated *Acinetobacter calcoaceticus* BD413 (Juni & Janik, 1969). Plasmids were maintained in *Escherichia coli* DH5 α (Gibco BRL). All bacterial cultures were grown in Luria-Bertani (LB) broth or minimal medium (MM) at 37 °C as previously described (Sambrook *et al.*, 1989; Shanley *et al.*, 1986). Carbon sources were supplemented to LB or MM at the following final concentrations: anthranilate, 3 mM; benzoate, 3 mM; *cis, cis*-muconate (CCM), 2.5 mM; and succinate, 10 mM. Benzaldehyde, benzyl acetate, benzyl alcohol, ethyl salicylate and salicylate were provided as sole carbon sources in a range of concentrations from 0.5 to 2.5 mM. Volatile compounds, such as the esters, were spotted onto filter paper in the lids of inverted petri dishes containing minimal medium. Antibiotics were added as necessary at the following final concentrations: ampicillin, 150

Table 2.1. Bacterial Strains and plasmids.

Strain or Plasmid(s)	Relevant Characteristic(s) ^{*†}	Reference or source
<u>Escherichia coli Strains</u>		
DH5 α	F ⁻ (Φ 80d <i>lacZ</i> Δ M15) Δ (<i>lacZYA-argF</i>)U169 <i>deoR recA1 endA1 hsdR17</i> (r _K ⁻ m _K ⁺) <i>phoA supE44</i> λ <i>thi-1 gyrA96 relA1</i>	Gibco BRL
BL21-Gold (DE3)	F ⁻ <i>dcm</i> ⁺ <i>Hte ompT hsdS</i> (r _B ⁻ m _B ⁻) <i>gal</i> λ (DE3) <i>endA</i> Tc ^r	Stratagene
<u>Acinetobacter Strains</u>		
ADP1	Wild type (BD413)	(Juni and Janik, 1969)
ISA13	<i>catM</i> :: Ω S4013	(Romero-Arroyo, et al., 1995)
ISA25	Δ (<i>catBCIJF</i>)4025	(Gaines et al., 1996)
ISA36	<i>benM</i> :: Ω S4036	(Romero-Arroyo, et al., 1995)
ACN9	<i>benM</i> :: Ω K5008 <i>catM</i> :: Ω S4013	(Collier, et al., 1998)
ACN32	<i>benA</i> :: <i>lacZ</i> -Km ^r 5032	(Collier, et al., 1998)
ACN450	<i>benP</i> :: Ω S5450	This study
<u>Plasmids</u>		
pUC19	Ap ^r ; cloning vector	(Yanisch-Perron et al., 1985)
pRK415	Tc ^r ; cloning vector	(Keen et al., 1988)
pET-21b	Ap ^r ; T7 expression vector	Novagen
pCR-Blunt II-TOPO	Km ^r ; PCR product cloning vector	Invitrogen
pHP45	Ap ^r , Sm ^r Sp ^r ; Source of Ω S	(Prentki & Krisch, 1984)
pBAC14	Ap ^r ; 2.4-kbp <i>Eco</i> RI- <i>Pst</i> I fragment containing <i>benM</i> in pRK415	(Collier, et al., 1998)
pBAC68	Ap ^r ; 7.0-kbp <i>Bgl</i> II/ <i>Kpn</i> I fragment containing the <i>areR-benK</i> region in pUC19	(Jones, et al., 1999)
pBAC84	Ap ^r ; 3.4-kbp <i>Sma</i> I- <i>Eco</i> RI fragment containing <i>benP</i> from pBAC68, inserted into <i>Hin</i> cII- <i>Eco</i> RI of pUC19	This study
pBAC370	Ap ^r , Sm ^r Sp ^r ; Ω S in <i>benP</i> of pBAC84	This study
pBAC381	Ap ^r ; PCR amplified fragment containing <i>catM</i> inserted into <i>Nde</i> I [†] / <i>Bam</i> HI [†] sites of pET-21b	This study
pBAC382	Ap ^r ; PCR amplified fragment containing <i>benM</i> inserted into <i>Nde</i> I [†] / <i>Eco</i> RI [†] sites of pET-21b	This study
pBAC539	Km ^r ; 0.3-kbp fragment containing <i>pobRAO/P</i> region in pCR-Blunt II-TOPO	(Brzostowicz, 1997)
pIB25	Ap ^r ; 1.3-kbp <i>Hin</i> dIII fragment containing <i>catM</i> in pRK415	(Neidle et al., 1989)

* Ap^r, ampicillin resistant; Sm^rSp^r, streptomycin and spectinomycin resistant; Km^r kanamycin resistant; Ω S, omega cassette conferring Sm^rSp^r; Ω K, omega cassette conferring Km^r.

† Indicates restriction sites added by PCR (See Table 2.2).

$\mu\text{g ml}^{-1}$; kanamycin, $25 \mu\text{g ml}^{-1}$; streptomycin, $25 \mu\text{g ml}^{-1}$; and spectinomycin, $25 \mu\text{g ml}^{-1}$. Bacterial growth was monitored by spectrophotometric measurement of the OD_{600} of cultures (Sambrook, et al., 1989).

DNA manipulations, plasmid construction, and interposon mutagenesis

Standard methods were used for plasmid DNA purifications, restriction enzyme digestions, polymerase chain reactions (PCR), electrophoresis, ligations, and *E. coli* transformations (Sambrook, et al., 1989). Oligonucleotides were purchased from Genosys (Table 2.2). Plasmid pBAC84, carrying *benP* was constructed by ligating a 3.4-kbp *Sma* I-*Eco* RI fragment from pBAC68, into *Hinc* II-*Eco* RI digested pUC19. Plasmid pBAC370, used for interposon mutagenesis of *benP*, was constructed by inserting an omega cassette conferring resistance to streptomycin and spectinomycin (ΩS), into the center of *benP*. A 2.0-kbp *Pst* I fragment from pHP45, with ΩS followed by translational and transcriptional stop signals, was ligated into a 500 bp deletion in pBAC84 created by *Cla* I digestion at *benP* sites, at nucleotide positions 2323 and 2719 (numbering system of Fig. 2.2.)

The CatM expression plasmid, pBAC381, was constructed after PCR amplifying *catM* from plasmid pIB25 with the primers CatM-NDEI and CatM-BAMHI (Table 2.2). The PCR product was electrophoresed on a 1.0 % agarose gel, excised, and purified with the QIAquick gel extraction kit (Qiagen). At sites introduced by the amplification primers, the PCR product was digested with *Nde* I and *Bam* HI and ligated into the similarly digested pET-21b expression vector (Novagen). The BenM expression plasmid pBAC382, was similarly constructed with primers BenM-NDEI and BenM-ECORI

Table 2.2. Oligonucleotide primers.

Primer	Sequence (5'-3') [*]	Relative [†] position	Restriction site
BENP-FOR	GACTTTAAGACCGCAACAGGTCTG	(3047-3070)	
BENP2-FOR	GGGCGTTAGCCTCAATTCGAAACT	(2569-2592)	
BENK-REV	CATCATCGTACTAAACGCACGCTG	(4038-4062)	
BENP-PE	ATAAACTGATAAAGACGCGT	(2102-2121)	
CATM-NDEI	TCAATTC CATATG GAACTAAGACACCTCAGA	(16276-16296)	<i>Nde</i> I
CATM-BAMHI	ATAG GATC CTTATTTCGATGAGTGGCCTGAT	(15385-15405)	<i>Bam</i> HI
BENM-NDEI	TCAATTC CATATG GAACTTAGACATCTCCGC	(5617-5637)	<i>Nde</i> I
BENM-ECORI	ATAG AATT CCTTACCAGTTTGGCGGCTCAGT	(4723-4743)	<i>Eco</i> RI
BENPO/P-FOR	TATTGCATAGGTCCTTCCCAAAG	(2071-2094)	
BENPO/P-REV	CCAGTCACGACTTGATGAAATTTG	(1777-1800)	

^{*} Bolded letters indicate restriction site

[†] Relative to complementary sequence of *areR*. Nucleotide 1 corresponds to the last position of the stop codon as depicted in fig. 2.2.

(Table 2.2) and plasmid pBAC14 as the template for PCR amplification. The DNA sequence of the entire *catM* and *benM* genes of pBAC381 and pBAC382, respectively, were verified.

To generate an *Acinetobacter* strain with an inactivated chromosomal *benP* gene, plasmid pBAC370 was digested with *Nde* I to yield a linear fragment with the disrupted *benP::ΩS5450* allele. This fragment was purified from a 1% agarose gel using the Qiaquick purification kit (Qiagen). As described previously (Neidle, et al., 1989), the linearized DNA fragment was used to transform and to replace the corresponding chromosomal region of strain ADP1 generating ACN450. The correct chromosomal configuration of ACN450 was confirmed by Southern hybridization analysis as previously described (Gregg-Jolly & Ornston, 1990).

Expression and purification of CatM and BenM

E. coli strain BL21-Gold (DE3) (Novagen) was transformed with pBAC381 or pBAC382 and plated on solid medium with ampicillin. An isolated colony was used to inoculate 5-ml of LB broth with ampicillin, and the culture was grown at 37°C with agitation until reaching an OD₆₀₀ between 0.4 and 0.8. This 5 ml culture was used to inoculate 1 L of fresh medium and allowed to grow to an OD₆₀₀ of 0.4 to 0.8 at which point the culture was put on ice. After 10 min on ice, the culture was transferred to a 16°C incubator, and protein expression was induced with the addition of IPTG to a final concentration of 1 mM. After over-night incubation (10-14 h), each 1-L culture was divided into 100 ml batches that were harvested by centrifugation at 7000 X g for 10 min.

at 4°C. After removal of the supernatant fluid, cell pellets were immediately stored at -70°C.

Cell pellets containing CatM or BenM were suspended on ice in 10 ml of buffer A1 (50 mM Tris-HCl pH 6.0, 50 mM NaCl, 5% [v/v] glycerol, 0.5 mM EDTA, and 0.5 mM DTT) containing PMSF at a final concentration of 100 µg ml⁻¹. Cells were lysed by two passages through a 4°C chilled French pressure cell at 15000 psi (103,500 kPa). The resulting lysate was centrifuged at 15,000 X g for 15 min at 4°C. All column purification steps were done with an FPLC system from Amersham-Pharmacia. A 10 ml sample of the supernate was loaded onto a 5ml HITRAP SP cation-exchange column that had been equilibrated with 25 ml of Buffer A. Protein was eluted from the column at a flow rate of 1 ml min⁻¹ over a linear gradient of Buffer B1 (Buffer A1 with 1M NaCl) and immediately placed on ice. Fractions containing CatM (300-350 mM NaCl) or BenM (250-350 mM NaCl) were pooled following analysis by 12% SDS-PAGE (Sambrook, et al., 1989).

To lower the NaCl concentration and allow subsequent binding of CatM or BenM to additional columns, pooled samples were diluted 5X with buffer A2 (50 mM Tris-HCl pH 7.0, 50 mM NaCl, 5% (v/v) glycerol, 0.5mM EDTA, and 0.5 mM DTT). The mixture was concentrated to a 10 ml volume with an Ultrafree S-10 centrifuge concentrator (Millipore). Samples were loaded onto a 5ml HITRAP heparin agarose affinity column that had been equilibrated with 25 ml of buffer A2. Protein was eluted over a linear gradient of buffer B2 (Buffer A2 with 1M NaCl) at 1 ml min⁻¹. Fractions containing CatM (500-600 mM NaCl) or BenM (300-400 mM NaCl) were identified by SDS-PAGE. Samples containing pure protein were pooled, diluted 5X with buffer A2, and

concentrated to 1-3 ml using an Ultrafree S-10 centrifuge concentrator. Samples were stored in 20 μ l aliquots at -70°C , at a final concentration of 0.5-1.0 mg ml^{-1} .

Protein concentrations were determined by the method of Bradford (Bradford, 1976) with bovine serum albumin as the standard. Molecular mass of CatM was estimated with gel filtration chromatography. A 5 mg sample of purified CatM (1.0 mg ml^{-1}) was loaded onto a HiPrep sephacryl S-200 gel filtration column that had been equilibrated with buffer A2. Protein was eluted and fractions analyzed by SDS-PAGE to determine the elution volume for CatM. Known proteins served as standards according to the directions of the Molecular Weight-Gel Filtration-200 kit (Sigma).

RNA extraction, RT-PCR, and primer extension analysis

Total RNA was extracted from mid-log phase ($\text{OD}_{600} = 0.3-0.5$) *Acinetobacter* cultures with a hot phenol extraction method as previously described (Williams & Rogers, 1987). RNA samples were treated with DNase I (Promega). The Dnase I was later removed from the RNA with RNeasy columns (Qiagen) in accordance with the manufacturers' specifications. Total RNA concentrations were estimated spectrophotometrically and rRNA bands were visualized on a 1.0 % agarose gel (Sambrook, et al., 1989).

The Omniscript reverse transcriptase kit (Qiagen) was used for both RT-PCR and primer extension methods. *Taq* polymerase (Fisherbrand), and RNasin ribonuclease inhibitor (Promega) were used for RT-PCR reactions. Products were analyzed on 1.0 % agarose gels and sometimes purified with the QIA-quick gel extraction kit (Qiagen). For primer extension reactions, the BENP-PE primer (Table 2.2) was end labeled with T4

Polynucleotide Kinase (Promega) and [γ - 32 P] ATP (ICN Biomedicals) according to the manufacturer's instructions. G-25 spin columns (Amersham-Pharmacia) were used to remove free [γ - 32 P] ATP from the labeling reactions. 1 μ l of the end-labeled primer was combined with 2 μ g of total RNA in a final volume of 6 μ l and incubated at 65°C for 5 min to allow primer annealing. A DNA sequencing ladder was generated with the fmol DNA Cycle Sequencing kit (Promega), [γ - 32 P] end-labeled BENP-PE primer, and plasmid pBAC84 containing the wild-type *benP* region as template. Primer-extension products and sequencing reactions were analyzed by 6% denaturing PAGE and visualized by autoradiography (Sambrook, et al., 1989).

Gel-retardation assays

A double stranded DNA fragment with the *benP* operator-promoter region (P_{bp}) was radio-labeled as previously described (Parsek *et al.*, 1994). The BENPO/P-FOR and BENPO/P-REV primers, after being 5' end-labeled with [γ - 32 P] ATP and T4 Polynucleotide Kinase (Promega), were used to PCR amplify a 317 bp DNA fragment from pBAC84. This labeled fragment was purified following separation by 5% PAGE. The conditions for DNA binding reactions were previously described (Romero-Arroyo, et al., 1995). Binding reactions were initiated by mixing 5-1000 ng of CatM or BenM with 1000 c.p.m. of the 32 P-labeled *benP* fragment (approximately 10 nM) in the presence or absence of 50 mM CCM. The DNA-protein complexes were analyzed as previously described (Parsek, et al., 1994).

Unlabeled DNA fragments were used in competition studies with the labeled fragment to verify the specificity of CatM and BenM binding. For use as a specific

competitor, a DNA fragment with P_{bp} was generated by PCR as described above except that the BENPO/P-FOR and BENPO/P-REV primers were not labeled with ^{32}P . To generate a fragment for non-specific DNA competition studies, the M13 forward and M13 reverse universal primers (Promega) were used in PCR to amplify a 656 bp fragment from pBAC539 (Table 2.1), which contains the *pobRA* operator-promoter region. This region of the ADP1 chromosome regulates the catabolism of *p*-hydroxybenzoate (DiMarco *et al.*, 1993) and does not contain a recognizable binding sequence for CatM or BenM. Competition studies were done by adding a range of competitor DNA, from 1- to 50-fold molar excess, to the reaction as previously described (Tobiason *et al.*, 1999).

RESULTS

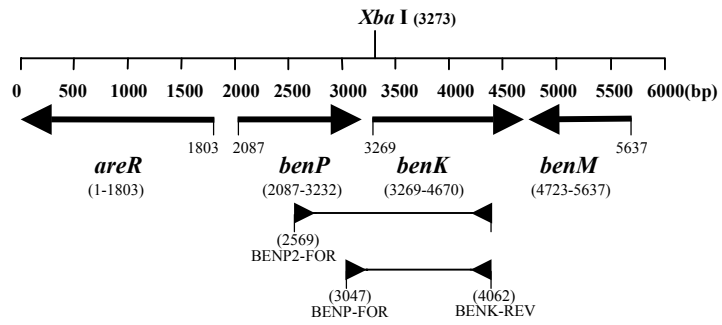
Co-expression of *benP* and *benK*

The orientation of other genes in the vicinity suggested that *benP* and *benK* would be transcribed either individually or as a bicistronic operon (Fig. 2.1). To understand the regulation of gene expression, we first explored the possibility that the two adjacent genes were co-transcribed. Total RNA was isolated from the wild-type strain, ADP1, grown with sole carbon sources that are degraded via the catechol branch of the β -ketoacid pathway (benzoate or CCM). In addition, RNA was isolated from ADP1 grown with succinate as the sole carbon source, a growth condition that does not induce expression of genes associated with the β -ketoacid pathway.

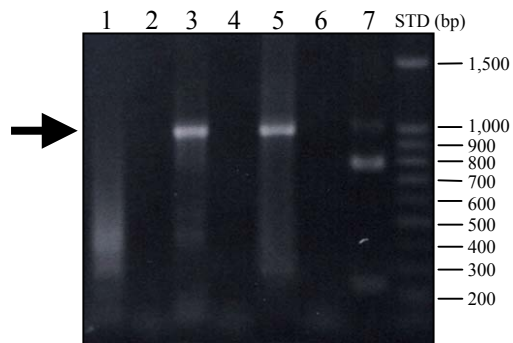
RT-PCR analysis was carried out with the BENP-FOR primer in *benP* and the BENK-REV primer in *benK* (Fig. 2.2, Table 2.2). With RNA from ADP1 grown on

Fig. 2.2. Co-expression of the *benP* and *benK* genes. The relative positions of genes (arrows), primers (triangles), and RT-PCR products (lines) are indicated (a). Numbers correspond to DNA sequence such that position 1 corresponds to the last position of the stop codon of the complementary sequence of *areR*. RT-PCR products were separated on an agarose gel (b) from reactions with the BENP-FOR and BENK-REV primers and total RNA from ADP1 grown on succinate (lanes 1 and 2), benzoate (lanes 3 and 4), or CCM (lanes 5, 6 and 7). An RT-PCR product from a previous reaction was digested with *Xba* I (lane 7). No reverse transcriptase was added to reactions in the even numbered lanes. An arrow shows the 1015 bp product. DNA size standards (STD) are indicated on the side.

(a)



(b)

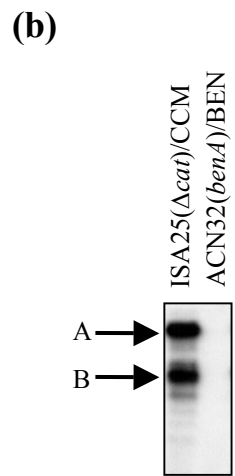
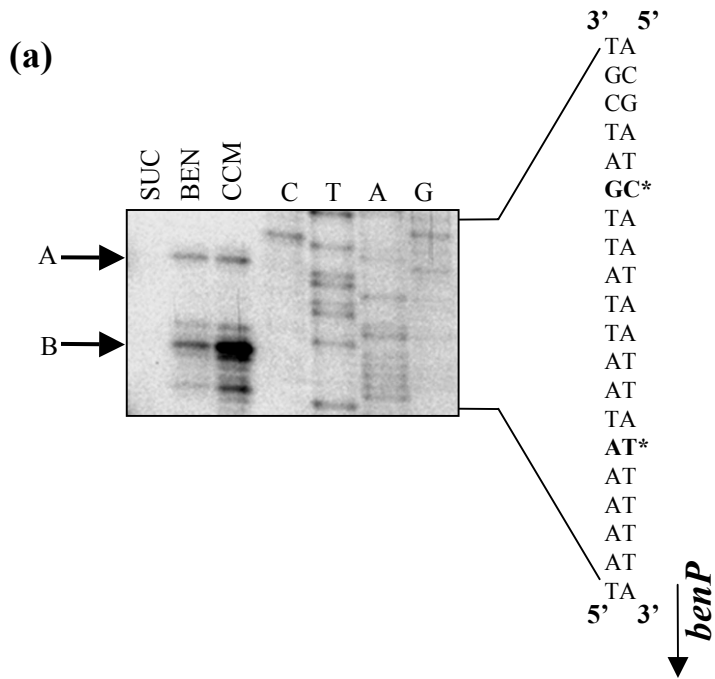


benzoate or CCM, but not succinate, a 1015-bp product of the size expected for these primers was obtained, Fig. 2.2 (b). Control reactions lacking reverse transcriptase did not yield a product, indicating no significant DNA contamination in the RNA samples. RT-PCR products were isolated and digested with *Xba*I to confirm the presence of a known recognition sequence in *benK*. Although complete digestion was not always achieved, the sizes of the cleavage products were consistent with the correct fragments having been amplified, as shown for CCM-grown cells in Fig. 2.2 (b) lane 7. Additional RT-PCR experiments with the same BENK-REV primer and a primer closer to the 5' end of *benP* (BENP2-FOR, Table 2.2) yielded a product of the expected size with RNA from cells grown on CCM (data not shown). Thus, there were *benK* transcripts that initiate more than 700 nt upstream of its translational start codon. These results indicate that *benP* and *benK* are co-transcribed and that expression of the *benPK* operon occurs during growth on CCM or benzoate, but not succinate.

Transcript initiation and inducible expression of *benPK*

Expression of *benP* was further explored with primer extension methods. The primer used for these experiments (BENP-PE, Table 2.2) annealed to a region downstream of the predicted *benP* AUG start codon. In extension reactions with total RNA from ADP1 grown on benzoate or CCM as the carbon source, two prominent products were generated. Their sizes would correspond to transcripts that initiate at sites 49 and 40 nt upstream of the start codon, labeled A and B in Fig. 2.3 (a). No extension products were detected in reactions with RNA from succinate-grown cells, despite multiple repetitions with independently isolated RNA samples. Spectral analysis of total

Fig. 2.3. Primer extension analysis of *benP*. RNA was extracted from the wild-type strain ADP1 grown on succinate (SUC), benzoate (BEN), or CCM as a sole carbon source (a). Lanes C, T, A, and G indicate the DNA sequencing ladder. Arrows A and B mark major products of sizes corresponding to transcripts initiating 49 and 40 nucleotides upstream of the predicted *benP* translational start site. Nucleotides at these positions are highlighted and marked with an asterisk. RNA was analyzed from LB-grown mutants (b). Strain ISA25 has a large *cat*-region deletion (Δcat) that prevents CCM catabolism and strain ACN32 has an insertion (in *benA*) that prevents benzoate catabolism. CCM was added to the growth medium of the former and benzoate (BEN) to the latter. Arrows showing major products (A and B) are of identical sizes in panels (a) and (b).



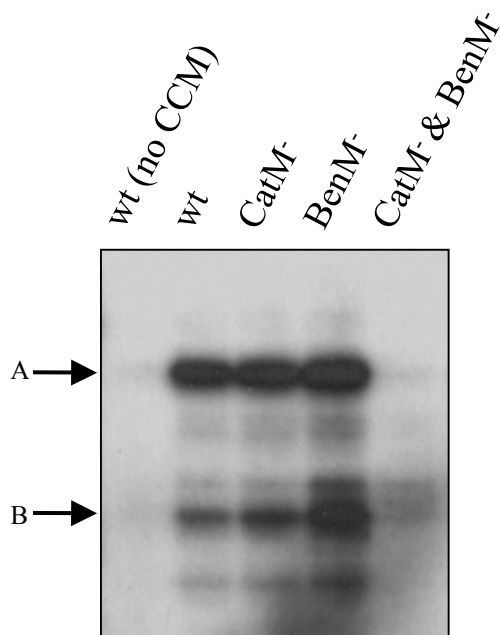
RNA and electrophoretic detection of rRNA revealed no obvious differences among the RNA samples from cells grown on different carbon sources. Consistent with the RT-PCR results, these studies indicated that *benP* expression is inducible.

Mutants were used to determine whether benzoate or CCM, in the absence of catabolism, could induce gene expression. RNA was isolated from ISA25, a strain with a large *cat*-gene deletion that prevents CCM catabolism. Primer extension analysis indicated that *benP* is expressed when this strain is grown on rich medium in the presence of CCM, Fig. 2.3 (b). Therefore, CCM itself, rather than a catabolite generated during growth on CCM, appears to cause increased *benP* expression. CCM similarly stimulated *benP* expression in ACN32, which has a large insertion in *benA* that prevents benzoate catabolism (data not shown). However, when ACN32 was grown on rich medium supplemented with benzoate, no *benP* expression was detected, Fig. 2.3 (b). Consistent with this result, benzoate does not increase expression of a chromosomal *benK::lacZ* transcriptional fusion in the absence of benzoate catabolism (Collier, et al., 1997). Therefore, transcription from the *benPK* promoter, P_{bp} , in benzoate-grown wild-type cells most likely results from the endogenous generation of CCM during benzoate degradation.

Roles of CatM and BenM in regulating P_{bp}

The identification of CCM as an inducer raised the possibility that CatM or BenM can activate transcription from P_{bp} . To test this possibility, *benP* expression was studied in mutants (listed in Table 2.1) lacking CatM (strain ISA13), BenM (strain ISA36), or both of these transcriptional regulators (strain ACN9). Total RNA was isolated from the

Fig. 2.4. Primer extension analysis of *benP* in mutants. RNA was extracted from LB-grown wild-type (wt) strain ADP1 and mutant strains ISA13 (CatM⁻), ISA36 (BenM⁻), and ACN9 (CatM⁻ & BenM⁻). The growth medium was supplemented with CCM except where noted for the wild-type control. Two major products marked by arrows are of the identical size to those labeled A and B in Fig. 2.3.



wild type and from each of these mutants grown on rich medium supplemented with CCM. Primer extension reactions with the *benP* primer (BENP-PE, Table 2.2) indicated that the loss of both transcriptional regulators significantly reduced transcription from P_{bp} . (Fig. 2.4). In contrast, the absence of either CatM or BenM alone had little effect on transcription relative to that in the wild-type strain under the same growth conditions (Fig. 2.4). These results suggested that both BenM and CatM are individually able to regulate P_{bp} in response to CCM. The overlap of their regulatory capabilities may account for the requirement that both BenM and CatM be absent in order to observe the loss of regulated gene expression. A similar overlap in regulation by BenM and CatM occurs for the expression of *catA* from its promoter region P_{cA} (Romero-Arroyo, et al., 1995).

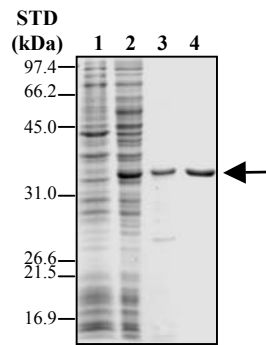
Protein purification following expression of *catM* and *benM* in *E. coli*

To study the interactions of BenM and CatM with DNA in the vicinity of P_{bp} *in vitro*, the two regulators were purified. Expression vectors pBAC381 and pBAC382 (Table 2.1) were constructed for the production of CatM and BenM, respectively, in *E. coli*. When protein production was induced at 37 °C, problems were encountered with inclusion body formation. As described in the Methods section, conditions were identified for purification following protein induction at 16 °C. CatM was purified by cation-exchange and heparin-agarose affinity chromatography. From 1 g of dry cell mass, CatM protein (approximately 2 mg total) was obtained with an estimated purity of >95%, Fig. 2.5 (a). BenM was similarly purified yielding approximately 1.5 mg g⁻¹ of dry cell mass, Fig. 2.5 (b). Gel filtration analysis indicated that the sole oligomeric form

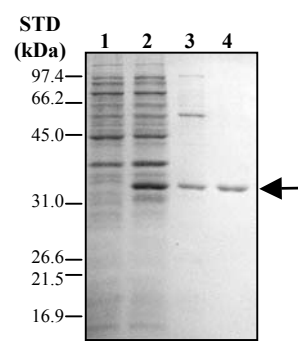
Fig. 2.5. Purification of CatM (a) and BenM (b) after induction in *E. coli*.

Coomassie stained 12% SDS-polyacrylamide gel of protein from (lane 1) soluble extract from uninduced *E. coli* cells with plasmid-borne *catM* or *benM*, (lane 2) soluble extract from IPTG-induced *E. coli* cells with plasmid-borne *catM* or *benM*, (lane 3) after cation-exchange (SP) chromatography, and (lane 4) after elution from the heparin agarose column. The position and molecular mass of protein standards (STD) are indicated. The arrows indicate the approximately 36 kDa CatM or BenM.

(a) CatM



(b) BenM



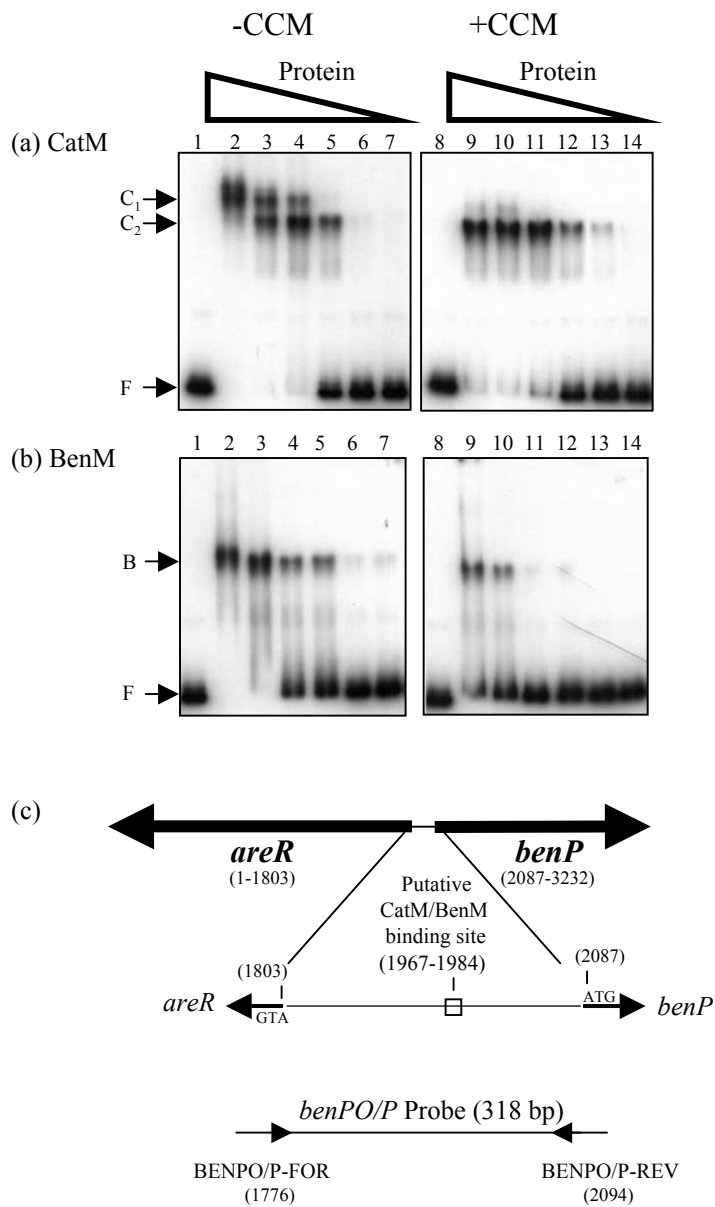
of CatM was approximately 140 kDa. Since denaturing SDS-PAGE analysis was consistent with the prediction that the monomeric protein is 35.5 kDa, the CatM protein was inferred to be tetrameric in solution. A similar conclusion was drawn from gel filtration analysis of BenM (Bundy, 2001).

Binding of CatM and BenM to the *benP* regulatory region

Based on studies of other LysR-type transcriptional regulators (McFall *et al.*, 1998), we predicted that if CatM and BenM activate *benP* expression, then they should bind to DNA in the region of P_{bp} in the presence or absence of the inducer, CCM. Gel retardation assays were used to test this prediction. Samples of purified CatM and BenM were incubated with a radiolabeled fragment carrying P_{bp} (Fig. 2.6). Increasing amounts of either protein increased the proportion of DNA with retarded electrophoretic mobility. To confirm that the changes in mobility patterns resulted from BenM or CatM binding specifically to the P_{bp} region, competition experiments were done with unlabeled DNA (described in the Methods section). In the presence of 100 ng of either BenM or CatM, reactions containing the unlabeled P_{bp} fragment in 50-fold molar excess to the ^{32}P -labeled probe resulted in the complete absence of fragments with retarded mobility (data not shown). In contrast, reactions containing the non-specific competitor DNA fragment in 50-fold molar excess did not reduce the ability of CatM or BenM to retard the mobility of the fragments with P_{bp} (data not shown).

The presence of CCM in the binding reaction with CatM resulted in altered patterns of fragment mobility at the higher protein concentrations, Fig. 2.6 (a) lanes 2, 3, and 4 compared to lanes 9, 10, and 11. In the presence of CCM, labeled fragments were

Fig. 2.6. Gel retardation assays of CatM or BenM bound to the P_{bP} region. Purified CatM (a) or BenM (b) was incubated with the ^{32}P -labeled P_{bP} fragment in the absence of CCM (lanes 1-7) or in presence of 50 mM CCM (lanes 8-14). Lanes 1 and 8 contained no protein. The following amounts of CatM or BenM were used in the binding reactions: lanes 2 and 9, 1000 ng; 3 and 10, 500 ng; 4 and 11, 100 ng; 5 and 12, 50 ng; 6 and 13, 10 ng; 7 and 14, 5 ng. The arrow marked F indicates the mobility of free DNA in the absence of protein. The retarded mobility of fragments at positions labeled C₁, C₂, and B presumably results from the binding of CatM or BenM to form protein-DNA complexes. The position of a putative binding site for these regulators is schematically indicated by a box (c). Also indicated are the primers and the position of the ^{32}P -labeled fragment (P_{bP} Probe) used in these studies. The numbering system is that used in Fig. 2.2.



observed at the position labeled C₂, whereas in the presence of CCM there were additional fragments observed at the position labeled C₁. In the reactions with BenM, the presence or absence of CCM did not alter the position of the fragments with retarded mobility. However, in the absence of CCM, BenM may have a higher affinity for the *P_{bp}* probe. Although the significance of the specific patterns is difficult to infer, the ability of the inducer to alter the mobility of DNA-protein complexes has been observed for similar LysR-type regulators (McFall, et al., 1998; Parsek *et al.*, 1992; Schell, 1993).

The function of *benP*

The regulation of *P_{bp}* by BenM and CatM should coordinate the transcription of the *benPK* operon with the expression of additional *ben* and *cat* genes involved in benzoate degradation (Fig. 2.1). Therefore, the ability to degrade benzoate and related compounds was tested in ACN450, a strain in which the chromosomal copy of *benP* was disrupted by insertional inactivation (Table 2.1, Methods section). ACN450 was capable of growing on solid medium using benzoate, benzaldehyde, benzyl alcohol, benzyl acetate, ethyl salicylate, salicylate, or anthranilate as the sole carbon source (data not shown). With these substrates, possible differences in growth rates between ACN450 and the wild-type strain were not characterized. The mutation in ACN450 should also prevent expression of *benK*, a gene known to affect the rate of growth on some of these compounds (Collier, et al., 1997). These results indicate that neither BenP nor BenK is essential for the cellular entry of this set of aromatic compounds under the laboratory conditions tested. Different experimental conditions, different substrates and/or different

Fig. 2.7. Modified alignment of the deduced BenP protein sequence with the sequences of known or putative porins from *Acinetobacter* and *Pseudomonas*. Boxes A-F display the regions of greatest similarity and asterisks mark residues (bolded) identical in all sequences. These regions are connected by less conserved stretches of amino acids (aa) of variable length. The total number of amino acids is shown parenthetically. In the VanORF and BenF sequences there are insertions of 10 and 4 amino acids respectively, that do not resemble those aligned in other peptide sequences. Sequences in OprD that may form transmembrane β -strands are underlined and numbered to correspond with the sixteen- β -stranded OprD topology model of Huang et al. (Huang *et al.*, 1995) that was recently modified (Ochs *et al.*, 2000). According to this model, short loops between strands 2 and 3 (box B), 4 and 5 (box C), 10 and 11 (box D) are in the periplasmic space, and the residues of box A are part of the first of eight loops external to the outer membrane. The Genbank accession numbers for each sequence are as follows: OprE1 (D12711), OprE3 (AB006797), OprD3 (AF033849), VanORF (AF009672), PhaK (AF029714), BenF (AAF63454), BenP (this study), and OprD (X63152).

A			B			C		
OprE1	39aa	LTLRNFYINIDN	12aa	WGQGFILNYQSGFTQGTVGVGVDA	42aa	GLTAKAKVSNTEFRYGTLPKLPVVVYNDGRLLPVTFEGGQVTS		
OprE3	37aa	LFFRNGYISRDI	9aa	WCQAATATFTSGFTQGTVGVGVDA	38aa	GAAVKFRESNTVLKYGDMPSLPVLSDNSRLLPESYSGTLITS		
OprD3	44aa	LLLRNFYFNRF	15aa	WVQGFMANFSSGFTQGTLVGVGIDA	39aa	GGAVKLRWYGTVLRVGDVFPLLPVIQYGNRLLFPSSFRGFTLVN		
VanORF	31aa	LTLRNFYFDRDY	12aa	WAQGVIFKQSGSYTDGPGVGVGVDA	37aa	GITGKAKYRNNELVGDLVPLLPITIFSSPARLFPQTYRGRVFLS		
PhaK	39aa	LELRNHYINRDI	12aa	WGQGF TAKLES GFTEGPGVGVGVDA	36aa	GLTGKIRVSKSTLRGLTLPILPVVVYNDTRLLASTPQGGLTS		
BenF	32aa	LSARNHYFSRDI	14aa	WAQGFILDFKSGYTPGTVGVGVGMDA	35aa	APTFKARLSKTEL RVGELQPNLPVLTFSDIRLLPPTVQGSVSS		
BenP	39aa	LSLKNAYIDRDY	10aa	WSQGASL F YKSDYKTFID-GL E I	39aa	GGT L K L K Y D Q T E L R V G E L W P D L P V T A V D R S R Q L L T S Y Q G V S L N S		
OprD	43aa	LLLRNFYFNRDG	9aa	W I O G F L I T T Y E S G F T Q G T V G V G V D A	35aa	GGAVKVRISK T M L K W G E M Q P T A P V F A A G G S R L F P Q T A T G F Q L Q S		
				2	3	4	5	

D			E			F		
OprE1	127aa	EVDNRAFSGLFYTVSGHSIGAGYQILNGD	38aa	YGYDFATVGVPGLTFFNTIYLSGDK	62aa	DQDENRLIVSYTLPLL		(460)
oprE3	99aa	NRDNKIWSLAASYTIDGHTFMIAHQRTNGD	42aa	YALDFAKYGVPGLT YRVAYVRGDN	50aa	DQDENRAFVEY PFSVF		(425)
oprD3	107aa	ELDNDIWSVRGGFAYGPHQVLLSYQRNNGD	34aa	YDLDMAAFGVPGLSFMTRYAKGED	60aa	DLDEVRLIVEYPLQVL		(448)
VanORF	108aa	EVDNRHLSGLFGLNYQNHITISLGYMQSFGA	33aa	YEYFK-10--GLRFMTRYAKGED	49aa	AVDENRLICYTLALW		(409)
PhaK	100aa	NIDNRNFAMFTLGVRAHKFTATWQMSGD	33aa	YDYDFVAMGIPGLSFMTRYTDGRH	47aa	AVDENRLICYTLALW		(417)
BenF	107aa	NIDNQAFFSMFTARHGGHSPHAGYQGIYGD	33aa	YDYNFAAMGVPGLTATVRYITGNN	9aa	RDRE-RD-4-YAVQSG		(398)
BenP	68aa	NIDSQNF G I L E T L K Y R N H T V G L G Y Q Q I V G D	33aa	YGYDFKDY-VPGLNPTFKHYGYD	45aa	DFNENRFLTYTKKF		(381)
OprD	103aa	DISNTTWSLAAYTIDAHITFLAYOKVHGD	42aa	YDINLASYGVPGLT F M V R Y I N G K D	61aa	DQNEEFLIVDYPLSLL		(443)
		10	11	13		16		

genetic backgrounds may be needed to reveal the phenotypic effects caused by the loss of BenK and BenP.

Initial analysis of BenP detected relatively low, but significant, sequence identity in pairwise alignments with known porins. However, computer-based programs failed to optimize the alignment of BenP and other proteins throughout their entire lengths. As shown in Fig. 2.7, generated by a combination of computer-based methods and hand-made alignments, there are segments of BenP with strong sequence similarity to known or putative porins that are interspersed with regions, of variable size, containing little or no identity to the other sequences. According to the transporter classification (TC) system of Saier, BenP and several other putative porins involved in aromatic compound transport form a family that includes the OprD porin of *Pseudomonas aeruginosa* (TC# 1.B.25; <http://tcds.ucsd.edu/tcds/search2.php>) (Saier, 2000). The substrates of OprD include cationic amino acids, peptides, and an analogous compound, the antibiotic imipenem (Trias & Nikaido, 1990).

No protein structure has yet been determined for a BenP-like porin, although various bacterial porins have a β -barrel structure (Koebnik *et al.*, 2000). A 16 β -strand topology model proposed for OprD has been tested by deletion mutagenesis (Huang, *et al.*, 1995; Ochs, *et al.*, 2000). The predicted OprD β -strands with sequences similar to those of BenP are underlined in Fig. 2.7. Furthermore, 23 amino acid residues that are conserved among all sequences in the alignment, marked by asterisks, are likely to have a role in protein structure or function. Proteins in the alignment that may be involved in aromatic compound catabolism include PhaK and BenF of *Pseudomonas putida*. PhaK was inferred to form an outer membrane channel with narrow substrate specificity since

inactivation of its gene prevents the use as a sole carbon source of phenylacetate but not 4-OH-phenylacetate or additional phenylacetate-related compounds (Olivera, et al., 1998). A predicted role for BenF in aromatic compound catabolism is based on the coexpression of *benF* with several genes in an operon for benzoate dissimilation (Cowles, et al., 2000; Olivera, et al., 1998).

DISCUSSION

Regulation of transcription initiation

A region of transcription initiation for the *benPK* operon was identified (Figs. 2.3 and 2.4). Alignment of this P_{bP} region with other CatM- and BenM-controlled promoters helped identify potential regulatory sequences Fig. 2.1 (c). Recent studies with DNase I footprinting demonstrated that CatM and BenM bind strongly to the P_{bA} region, which controls expression of the divergently transcribed *benM* and *benA* genes. CatM and BenM each recognize a consensus LysR-type binding sequence in P_{bA} (T 11 nt A, with a small region of dyad symmetry), boxed in Fig. 2.1 (c) (Collier, 2000). An identical sequence to that in P_{bA} , ATAC 7 nt GTAT, is recognized by CatM in the P_{cB} region, which controls expression of the divergently transcribed *catM* and *catB* genes (Romero-Arroyo, et al., 1995). Similar sequences are recognized by a subfamily of LysR-type transcriptional regulators involved in bacterial aromatic compound catabolism, to which CatM and BenM belong (Coco *et al.*, 1994). Therefore, the boxed regions of P_{bP} and P_{cA} are also likely to serve as BenM and CatM binding sites, Fig. 2.1 (c). Furthermore, six additional nucleotides, which are highlighted in Fig. 2.1 (c), are identical in all these

promoter regions and occur in locations shown to be important for the regulation of P_{bA} (Bundy, 2001).

This sequence alignment places the previously identified transcriptional start sites of the *benA*, *catA*, and *catB* genes in an identical position (+1), Fig. 2.1 (c) (Collier, 2000; Romero-Arroyo, et al., 1995). This position of *benP* would correspond to a primer extension product of the size denoted as "A" in Figs. 2.3 and 2.4. Thus, the placement of putative regulatory sequences and the observation that "A" is the largest observed primer extension product suggest that *benP* transcription initiates at a position corresponding to that of the other CatM- and BenM-regulated genes. The multiple products in the *benP* primer extension reactions may result from RNA secondary structure, RNA processing and/or degradation, multiple transcription initiation sites, or some combination of these factors. The significance of the experimental variation in relative intensities of the products is not evident. Nevertheless, the presence of the primer extension products clearly indicated the conditions under which *benP* is expressed.

The regulon controlled by CatM and BenM

CCM caused transcription from P_{bP} to increase in strains with CatM or BenM (Figs. 2.3 and 2.4). The absence of both regulators significantly reduced *benP* expression, although the resultant expression was higher than that of the wild-type strain grown in the absence of CCM (Fig. 2.4). Similarly, in a mutant lacking both BenM and CatM, the expression of *benA* is approximately 4-fold higher than in strains with the regulators when no inducer is present (Cosper *et al.*, 2000). This increased expression results from the ability of CatM or BenM, in the absence of inducers, to bind to a

segment of P_{bA} and repress basal *benA* expression by preventing access to RNA polymerase (Bundy, 2001). BenM and CatM, which are able to bind to the P_{bP} region in the absence of CCM (Fig. 2.6), may similarly repress basal *benP* expression.

The gel retardation studies indicate that CatM can form at least two different complexes with the P_{bP} region. The presence of CCM may alter the interactions between the regulatory proteins and one or more binding site in this region. Multiple binding sites for BenM and CatM have been demonstrated in the P_{bA} region (Bundy, 2001). Multiple binding sites in the target genes have also been identified in *Pseudomonas putida* for the CatR and ClcR regulators, which control catechol and chlorocatechol degradation, respectively (McFall, et al., 1998). Based on structural studies of transcriptional regulators, the putative CatM/BenM binding site in the P_{bP} region, boxed in Fig. 2.1 (c), should bind a protein dimer (Branden & Tooze, 1999). However, BenM and CatM, like many LysR-type regulators, were tetrameric in solution (Schell, 1993). Additional studies are needed to determine if the presence of CCM affects the oligomeric structure of CatM or BenM and to characterize the specific binding of these regulators to the P_{bP} region.

While CatM and BenM both regulate transcription from P_{bP} , P_{bA} , P_{cA} , and P_{cB} (depicted in Fig. 2.1), the specific regulation at each locus varies considerably. For example, benzoate interacts with BenM to activate transcription from P_{bA} , and most likely from P_{cA} , as well (Collier, et al., 1998; Romero-Arroyo, et al., 1995). In contrast, despite the ability of BenM to regulate transcription from P_{bP} , benzoate did not serve as an inducer in the absence of its conversion to CCM (Figs. 2.3 and 2.4). Regulated expression from P_{bP} appeared to be mediated equally well by CatM or BenM in response

to CCM (Fig. 2.4). Similarly, CCM enables CatM and BenM each to activate high-level transcription from P_{cA} (Romero-Arroyo, et al., 1995). In contrast, at P_{bA} or P_{cB} , BenM or CatM, respectively, acts as the principal regulator of the expression of a multi-gene operon (Collier, et al., 1998; Romero-Arroyo, et al., 1995). Thus CatM and BenM control the expression of numerous genes with related functions. The demonstration in this report that the *benPK* operon is part of this complex regulon strongly suggests a role for BenP and BenK in the degradation of aromatic compounds.

Transporters in aromatic compound catabolic pathways

The proposed porin functions have yet to be demonstrated for BenP or for similar proteins likely to be involved in aromatic compound uptake. However, open reading frames encoding hypothetical bacterial porins are frequently located in the vicinity of genes known to participate in aromatic compound degradation. For example, two different BenP/PhaK-like hypothetical proteins of *Pseudomonas* sp. strain CA10 are encoded in genetic regions involved in the degradation of the heterocyclic aromatic compound carbazole via the catechol branch of the β -keto adipate pathway (Nojiri *et al.*, 2001). Moreover, the putative porin-encoding genes are often located near genes coding for proteins resembling inner-membrane permeases such as BenK, PcaK and MucK that are involved in the uptake of compounds degraded via the β -keto adipate pathway (Nichols & Harwood, 1997; Williams & Shaw, 1997). Taken collectively, the data support a model in which a porin, such as BenP, and permease, such as BenK, function together to facilitate the cellular entry of some substrates of bacterial aromatic compound catabolic pathways.

ACKNOWLEDGEMENTS

We are grateful to Drs. Lauren S. Collier, Becky M. Bundy, and James E. Posey for their contributions to protein purification and primer extension analysis. We also thank Drs. Frank Gherardini, Timothy R. Hoover, Anna C. Karls, and Mark A. Schell for many helpful discussions. This research was supported by NSF grant MCB-9808784 (to E.L.N).

REFERENCES

Bradford, M. M. (1976). A rapid and sensitive method for the quantitation of microgram quantities of protein utilizing the principle of protein-dye binding. *Anal. Biochem.* **72**, 248-254.

Branden, C. & Tooze, J. (1999). *Introduction to Protein Structure - Second Edition*, Second ed. New York, NY: Garland Publishing, Inc.

Brzostowicz, P. C. (1997). Carbon-source dependent expression of the *pobA* gene needed for 4-hydroxybenzoate degradation in *Acinetobacter* sp. Strain ADP1. M.S. Thesis. In *Department of Microbiology*. : University of Georgia.

Bundy, B. M. (2001). Transcriptional regulation of the *benABCDE* operon of *Acinetobacter* sp. Strain ADP1: BenM-mediated synergistic induction in response to benzoate and *cis,cis*-muconate. Ph.D. Thesis. In *Department of Microbiology*. : University of Georgia.

Coco, W. M., Parsek, M. R. & Chakrabarty, A. M. (1994). Purification of the LysR family regulator, ClcR, and its interaction with the *Pseudomonas putida clcABD* chlorocatechol operon promoter. *J Bacteriol* **176**, 5530-3.

Collier, L. S. (2000). Transcriptional regulation of benzoate degradation by BenM and CatM in *Acinetobacter* sp. strain ADP1. Ph.D. Thesis. In *Department of Microbiology*. : University of Georgia.

Collier, L. S., Gaines, G. L., III & Neidle, E. L. (1998). Regulation of benzoate degradation in *Acinetobacter* sp. strain ADP1 by BenM, a LysR-type transcriptional activator. *J. Bacteriol.* **180**, 2493-2501.

Collier, L. S., Nichols, N. N. & Neidle, E. L. (1997). *benK* encodes a hydrophobic permease-like protein involved in benzoate degradation by *Acinetobacter* sp. Strain ADP1. *J. Bacteriol.* **179**, 5943-5946.

Cosper, N. J., Collier, L. S., Clark, T. J., Scott, R. A. & Neidle, E. L. (2000). Mutations in *catB*, the gene encoding muconate cycloisomerase, activate transcription of the distal *ben* genes and contribute to a complex regulatory circuit in *Acinetobacter* sp. Strain ADP1. *J. Bacteriol.* **182**, 7044-7052.

Cowles, C. E., Nichols, N. N. & Harwood, C. S. (2000). BenR, a XylS homologue, regulates three different pathways of aromatic acid degradation in *Pseudomonas putida*. *J. Bacteriol.* **182**, 6339-6346.

DiMarco, A. A., Averhoff, B. & Ornston, L. N. (1993). Identification of the transcriptional activator *pobR* and characterization of its role in the expression of *pobA*, the structural gene for *p*-hydroxybenzoate hydroxylase in *Acinetobacter calcoaceticus*. *J. Bacteriol.* **175**, 4499-4506.

Gaines, G. L., III, Smith, L. & Neidle, E. L. (1996). Novel nuclear magnetic resonance spectroscopy methods demonstrate preferential carbon source utilization by *Acinetobacter calcoaceticus*. *J. Bacteriol.* **178**, 6833-6841.

Gregg-Jolly, L. A. & Ornston, L. N. (1990). Recovery of DNA from the *Acinetobacter calcoaceticus* chromosome by gap repair. *J. Bact.* **172**, 6169-6172.

Harwood, C. S. & Parales, R. E. (1996). The β -ketoadipate pathway and the biology of self-identity. *Annu. Rev. Microbiol.* **50**, 553-590.

- Huang, H., Jenateur, D., Pattus, F. & Hancock, R. E. W. (1995).** Membrane topology and site-specific mutagenesis of *Pseudomonas aeruginosa* porin OprD. *Mol. Microbiol.* **16**, 931-941.
- Jones, R. M., Collier, L. S., Neidle, E. L. & Williams, P. A. (1999).** *areABC* Genes determine the catabolism of aryl esters in *Acinetobacter* sp. Strain ADP1. *J. Bacteriol.* **181**, 4568-4575.
- Jones, R. M., Pagmantidis, V. & Williams, P. A. (2000).** *sal* genes determining the catabolism of salicylate esters are part of a supraoperonic cluster of catabolic genes in *Acinetobacter* sp. Strain ADP1. *J. Bacteriol.* **182**, 2018-2025.
- Jones, R. M. & Williams, P. A. (2001).** *areCBA* is an operon in *Acinetobacter* sp. Strain ADP1 and is controlled by AreR, a σ^{54} -dependent regulator. *J. Bacteriol.* **183**, 405-409.
- Juni, E. & Janik, A. (1969).** Transformation of *Acinetobacter calco-aceticus* (*Bacterium anitratum*). *J. Bacteriol.* **98**, 281-288.
- Keen, T., Tamaki, S., Kobayashi, D. & Trollinger, D. (1988).** Improved broad-host-range plasmids for DNA cloning in Gram-negative bacteria. *Gene* **70**, 191-197.
- Koebnik, R., Locher, K. P. & Van Gelder, P. (2000).** Structure and function of bacterial outer membrane proteins: barrels in a nutshell. *Mol Microbiol* **37**, 239-253.
- McFall, S. M., Chugani, S. A. & Chakrabarty, A. M. (1998).** Transcriptional activation of the catechol and chlorocatechol operons: variations on a theme. *Gene* **223**, 257-67.
- Neidle, E. L., Hartnett, C. & Ornston, L. N. (1989).** Characterization of *Acinetobacter calcoaceticus catM*, a repressor gene homologous in sequence to transcriptional activator genes. *J. Bacteriol.* **171**, 5410-5421.

- Nichols, N. N. & Harwood, C. S. (1997).** PcaK, a high-affinity permease for the aromatic compounds 4-hydroxybenzoate and protocatechuate from *Pseudomonas putida*. *J Bacteriol* **179**, 5056-5061.
- Nojiri, H., Sekiguchi, H., Maeda, K., Urata, M., Nakai, S., Yoshida, T., Habe, H. & Omori, T. (2001).** Genetic characterization and evolutionary implications of a *car* gene cluster in the carbazole degrader *Pseudomonas* sp. Strain CA10. *J Bacteriol* **183**, 3663-3679.
- Ochs, M. M., Bains, M. & Hancock, R. E. W. (2000).** Role of putative loops 2 and 3 in imipenem passage through the specific porin OprD of *Pseudomonas aeruginosa*. *Antimicrob Agents Chemother* **44**, 1983-1985.
- Olivera, E. R., Minambres, B., Garcia, B., Muniz, C., Moreno, M. A., Ferrandez, A., Diaz, E., Garcia, J. L. & Luengo, J. M. (1998).** Molecular Characterization of the phenylacetic acid catabolic pathway in *Pseudomonas putida* U: The phenylacetyl-CoA catabolon. *Proc. Natl. Acad. Sci.* **95**, 6419-6424.
- Parsek, M. R., Coco, W. M. & Chakrabarty, A. M. (1994).** Gel-shift assay and DNase I footprinting analysis of transcriptional regulation of biodegradation genes. *Methods Mol. Genet.* **3**, 273-290.
- Parsek, M. R., Shinabarger, D. L., Rothmel, R. K. & Chakrabarty, A. M. (1992).** Roles of CatR and *cis,cis*-muconate in activation of the *catBC* operon, which is involved in benzoate degradation in *Pseudomonas putida*. *J. Bacteriol.* **174**, 7798-7806.
- Prentki, P. & Krisch, H. M. (1984).** In vitro insertional mutagenesis with a selectable DNA fragment. *Gene* **29**, 303-313.

- Romero-Arroyo, C. E., Schell, M. A., Gaines III, G. L. & Neidle, E. L. (1995).** *catM* encodes a LysR-type transcriptional activator regulating catechol degradation in *Acinetobacter calcoaceticus*. *J. Bacteriol.* **177**, 5891-5898.
- Saier, M. H. (2000).** Families of proteins forming transmembrane channels. *J Membr Biol* **175**, 165-180.
- Sambrook, J., Fritsch, E. F. & Maniatis, T. (1989).** *Molecular cloning: a laboratory manual, 2nd ed.* Cold Spring Harbor, N. Y.: Cold Spring Harbor Laboratory Press.
- Schell, M. A. (1993).** Molecular biology of the LysR family of transcriptional regulators. *Annu. Rev. Microbiol.* **47**, 597-626.
- Segura, A., Bunz, P. V., D'Argenio, D. A. & Ornston, L. N. (1999).** Genetic Analysis of a chromosomal region containing *vanA* and *vanB*, genes required for conversion of either ferulate or vanillate to protocatechuate in *Acinetobacter*. *J. Bacteriol.* **181**, 3494-3504.
- Shanley, M. S., Neidle, E. L., Parales, R. E. & Ornston, L. N. (1986).** Cloning and expression of *Acinetobacter calcoaceticus catBCDE* genes in *Pseudomonas putida* and *Escherichia coli*. *J. Bacteriol.* **165**, 557-563.
- Tobiason, D. M., Lenich, A. G. & Glasgow, A. C. (1999).** Multiple DNA binding activities of the novel site-specific recombinase, Piv, from *Moraxella lacunata*. *J. Biol. Chem.* **274**, 9698-9706.
- Trias, J. & Nikaido, H. (1990).** Protein D2 channel of the *Pseudomonas aeruginosa* outer membrane has a binding site for basic amino acids and peptides. *J Biol Chem* **265**, 15680-15684.

Williams, M. G. & Rogers, M. (1987). Expression of the *arg* genes of *Escherichia coli* during arginine limitation dependent upon stringent control of translation. *J. Bacteriol* **169**, 1644-650.

Williams, P. A. & Shaw, L. E. (1997). *mucK*, a gene in *Acinetobacter calcoaceticus* ADP1 (BD413) encodes the ability to grow on exogenous *cis*, *cis*-muconate as sole carbon source. *J. Bacteriol.* **179**, 5935-5942.

Yanisch-Perron, C., Vieira, J. & Messing, J. (1985). Improved M13 phage cloning vectors and host strains: nucleotide sequences of the M13mp18 and pUC19 vectors. *Gene* **33**, 103-119.

Young, D. M., Parke, D., D'Argenio, D. A., Smith, M. A. & Ornston, L. N. (2001). Evolution of a catabolic pathway. *ASM News* **67**, 362-369.

CHAPTER 3

CHARACTERIZATION OF THE EFFECTOR-BINDING PROPERTIES OF BENM USING FLUORESCENCE EMISSION SPECTROSCOPY¹

¹Clark, T. J., C. Momany, E. L. Neidle, and R. S. Phillips. 2002. To be submitted to *J. Bacteriol.*

ABSTRACT

BenM, a member of the LysR-type family of transcriptional regulators, positively regulates genes necessary for benzoate degradation in the gram type-negative bacterium *Acinetobacter* sp. strain ADP1. Recent in vitro studies demonstrated that BenM activates *benABCDE* expression synergistically in response to two distinct effectors, *cis,cis*-muconate and benzoate. Direct binding of either effector by BenM has never been demonstrated. Both ligands alter interactions between BenM and DNA. Similarly, both ligands alter the ability of BenM to activate transcription in vitro. Therefore, it was inferred that benzoate and *cis,cis*-muconate interact directly with BenM. In this study, interactions of BenM with benzoate and *cis,cis*-muconate were characterized by fluorescence emission spectroscopy. The data presented here suggest that BenM binds to benzoate and to *cis,cis*-muconate. However, the conformational changes in BenM caused by each effector were distinct. These studies demonstrated that benzoate and *cis,cis*-muconate compete for a common binding site in BenM. A truncated version of BenM lacking the N-terminal, putative DNA-binding domain was also able to interact with benzoate and CCM. Lastly, we measured the effects of various benzoate derivatives on the fluorescence spectra of BenM to investigate effector-binding specificity.

INTRODUCTION

LysR-type transcriptional regulators (LTTRs) constitute one of the largest families of prokaryotic regulatory proteins, with over 150 members having been described or putatively identified in bacteria and archae (Perez-Rueda & Collado-Vides, 2001). Although found to regulate genes controlling a diverse array of biological processes (Schell, 1993), all LTTRs share the common function of binding to a DNA consensus sequence upstream of a target promoter and positively regulating gene transcription in response to an effector. Mutational studies have identified three separate domains within LTTRs: an N-terminal DNA-binding domain containing a helix-turn-helix motif, a central domain shown to be necessary for effector-binding and recognition, and a C-terminal domain responsible for protein multimerization (Jorgenson & Dandanell, 1999; Kullik *et al.*, 1995; Lochowska *et al.*, 2001).

BenM, an LTTR found in the gram-type negative bacterium *Acinetobacter* sp. strain ADP1, positively regulates genes necessary for benzoate catabolism (Collier *et al.*, 1998). Recent *in vitro* studies suggest that BenM activates the expression of the *benABCDE* operon synergistically in response to two distinct metabolites, *cis,cis*-muconate (CCM) and benzoate (Bundy *et al.*, 2002). *In vitro* transcription studies using purified BenM containing a C-terminal hexahistidine tag (BenM-His), showed that either CCM or benzoate could act as an effector molecule to activate *benA* expression. The presence of both effectors resulted in greater levels of BenM-mediated *benA* expression than the sum of expression due to either compound alone. Similarly, DNase I footprinting studies showed that the BenM-His protection pattern of the *benA* promoter

region changed more significantly in the presence of both effectors, than with either alone (Bundy, et al., 2002).

The mechanism controlling the synergistic effect of CCM and benzoate on BenM-mediated transcriptional activation is unknown. Efforts to determine the region(s) involved in effector-binding using crystallization studies have been hampered by difficulties in purifying and stabilizing full-length BenM at high concentrations. This problem, common to LTTRs, may result from flexibility between the DNA and effector-binding domains of the regulator (Schell, 1993; Tyrrell *et al.*, 1997). Much of the current work on LTTRs has focused on characterizing the DNA-binding function of the proteins. There are few reports describing LTTR-effector-binding. In general, LTTR-effector interactions have been inferred from changes in DNA-binding or regulatory functions. One previous study has characterized the effector-binding by an LTTR. Lynch and co-workers used fluorescence emission spectroscopy to study the effector-binding properties of the CysB protein from *Klebsiella aerogenes*. They showed that the intensity of the fluorescence spectra of CysB increased in the presence of N-acetylserine. From these studies, they concluded that CysB specifically interacted with N-acetylserine, suggesting protein-effector binding (Lynch *et al.*, 1994).

Here, we report the use of fluorescence emission spectroscopy to characterize BenM-effector-binding to help understand how a single transcriptional regulator responds to distinct effectors. BenM contains a single tryptophan residue located at the C-terminus of the protein. Conformational changes in BenM altering the immediate environment of this tryptophan residue caused from the binding of a ligand were detected by monitoring the fluorescence emission spectra between 330-350 nm, the wavelength range that

corresponds to emissions by the indole group of tryptophan (Lakowicz, 1999). Changes in BenM resulting from the binding of effector are assessed by monitoring changes in the fluorescence emission spectra of the protein in the presence of effector compounds. In addition, the binding characteristics of full-length BenM were compared to those of a truncated version of BenM containing the putative effector-binding domain (BenM-EBD-His).

METHODS

Chemicals. *Cis,cis*-muconate (CCM) was purchased from Acros chemicals. All other compounds used for ligand-binding studies were obtained from Sigma-Aldrich.

Imidazole was purchased from Fluka.

Purification of full-length BenM. Full-length BenM, containing a C-terminal hexahistidine purification tag (BenM-His), was expressed and purified as previously described (Bundy, 2001).

Cloning and expression of BenM-EBD. The BenM-EBD-His expression plasmid was constructed by Becky Bundy (unpublished data). DNA encoding the putative effector-binding domain (residues 81-304) of BenM (BenM-EBD) was PCR amplified from plasmid pBAC14 (Collier, et al., 1998) using *Pfu* polymerase (Stratagene) and the oligonucleotide primers BENM-81, (5'-TCAATTCATATGACCAAGCGCATTGCC-3') and BENM-PET3 (5'-TCAATTCTCGAGTTCGATGAGTGGCCTGATATG-3'). These primers contain *Nde*I and *Xho*I restriction sites (bold print), respectively. The PCR

product was electrophoresed on a 1.0% agarose gel, excised, and gel-purified using the QIAquick gel extraction kit (Qiagen). The purified PCR product was digested with the restriction enzymes *NdeI* and *XhoI* and ligated into similarly digested pET-21b. Cloning the PCR fragment into the *XhoI* site of pET-21b translationally fused a hexahistidine purification tag to the C-terminus of BenM-EBD. The resulting plasmid, pBAC435, was transformed into *E. coli* strain DH5 α (Gibco-BRL). The plasmid sequence was confirmed by DNA sequencing (data not shown).

To ensure reproducible BenM-EBD-His expression, pBAC435 was freshly transformed into *E. coli* BL21-Gold(DE3) (Stratagene) cells prior to each protein purification repetition. A single *E. coli* transformant containing pBAC435 that grew on solid LB medium containing 150 μ g/ml ampicillin was used to inoculate 5 ml of similarly supplemented LB broth and incubated with agitation for 3 to 4 h at 37 $^{\circ}$ C. The entire culture was transferred into 1.0 l of the same medium, and incubated as before. After the culture reached an OD₆₀₀ of 0.5 to 0.8 (3-4 h), isopropyl- β -D-thiogalactoside (IPTG) was added to a final concentration of 0.5 mM, and the culture was incubated overnight (12 to 16 h). Cells were harvested the next morning by centrifugation at 7,000 g for 10 min at 4 $^{\circ}$ C and cell pellets stored at -70 $^{\circ}$ C.

Purification of the BenM-EBD. Frozen cell pellets (2-3 g dry weight) of cells expressing BenM-EBD were suspended in 20 ml of binding buffer (20 mM Tris-HCl pH 7.9, 500 mM NaCl, 10% glycerol, and 5 mM imidazole) at 4 $^{\circ}$ C. Cells were lysed via two passes through a chilled (4 $^{\circ}$ C) French pressure cell at 15,000 psi. The cell lysate was centrifuged at 15,000 g for 15 min at 4 $^{\circ}$ C to remove cell debris. All purifications

were done at room temperature using a Fast Performance Liquid Chromatography (FPLC) system (Amersham-Pharmacia). Cell lysate was applied to a 5 ml Hi-TRAP metal-chelating column (Amersham-Pharmacia) that was previously charged with Ni²⁺ (2.5 ml of 0.1 M NiSO₄) and equilibrated with 5 column volumes of binding buffer. Protein was eluted with a linear gradient of elution buffer (20 mM Tris-HCl pH 7.9, 500 mM NaCl, 10% [v/v] glycerol, and 250 mM imidazole) at a rate of 2 ml/min over 20 column volumes. 1.0 ml fractions were collected and immediately placed on ice. BenM-EBD containing fractions were identified on 12% SDS-PAGE gels stained with Coomassie dye (Sambrook *et al.*, 1989) (Data not shown). Samples containing purified protein were pooled and dialyzed (twice) for 4 h at 4 °C in 1.0 l of dialysis buffer (20 mM Tris-HCl pH 7.9, 500 mM NaCl, and 10% glycerol) using 10,000 -Da molecular weight cut-off snakeskin dialysis tubing (Pierce). Approximately 10-20 mg of BenM-EBD was obtained per liter of culture at ≥95% purity. Protein was stored at 4 °C.

Protein Determinations. Protein concentrations were determined using the protein assay kit (Bio-Rad) by the method of Bradford (Bradford, 1976). Bovine serum albumin (Pierce) was used to generate a standard curve.

Fluorescence emission spectroscopy. Tryptophan fluorescence data were obtained using an RSM-1000 instrument from OLIS, Inc. The excitation wavelength was generated using a 450 W Xe lamp with a 6 mm entrance slit, an 8 nm exit slit on the excitation monochromator, and a 4 nm slit in the scan disk of the emission monochromator. To control for decreased fluorescence by the addition of the various effectors, the

fluorescence emission of a 1 μM tryptophan solution was monitored in the presence of 1 mM amounts of the various ligands to be investigated using excitation wavelengths of 280 and 295 nm. CCM, which absorbs light at 280 nm, had a strong inner-filter effect on fluorescence, completely quenching the tryptophan fluorescence signal when an excitation wavelength of 280 nm was used for irradiation. To overcome this problem, all studies using CCM were done with an excitation wavelength of 295 nm. This wavelength resulted in a decrease in the emission spectrum intensities ($\sim 50\%$) of both BenM-His and BenM-EBD-His compared to those generated with an excitation wavelength of 280 nm. Samples containing all other effectors, including benzoate, were measured with an excitation wavelength of 280 nm. The fluorescence emission of 2 ml of BenM-EBD-His or BenM-His diluted with dialysis buffer to a final monomeric concentration of 2 μM , was measured at 25 $^{\circ}\text{C}$ in the presence or absence of effectors. Various concentrations of effector ranging from 10 μM to 10 mM were added (2-10 μl) to the protein solution in a quartz cuvette. After brief mixing by inversion, the fluorescence emission spectra were measured. Fluorescence emissions were scanned for 30 sec, at a rate of 31 scans/sec, over a wavelength range of 300-900 nm. Final spectra were averaged and compiled using the robust global analysis software supplied by OLIS (Matheson, 1990). The fluorescence spectra between 300-500 nm were normalized against the background fluorescence value at 500 nm and used for final data calculations. The final fluorescence values were the average of at least three separate experimentally determined values, with standard deviation values corresponding to $<20\%$ of the average values.

Data analysis. The equilibrium dissociation constants (K_d) for the various protein-effector complexes were obtained by plotting the changes in the intensity of the emission spectra (measured in volts) versus the effector concentrations and fitting the data to a binding isotherm (eq 1) using the Sigmaplot 2000 software hyperbolic regression wizard function (SPSS Inc.). In equation 1, $\Delta\text{Volts}_{\text{obs}}$ is the observed change in voltage, $\Delta\text{Volts}_{\text{max}}$ is the calculated maximum change in voltage, $[E]$ is the concentration of the effector, K_d is the dissociation constant for the effector, and c accounts for the inner filter effect of the effector on the fluorescence signal.

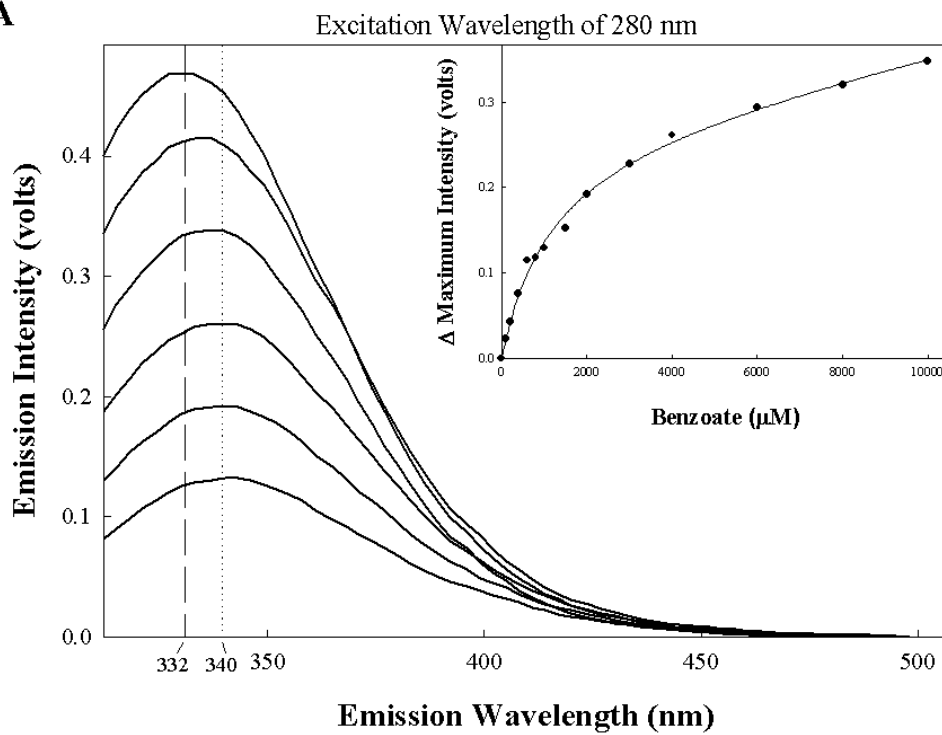
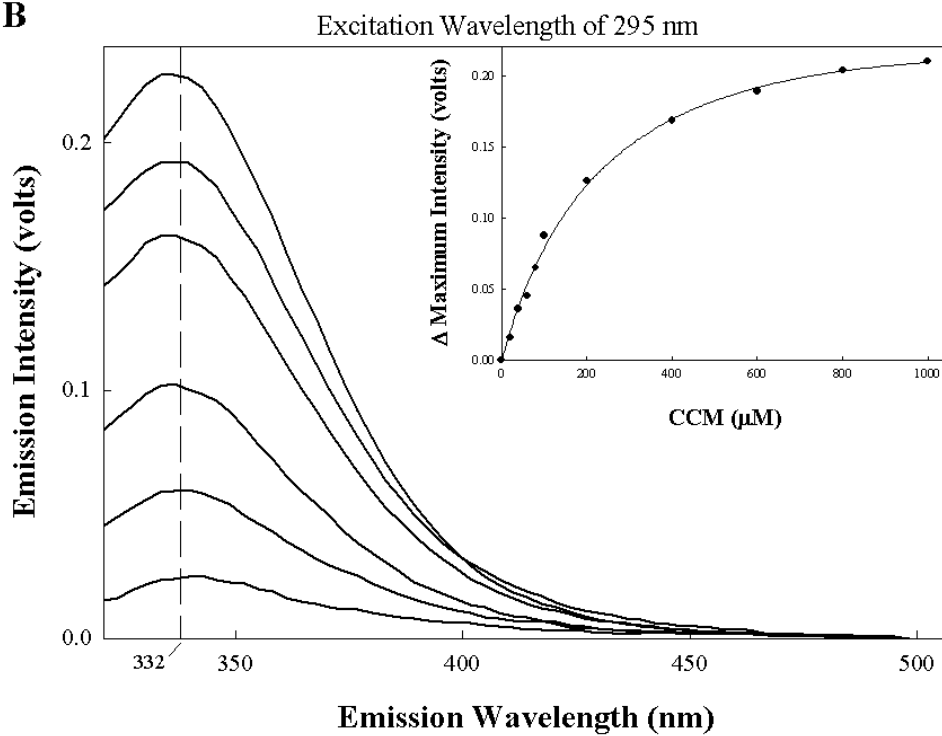
$$\Delta\text{Volts}_{\text{obs}} = (\Delta\text{Volts}_{\text{max}}[E]/K_d[E]) + c[E] \quad (1)$$

RESULTS

Effects of benzoate and CCM on the fluorescence emission spectra of BenM-His.

We used fluorescence emission spectroscopy to monitor the fluorescence signal of a single tryptophan residue in BenM-His as a means of determining interactions between the protein and benzoate or CCM. Initially, the BenM-His fluorescence spectrum showed a maximum emission peak at ~332 nm, suggesting that the tryptophan residue was buried within the protein and unexposed to solvent (Fig. 3.1) (Lakowicz, 1999). The presence of benzoate caused the BenM-His emission maximum peak to shift towards a higher wavelength. For example, in the presence of 200 μM benzoate the maximum was at 335 nm, whereas in the presence of benzoate at 2 mM and above the maximum was at 340 nm (shift is denoted by the vertical dashed lines, Fig. 3.1A). A shift of this nature is indicative of the tryptophan residue being exposed to a more hydrophilic environment, suggesting that the protein has undergone a conformational change affecting the

Fig. 3.1. The effect of benzoate and CCM on the fluorescence emission spectra of BenM-His. (A) The fluorescence emission spectra of BenM-His (from top to bottom) alone and in the presence of 200 μ M, 600 μ M, 2 mM, 4 mM, and 8 mM benzoate. (B) The fluorescence emission spectra of BenM-His with (from top to bottom) 0, 40, 80, 200, 400, or 800 μ M CCM. The vertical lines indicate maximum emission intensity at 332 nm (dashed lines) and the shift to 340 nm (dotted lines) in the presence of benzoate. The inset graph in each panel shows the change in maximum fluorescence emission peak (at 337 nm for benzoate and 333 nm for CCM) plotted against the concentration of benzoate (A) or CCM (B).

A**B**

C-terminus of the protein (Freifelder, 1982). The addition of benzoate also caused a steady decrease in the overall emission spectra of BenM-His that indicates interactions between the compound and the protein. Titration of BenM-His with up to 8 mM benzoate caused the overall spectrum intensity to decrease approximately 80%.

Compounds containing carboxyl groups, like benzoate, are known to quench the fluorescence of tryptophan through direct, non-specific interactions termed collisional quenching (Lakowicz, 1999). To rule out this possibility and to determine if the decrease in BenM-His fluorescence was due to specific binding of benzoate we plotted the change in fluorescence versus the concentration of benzoate. We predicted that if the decrease in the emission signal resulted from collisional quenching, we would expect to see a linear relationship between fluorescence and the concentration of benzoate (Lakowicz, 1999). Conversely, if a specific effector-protein binding interaction were occurring, we would expect a hyperbolic curve, similar to that from a typical protein-ligand binding reaction (Lakowicz, 1999). The plot of the change in the fluorescence emission maximum at 337 nm versus the concentration of benzoate is shown (Fig. 3.1A, inset). The resulting curve is indicative of a specific binding interaction between benzoate and BenM-His. Although several physical properties of the protein influence the overall fluorescence signal, the decrease in the emission spectrum and the spectral shift suggests that benzoate possibly has an effect on the conformation of BenM-His specifically affecting the residues proximal to the tryptophan residue.

The overall intensity of the emission spectrum of BenM-His differed depending on the excitation wavelength used. As shown in Fig. 3.1, the intensity of the overall emission spectrum generated using a wavelength of 280 nm (top line, Fig. 3.1A) was

almost twice the intensity of the signal generated with the 295 nm wavelength (top line, Fig. 3.1B). This is due to the intrinsic fluorescence properties of tryptophan where the polarization state of the indole group remains relatively constant when wavelengths between 260 and 290 nm are used for excitation (Lakowicz, 1999). A dramatic change in the polarization state occurs however, when wavelengths longer than 290 nm are used for excitation. This change in the polarization state results in an approximate 50% decrease in the fluorescence emission intensity, accounting for the change seen in BenM-His fluorescence.

To compare the effects of CCM to benzoate, we measured the fluorescence emission spectrum of BenM-His after titration with various amounts of CCM. An excitation wavelength of 295 nm was used for experiments using CCM due to the strong inner filter effect of the compound at 280 nm (see methods). The presence of CCM did not cause a shift in the emission maximum peak of BenM-His, but did cause a more significant decrease in the overall intensity of the emission spectra (Fig. 3.1B) than benzoate. Titration of BenM-His with 40 μ M CCM caused the fluorescence spectrum intensity to decrease approximately 10%. In contrast, with benzoate, a 10% change required a concentration of 200 μ M. The addition of 1 mM CCM resulted in an approximate 90% decrease of the overall emission spectra, a change requiring >8 mM benzoate. As with benzoate, the decrease in the maximum fluorescence emission of BenM-His at 332 nm was plotted versus the amount of CCM present (inset graph, Fig. 3.1B) to rule out collisional quenching by the carboxyl groups of CCM. The plot resulted in a hyperbolic curve. Similar to benzoate, the data indicate that CCM has a specific interaction with the proximal tryptophan residue of BenM-His.

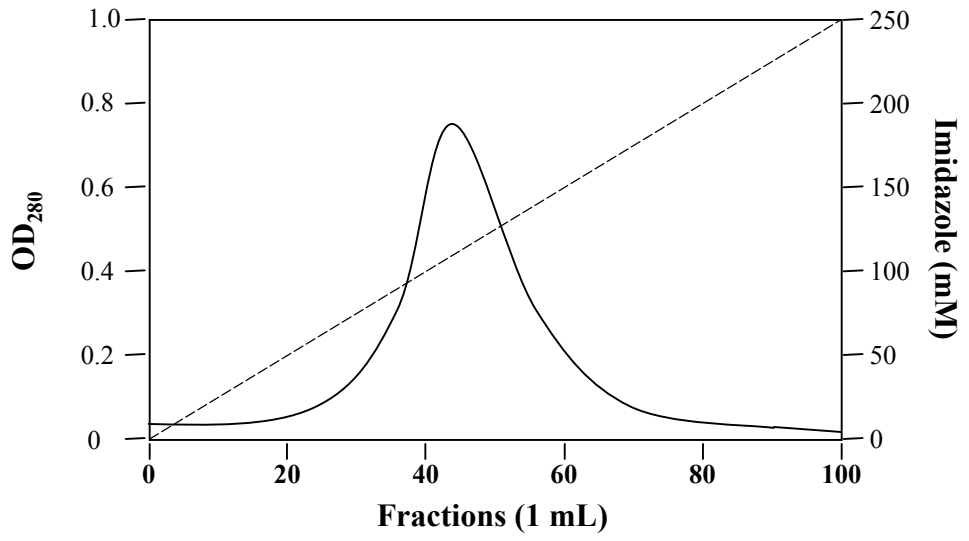
The results suggested that BenM-His binds both benzoate and CCM. However, the effect of each compound on the emission spectrum differed. The decrease in the overall fluorescence emission spectra of BenM-His in the presence of CCM was more dramatic than the decrease associated with benzoate. To compare the relative affinities of BenM-His for each ligand, the equilibrium binding constants were determined for the BenM-His-benzoate and BenM-His-CCM complexes as described in the Methods section. The dissociation constant of the BenM-His-benzoate complex was roughly four times that of the BenM-His-CCM complex (Table 3.1), which suggests that BenM-His has a higher affinity for CCM than benzoate. This conclusion is consistent with previous *in vitro* and *in vivo* results that showed higher BenM-mediated transcriptional activation in response to CCM than benzoate (Bundy, et al., 2002; Collier, et al., 1998).

Protein purification following expression of *benM*-EBD-His in *E. coli*.

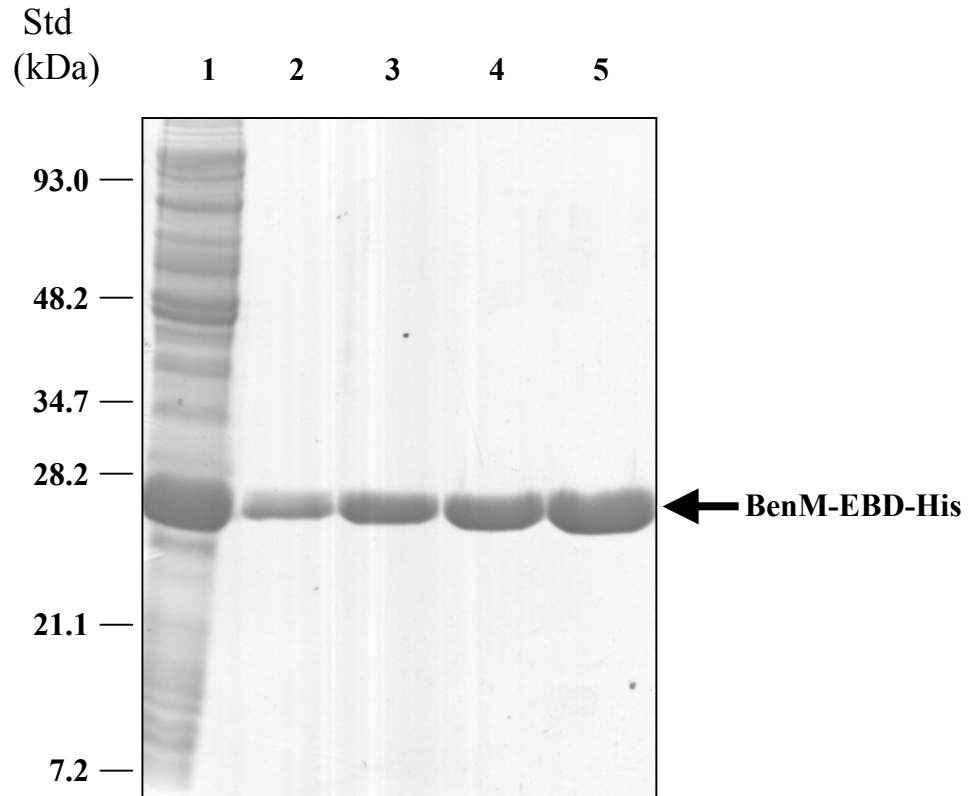
Based on studies of other LTTRs, we predicted that the effector-binding domain of BenM comprised the central and C-terminal segment of the protein (Choi *et al.*, 2001; Tyrrell, et al., 1997). In these previous studies, proteins with the N-terminal DNA binding domain (approximately residues 1 to 80) removed were still able to bind effectors. However, the efficiency of binding by these truncated versions was never compared to that of the full-length protein. In an effort to determine the influence of the N-terminal DNA binding domain on BenM effector-binding, Becky Bundy constructed pBAC435 to express a truncated version of the BenM, lacking the N-terminal domain. I used affinity chromatography to purify the protein, referred to as BenM-EBD-His,

Fig. 3.2. Purification of BenM-EBD-His after induction in *E. coli*. Panel A is a representation of the elution profile of BenM-EBD-His from a nickel-chelating affinity column with a linear imidazole gradient (dashed line). (B) Coomassie-stained 12% SDS-polyacrylamide gel with soluble extract from IPTG-induced *E. coli* cells (lane 1) and fractions 30 (lane 2), 35 (lane 3), 40 (lane 4) and 45 of BenM-EBD-His eluted from a Nickel affinity column as depicted in panel A. The positions and molecular masses of protein standards are indicated on the left side the gel. The arrow denotes the approximate 26 kDa BenM-EBD-His.

A



B



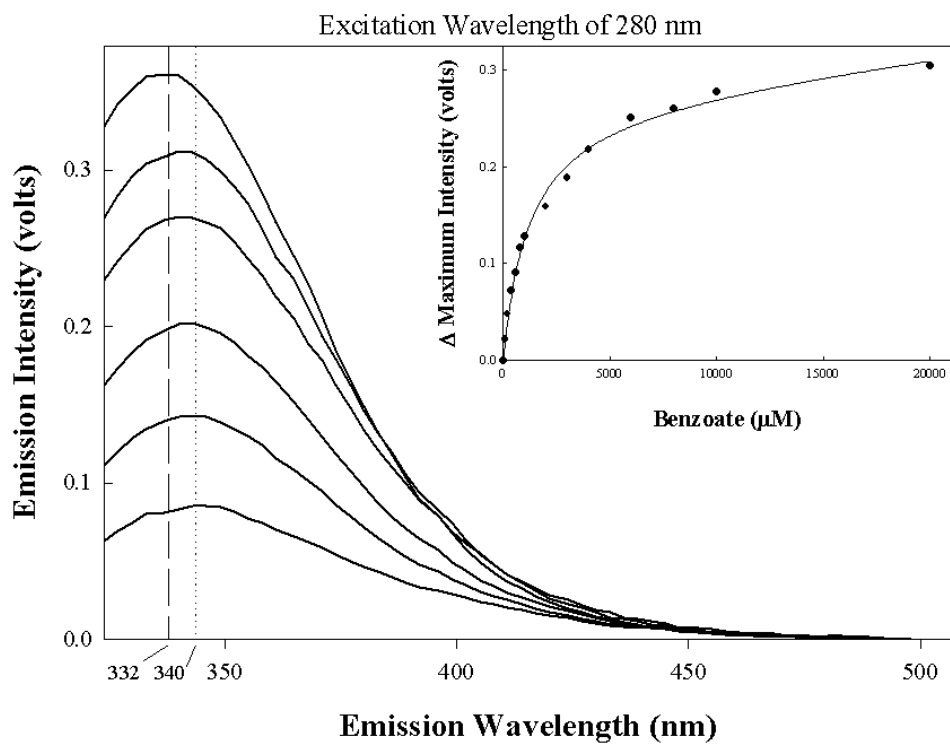
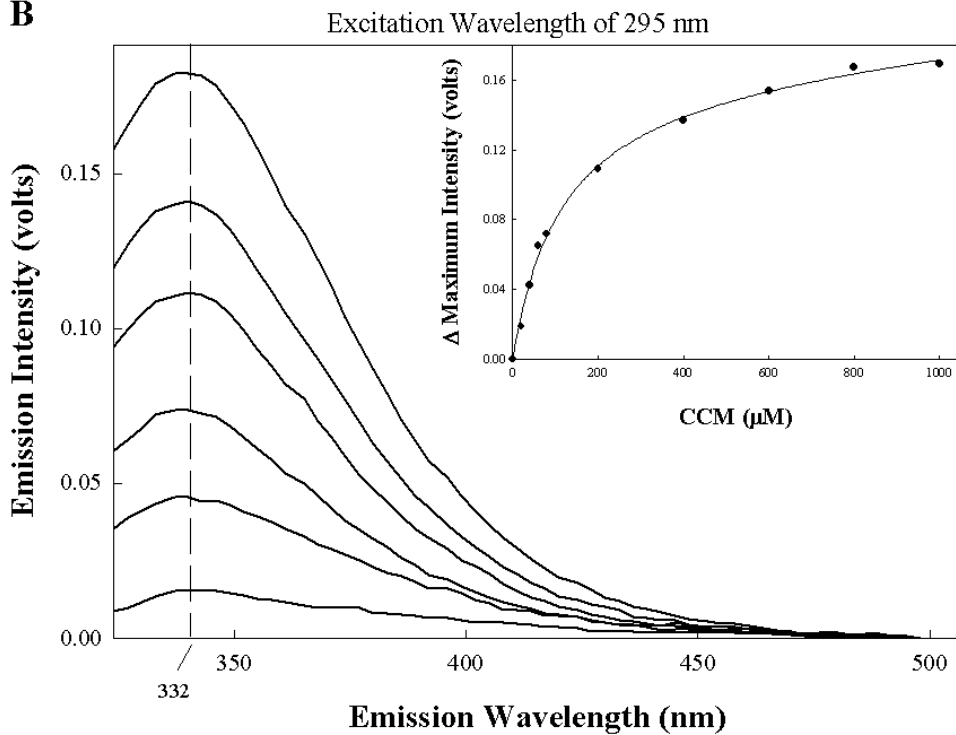
after it was expressed at high levels in *E. coli* with a hexahistidine tag. When induced, BenM-EBD-His comprised approximately 30% of the total cellular protein in *E. coli* BL21(DE3) cells (Fig. 3.2). BenM-EBD-His was purified using a nickel-chelating column. The protein eluted as a single peak with 100-150 mM imidazole (Fig. 3.2). Purified protein was estimated to be approximately 26,000 -Da by SDS-PAGE analysis and Coomassie-staining. This estimated size agreed with the computer predicted molecular mass for BenM-EBD-His of 26,372 -Da.

Effects of benzoate and CCM on the fluorescence emission spectra of BenM-EBD-His.

To demonstrate that BenM-EBD-His contains the functional effector-binding domain, the fluorescence emission spectra of purified BenM-EBD-His was monitored in the presence of benzoate and CCM. Like BenM-His, BenM-EBD-His has the single tryptophan residue at the distal C-terminal end of the protein allowing us to measure the fluorescence emission spectra of BenM-EBD-His, as done for BenM-His. Conditions for these studies of BenM-EBD-His were identical to those used to monitor full-length BenM-His protein.

In the absence of effectors, BenM-EBD-His gave an initial fluorescence spectrum with a maximum emission peak at 332 nm (top lines, Fig. 3.3A and 3.3B) similar to that of BenM-His. Likewise, the addition of benzoate up to 2 mM caused the maximum emission spectra of BenM-EBD-His to shift a total of 7 nm to 340 nm. The addition of 8 mM benzoate caused a decrease in intensity of almost 80%. The calculated dissociation

Fig. 3.3. The effect of benzoate and CCM on the fluorescence emission spectra of BenM-EBD-His. (A) The fluorescence emission spectra of BenM-EBD-His (from top to bottom) alone and in the presence of 200 μ M, 600 μ M, 2 mM, 4 mM, and 8 mM benzoate. Panel B shows the fluorescence emission spectra of BenM-EBD-His in the presence of (from top to bottom) 0, 40, 80, 200, 400, or 800 μ M CCM. The vertical lines indicate maximum emission intensity at 332 nm (dashed lines) and the shift to 340 nm (dotted lines) in the presence of benzoate. The inset graph in each panel shows the change in maximum fluorescence emission peak (at 337 nm for benzoate and 333 nm for CCM) plotted against the concentration of benzoate (A) or CCM (B).

A**B**

constant for the BenM-EBD-His-benzoate complex was approximately that of the BenM-His-benzoate complex (Table 3.1).

The change in the fluorescence emission spectra of BenM-EBD-His was similarly measured in the presence of increasing amounts of CCM. The titration of BenM-EBD-His with increasing amounts of CCM caused a steady decrease in the overall fluorescence spectra (Fig. 3.3B). As seen with BenM-His, there was no shift of the maximum emission peak at 332 nm (Fig. 3.1B). The dissociation constant determined for the BenM-EBD-His-CCM complex was almost half the K_d determined for the BenM-His-CCM complex (Table 3.1), suggesting that BenM-EBD-His has a higher affinity for CCM than BenM-His.

Combined effect of benzoate and CCM on the fluorescence emission spectra of BenM-His and BenM-EBD-His.

As noted previously, *in vitro* studies showed that the presence of both benzoate and CCM had a synergistic effect on BenM-mediated transcriptional activation (Bundy, et al., 2002). This observation suggested that BenM is capable of binding to both benzoate and CCM. However, the *in vitro* transcription assay did not reveal any information about possible binding sites. As described here, fluorescence spectroscopy was used to investigate whether binding of the two compounds was either cooperative or competitive. We titrated BenM-His and BenM-EBD-His with increasing amounts of CCM in the presence of 1 mM benzoate. This benzoate concentration was approximately equal to the K_d of both BenM-EBD-His and BenM-His for benzoate (Table 3.1). A decrease in the K_d for CCM in the presence of benzoate would suggest a cooperative

Fig. 3.4. Graphs showing the change in the maximum emission fluorescence for BenM-His (a) and BenM-EBD-His (b) versus the concentration of CCM (●) and the concentration of CCM in the presence of 1mM benzoate (■). The change in maximum fluorescence at 333 nm was used in plots for CCM only, and at 340 nm for CCM in the presence of benzoate.

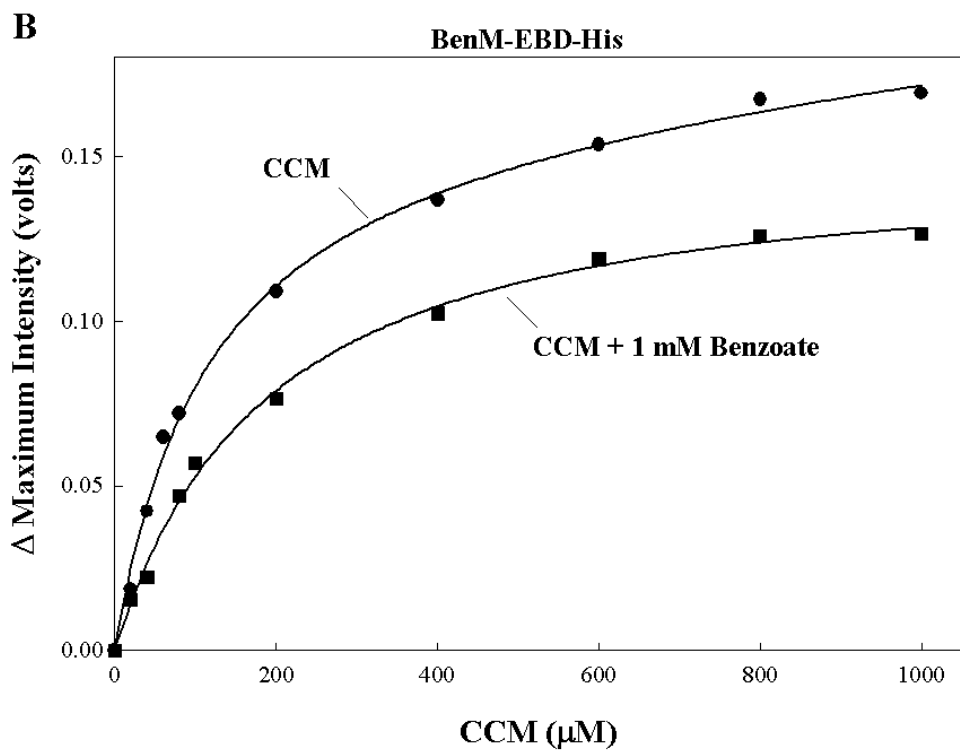
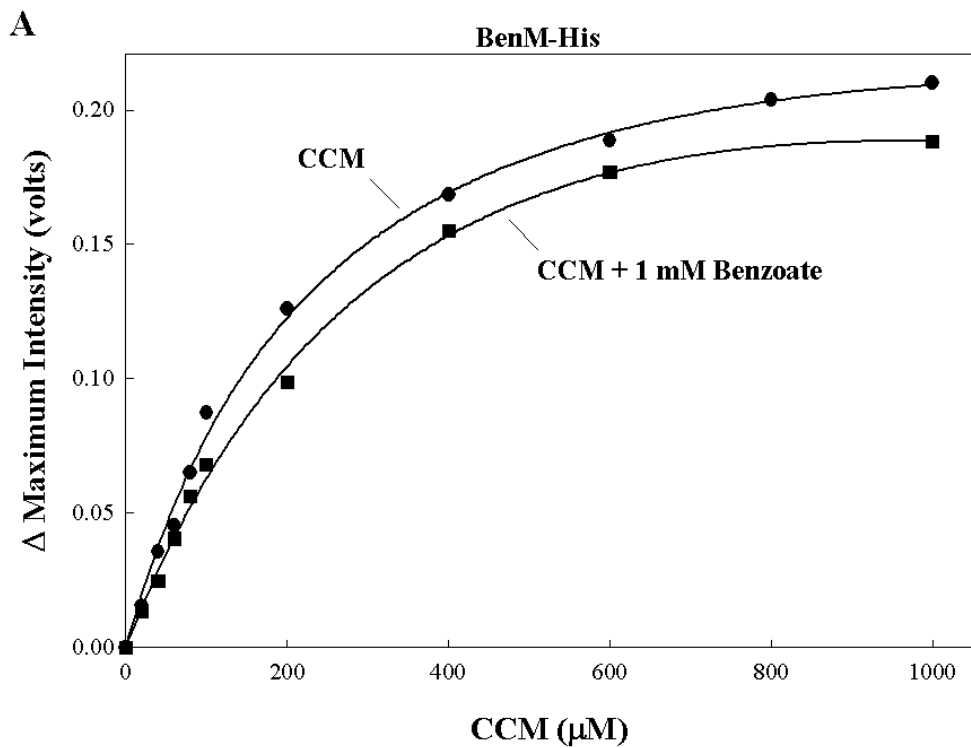


Table 3.1. Equilibrium binding constants for BenM-His and BenM-EBD

Effector Ligand	K_d (mM) ^a	
	BenM-His	BenM-EBD
Benzoate	1.2 ± 0.2	1.1 ± 0.1
CCM	0.28 ± 0.05	0.12 ± 0.02
CCM + 1 mM Benzoate	0.49 ± 0.09	0.20 ± 0.03
<i>m</i> -Chlorobenzoate	ND	0.31 ± 0.05

^a The values shown are the averages of at least three experiments. Standard deviations were no more than 20% of the values shown.

mechanism of binding for both effectors. In contrast, an increase in the K_d for CCM would suggest that the effectors were in competition for the same binding sites. With an excitation wavelength of 295 nm, changes in the fluorescence emission spectra of BenM-His or BenM-EBD-His were monitored following the addition of increasing amounts CCM in the presence or absence of benzoate. The change in the maximum emission intensity of each spectrum was plotted versus the concentration of CCM for each protein (Fig. 3.4A and 3.4B). Dissociation constants were determined for the BenM-His-CCM and BenM-EBD-His-CCM complexes in the presence of 1 mM benzoate (Table 3.1). These values were both roughly double their corresponding K_d values for CCM alone. This result indicated competition between benzoate and CCM for common binding sites within BenM.

Effect of benzoate derivatives on the fluorescence emission spectra of BenM-EBD-His.

We used fluorescence emission spectroscopy to monitor the effect of various benzoate derivatives on BenM-EBD-His in an attempt to gain insight into the chemical properties influencing effector-binding by BenM. Using an excitation wavelength of 280 nm, we measured the fluorescence spectrum of BenM-EBD-His in the presence of 1 mM amounts of *m*-chlorobenzoate, *o*-chlorobenzoate, *m*-toluate, isophthalate, or benzoate (Fig. 3.5). In contrast to the results with benzoate, none of the effector analogs caused a shift in the maximum fluorescence peak. *m*-chlorobenzoate and isophthalate caused an almost identical decrease in the overall emission spectrum of BenM-EBD-His. The size of the decrease was larger than that caused by an identical concentration of benzoate.

Fig. 3.5. The effect of various effector analogs on the fluorescence emission spectra of BenM-EBD-His. Using an excitation wavelength of 280 nm, the fluorescence emission spectra of BenM-EBD-His were measured in presence of 1 mM *o*-chlorobenzoate (●), 1 mM benzoate (■), 1 mM *m*-toluate (▲), 1 mM *m*-chlorobenzoate (+), and 1 mM isophthalate (○). The solid line is the fluorescence emission spectra of BenM-EBD-His alone.

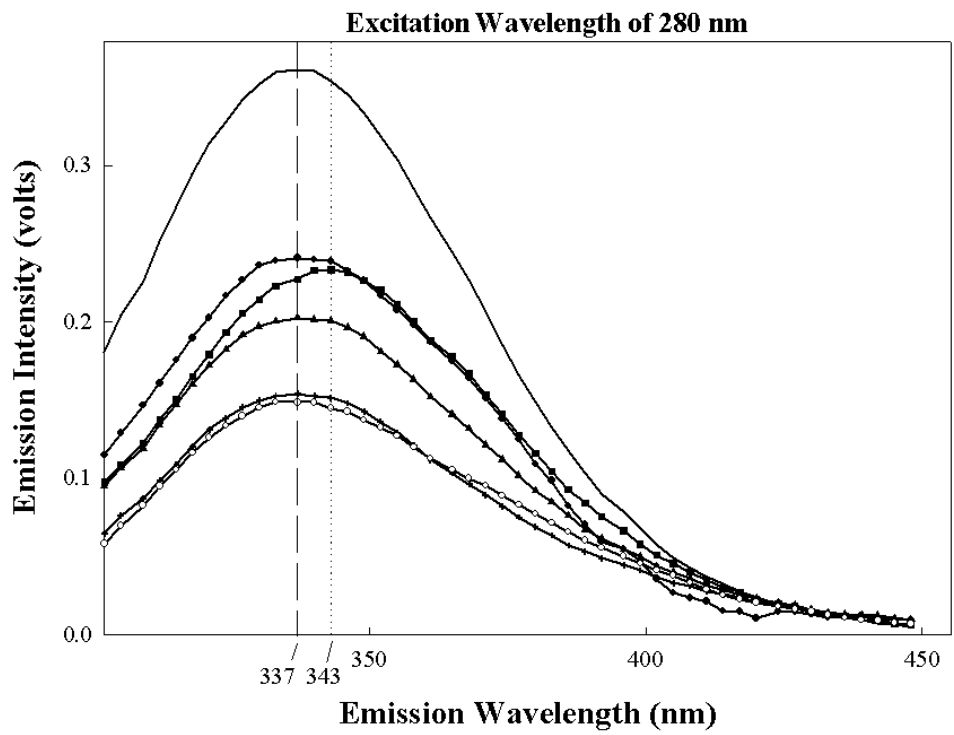
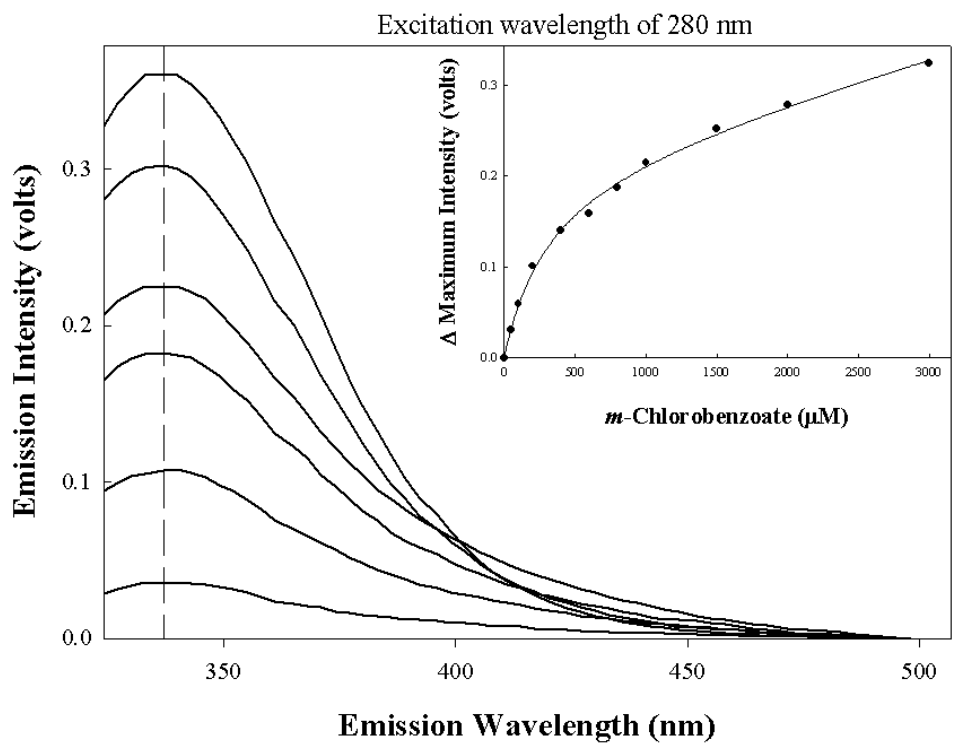


Fig. 3.6. The fluorescence emission spectra of BenM-EBD-His titrated with varying amounts of *m*-chlorobenzoate. The lines are, from top to bottom, the emission spectra of BenM-EBD-His only, in the presence 100 μM , 400 μM , 800 μM , 1.5 mM, and 3 mM *m*-chlorobenzoate. The inset graph shows the change in maximum fluorescence emission of BenM-EBD-His at 333 nm plotted against the concentration of *m*-chlorobenzoate.



Likewise, the addition of *m*-toluate caused a larger decrease in the BenM-EBD-His emission spectrum than benzoate. The presence of *o*-chlorobenzoate caused a decrease in the emission spectrum of BenM-EBD-His of comparable magnitude to that of benzoate.

These results suggested that BenM-EBD-His has a higher affinity for meta-substituted benzoate derivatives than benzoate. For direct comparison of the affinity of a meta-substituted benzoate derivative to that of benzoate, we determined the dissociation constant of BenM-EBD-His for *m*-chlorobenzoate (Fig. 3.6). The K_d for the BenM-EBD-His- *m*-chlorobenzoate complex was determined (Fig. 3.6 and Table 3.1) to be almost three times lower than the K_d for benzoate, suggesting that BenM-EBD-His has a higher affinity for *m*-chlorobenzoate than benzoate. The results imply that the chloro group at the meta position on *m*-chlorobenzoate (Fig. 3.6) provides some advantage for binding to BenM-EBD-His.

DISCUSSION

In this study we used fluorescence emission spectroscopy to analyze the equilibrium binding properties of BenM for various compounds including CCM and benzoate. Wild-type BenM contains a single tryptophan residue located at the absolute C-terminal end of the native protein. This residue directly precedes residues added as part of an artificial hexahistidine purification tag in BenM-His and BenM-EBD-His. Conformational changes in BenM altering the immediate environment of this tryptophan residue, such as those caused from the binding of a ligand, were detected by monitoring the fluorescence emission spectra between 330-350 nm. This wavelength range

corresponds to the fluorescence emissions by the indole group of tryptophan (Lakowicz, 1999).

Attempts to demonstrate BenM binding of benzoate or CCM using isothermal calorimetry (ITC) methods proved unsuccessful (data not shown). Failure to generate evidence of binding was attributed to BenM having a binding affinity for benzoate or CCM presumably below the detectable threshold of the ITC conditions. The dissociation constant values calculated for the BenM proteins complexed to CCM or benzoate (Table 3.1) are consistent with the binding of these molecules being 10- to 100-fold below the sensitivity of ITC measurements (Ladbury & Chowdhry, 1998).

The data suggest that BenM is capable of binding both benzoate and CCM at a common site, albeit with a greater affinity for CCM. CCM is toxic to the cell when accumulated to high levels (Gaines *et al.*, 1996). The high binding affinity of BenM for CCM may reflect the importance of detecting CCM levels in the cell. The high affinity for CCM may also reflect that BenM evolved from a progenitor with the primary function of detecting CCM.

In *Acinetobacter* sp. strain ADP1, BenM coordinates expression of the *ben* and *cat* genes in conjunction with the distinct LTTR CatM. CatM responds only to CCM and not benzoate (Bundy, et al., 2002). Yet, the two proteins are 59% identical and 75% similar in amino acid sequence (Collier, et al., 1998). The effector-binding region of BenM similarly shares from 30 to 60% sequence identity with comparable regions of CatM homologs (Collier, et al., 1998). Figure 3.7 shows a multiple sequence alignment of the putative effector-binding domains of several LTTRs that respond to CCM and halogenated CCM. With representatives from bacteria of several genera, this group of

Fig. 3.7. Multiple sequence alignment of the putative effector-binding domains of several LTTRs with homology to BenM. The alignment was generated with the CLUSTALX software using the default parameters (Thompson *et al.*, 1997). Regions of each protein relative to the DNA-binding domain of BenM were deleted. The proteins used in the alignment were (Genbank accession number): CbnR (Q9WXC7) from *Alcaligenes eutrophus* (Ogawa & Miyashita, 1999), TcbR (P27102) from *Pseudomonas* sp. strain P51 (van der Meer *et al.*, 1991), ClcR(Pp) (Q05840) from *Pseudomonas putida* (Coco *et al.*, 1993), TfdR (P10086) from *Alcaligenes eutrophus* (Kaphammer *et al.*, 1990), BenM (O68014) (Collier, *et al.*, 1998), CatM (P07774) from *Acinetobacter* sp. strain ADP1 (Romero-Arroyo *et al.*, 1995), CatR(Pp) (P20667) from *Pseudomonas putida* (Rothmel *et al.*, 1990), and CatR(AI) (O33945) from *Acinetobacter lwoffii* (Kim *et al.*, 1998). The asterisk (*) indicates the position of single, fully conserved residues. Conserved residues with a PAM250 matrix score >0.5, are designated with a colon (:). Conserved residues with a matrix score <=0.5 are designated with a period (.). Conserved and structurally related amino acid groups are denoted by the color scheme: Hydrophobic (A, V, F, M, I, L), blue; Polar (S, T, C, N, Q), green; Polar-Aromatic (H, Y, W), grey; Basic (D, E), purple; and Acidic (K, R), red. Glycine (orange) and proline (yellow) residues are colored individually. The numbers below the alignment correspond to the residue numbers of BenM.

```

      :: .      : :: : : * ::      : :      . * :: : *
CbnR  RSRAAARGDVGELSVAYFGTPIYRSLPLLLRAFLTSTPTATVSLTHMTKDEQVEGLLAGT
TcbR  RSRAAARGDVGELSVAYFGTPIYRSLPLLLRAFLTSTPTATVSLTHMTKDEQVEGLLAGT
ClcR (Pp) RSRAASRGEIGELRVAYFGTVVLHTLPLLLRQLLSVAPSATVSLTQMSKNRQIEALDAGT
TfdR  RSRAASRGEIGOLDIGYLGTAIYQTVPALHHAFTQAVPGATLSLALMPKVRQIEALRAGT
BenM  MTKRIAS-VEKTIRIGFVGSLLFGLLPRIIHLYRQAHPNLRIELYEMGTKAQTEALKEGR
CatM  MAKRIAT-VSQTLRIGYVSSLLYGLLPEIIYLFRCQNPEIHIELIECGTKDQINALKQGK
CatR (Pp) NTRRIGQGQRQWLGIGFAPSTLYKVLPELIRELRQDS-ELELGLNEMTTLQQVEALKSGR
CatR (Al) ATRRVGLHORSVLSIGFVASTLYGVLPTLMRKLROHAPELDIQMVELMSVQQIQAINTEGR
.....90.....100.....110.....120.....130.....

```

```

      * . . . * .      :      : *      :      : :: *
CbnR  IHVGFSRFFPRHPGIEIVNIAQEDLYLAVHRS--QSGKFGKTCKLADLRAVELTLFPRGG
TcbR  IHVGFSRFFPRHPGIEIVNIAQEDLYLAVHRS--QSGKFGKTCKLADLRAVELTLFPRGG
ClcR (Pp) IDIGFGRFYPYQEGVVVRNVINERLFLGAQKS--RARSFGEQVHCSALRNEPFILFPREG
TfdR  IHLGVGRFYPQEPGITVEHLHYERLYIAAGSS--IARQLRQDPTLLRLKSESLLVLPKEG
BenM  IDAGFGRLKISDPAIKRSLLRNERLMVAVHASHPLNQMKDKGVHLNDLIDEKILLYPSSP
CatM  IDLGFGRCLKITDPAIRRIVLHKEQLKLAHKKHHHLNQFAATGVHLSQIIDEPMILLYPVSQ
CatR (Pp) IDIAFGRRIRIDDPAIHQVLCEDPLVAVLPKDHPLA---SSPLTLAQLAGEAFILYPANP
CatR (Al) IDIGFGRVHHSDDPNVSSIVLHEERLAVALPMESPMARE-STPLPVHQLAGEKLIIVYPKEP
.....150.....160.....170.....180.....190.....

```

```

      :* :: : : :      :      : * : * . . . : * : :
CbnR  RPSFADEVIGLFKHAGIEPRIARVVEDATAALALTMAGAASSIVPASVVAIRWPDIAFAR
TcbR  RPSFADEVIGLFKHAGIEPRIARVVEDATAALALTMAGAASSIVPASVVAIRWPDIAFAR
ClcR (Pp) RPSFADEVIGVFKNARVEPKVVAIVEDVNAAMALALAGVVTIVPETVAMISWPDFGFTE
TfdR  RPSFADEVIALMRRAGVEPRVLAIVEDVNAALGLVAAAGAVTLVPASVVAIRPFVRTIME
BenM  KPNFSTHVMNIFSDHGLEPTKINEVREVQALGLVAAAGEGIVLVPASVVAIRPFVRTIME
CatM  KPNFATFIQSLFTELGLVPSKLTEIREIQALGLVAAAGEGVCIVPASAMDIGVKNLLYIP
CatR (Pp) RPSYADHVLALFAHHGMSIHVSQWANELQTAIGLVAVGVVTLVPASVQQHRTDIEYVS
CatR (Al) RPGFADQVLNILDRHDVQPGQVMEVREIQALGLVAAEFVGVIPASAR-QMRHDVHYRL
.....210.....220.....230.....240.....250.....

```

```

      : . . * :      :
CbnR  IVGTRVKVPISCFRKEKQPPILARFVEHVRRSAKD-----
TcbR  IVGTRVKVPISCTFRKEKQPPILARFVEHVRRSAKD-----
ClcR (Pp) LVGSKATVPVSCIYRHDHIAPILKTFLNLLPIRESQ-----
TfdR  MADASAKVPVSLTYLTDSDRVVLRFLDVARRGKQK-----
BenM  LLDPAITPIYIAVRNMEESTYIYSLYETIROIYAYEGFTEPPNW
CatM  ILDDAYSPISLAVRNMDHSNYIPKILACVQEVFATHHIRPLIE-
CatR (Pp) LLDSGAVSPIILSRKGDVSPIVQRCLTLIAQQAEE-----
CatR (Al) IDGDRATSPVIVSHRANDSSKYISLTKOLIREMYAEHPAWLDTHN
.....270.....280.....290.....300.....

```

proteins comprises a separate subfamily of LTTRs (Schell, 1993). The high degree of sequence identity between BenM and these proteins strongly suggests a common evolutionary lineage (see phylogenetic tree chapter 1). It seems likely that the effector-binding site of BenM primarily bound CCM and latter evolved to gain the ability to bind benzoate. Consistent with this idea, the putative effector-binding regions of NahR, a well-characterized LTTR from *Pseudomonas putida* that responds to the benzoate analog 2-hydroxybenzoate, and SalR, a NahR homolog in *Acinetobacter*, are only approximately 19% identical to that of BenM (Cebolla *et al.*, 1997; Jones *et al.*, 2000).

BenM may have evolved to modulate its CCM-mediated response by gaining the ability to bind benzoate. The fluorescence spectroscopy results with benzoate support the notion that the interactions between BenM and benzoate are different than those with CCM. The presence of benzoate caused a spectral shift in the wavelength of maximal emission intensity of BenM-His indicative of a conformational change affecting the C-terminal portion of the protein. This change, which was not detected by the addition of CCM, could reflect the differences between the chemical structures of CCM and benzoate. It seems likely that the common binding site shared by CCM and benzoate interacts with the carboxyl groups of both effectors. If this is the case, then the aromatic ring of benzoate could sterically hinder interactions within the binding pocket of BenM. The result might be the biological equivalent of a square peg in a round hole. The linearity of CCM might allow the molecule to be flexible within the binding pocket resulting in tighter binding and minimal conformational changes.

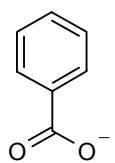
The data obtained with the various benzoate derivatives may refute the idea that the bulky aromatic ring of benzoate is the chief cause of the conformational change. The

meta and ortho substituted benzoate derivatives all failed to cause a shift in the emission spectra of BenM-EBD-His. The reasons for this are unclear. It could be that the substitutions at the meta or ortho positions of benzoate increase van der Waals interactions between the compound and the adjacent residues of the binding pocket. This may allow the meta-substituted compounds to slip into the binding pocket with a tighter affinity in a similar fashion to CCM (Fig. 3.8). It is not known whether any of these compounds are capable of acting as effectors or antagonists for BenM.

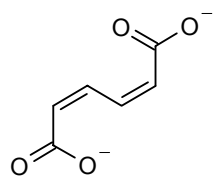
A model for BenM-mediated transcriptional activation has been previously suggested (Bundy, et al., 2002). Based in part on the results of Dnase I footprinting studies, the model shows that the *benA* promoter region contains three BenM-binding sites (Sites 1, 2, and 3). BenM, a tetramer in solution, is capable of binding two of these three sites at a time. Presumably one dimer binds to a single site. In the absence of effectors, BenM preferentially occupies sites 1 and 3 and represses *benA* transcription by blocking access of RNA polymerase to the promoter. In the presence of effectors, BenM binds to sites 1 and 2 and recruits RNA polymerase to the *benA* promoter region. BenM, like other LTTRs, most likely establishes contacts with the C-terminal domain of the α -subunit of RNA polymerase, resulting in transcriptional activation (Ishihama, 1993). The binding and release of effectors by BenM is presumed to establish an equilibrium between the activated state (BenM complexed to sites 1 and 2) and the repressed state (BenM bound to sites 1 and 3). Previous, in vitro transcription studies showed that maximal BenM-His-mediated transcriptional activation occurred with equimolar amounts of benzoate and CCM (Bundy, et al., 2002). It was suggested that the simultaneous binding of both benzoate and CCM was more effective in locking BenM into an activated

Fig. 3.8. Diagram (a) showing the chemical structures of benzoate, CCM, and various chemical analogs. (b) A diagram showing CCM overlain on top of benzoate, *m*-chlorobenzoate, and isophthalate to demonstrate the similar positioning of the functional groups.

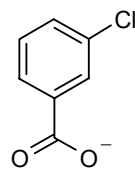
A



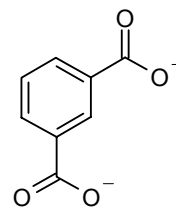
benzoate



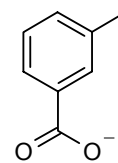
CCM



***m*-chlorobenzoate**

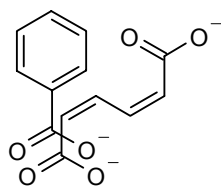


isophthalate

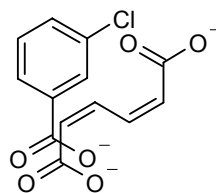


***m*-toluate**

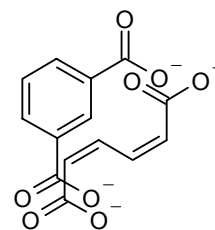
B



**benzoate
and CCM**



***m*-chlorobenzoate
and CCM**



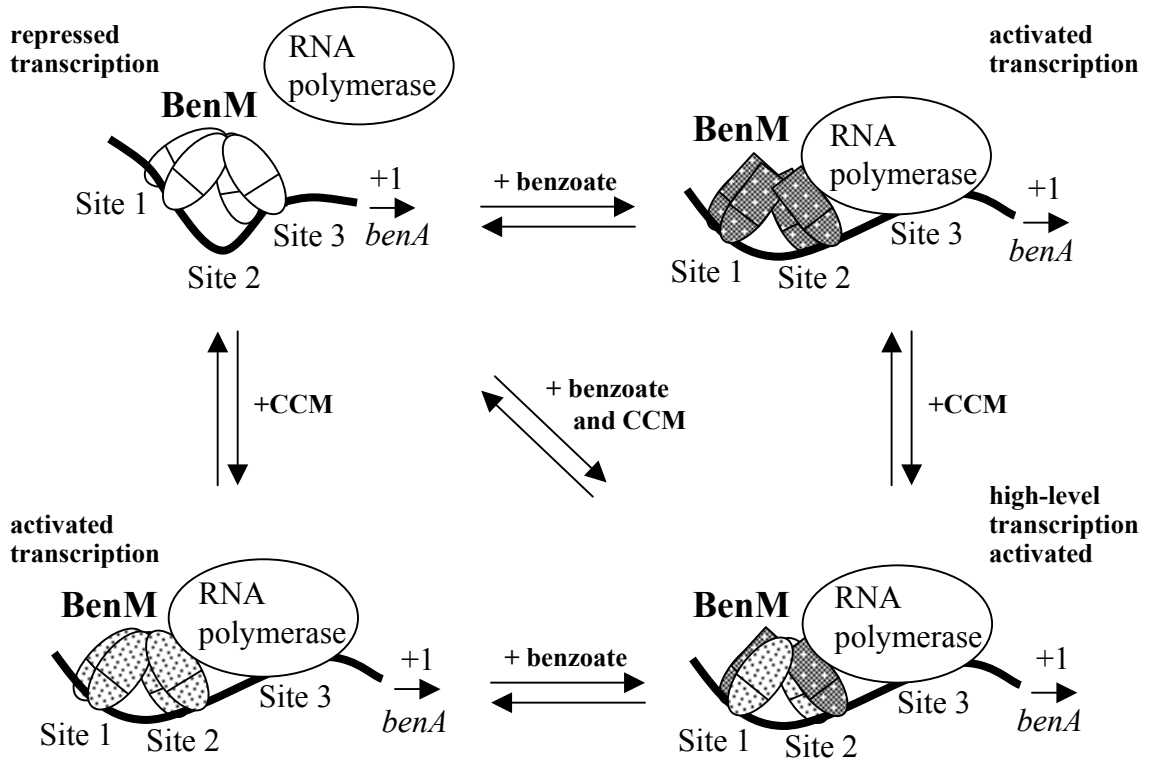
**Isophthalate
and CCM**

conformation than was the binding of either compound alone. The previous model did not suggest how this might occur.

The studies here show that benzoate and CCM compete for a common binding site and that benzoate binding causes a conformational change in BenM that is different from that with CCM. Our fluorescence spectroscopy results rule out a cooperative binding mechanism for benzoate and CCM. Instead, the data suggest that the highest level of transcriptional activation may be accomplished when BenM binds equal amounts of CCM and benzoate. Thus, we predict that the highest level of transcriptional activation occurs only with a BenM tetramer comprised of two monomers bound to CCM and two bound to benzoate. Consistent with this prediction, the previous model was revised and is shown in Figure 3.9.

This model depicts BenM activating transcription in response to either CCM or benzoate alone. However, the conformation of the BenM tetramer in each of the three active states is slightly different, as suggested by the fluorescence spectroscopy studies. The conformation of the BenM tetramer bound simultaneously with benzoate and CCM, in comparison to either alone, could result in interactions between BenM and DNA and/or BenM and RNA polymerase that are more effective for transcriptional activation. It is possible that the equilibrium between the repressed and activated states is shifted strongly to the active state under these dual effector-binding conditions. However, attempts to measure the kinetics of effector-binding to BenM were unsuccessful. A fast reaction appeared to occur during the 2 milliseconds "deadtime" of the stop-flow apparatus that prevented the determination of the kinetic binding constants (Clark & Phillips, 2002). Nevertheless, our results suggest that conformational changes associated

Fig. 3.9. Model of BenM-mediated regulation at *benA*, modified from (Bundy, et al., 2002). The model shows benzoate-bound BenM monomers after undergoing a conformational change in the C-terminal region of the protein (depicted as shaded gray bullet shapes). CCM-bound BenM monomers are shown as speckled ovals to indicate minimal conformational changes in the protein, in comparison to the changes detected with benzoate by fluorescence studies. In the presence of both effectors, one monomer of each BenM dimer is shown bound with either CCM or benzoate. Although depicted in this way, alternatively each dimer of BenM could be fully bound with benzoate or CCM.



with a BenM tetramer bound to equimolar amounts of benzoate and CCM underly the synergistic effect of both compounds on transcription.

REFERENCES

Bradford, M. M. (1976). A rapid and sensitive method for the quantitation of microgram quantities of protein utilizing the principle of protein-dye binding. *Anal. Biochem.* **72**, 248-254.

Bundy, B. M. (2001). Transcriptional regulation of the *benABCDE* operon of *Acinetobacter* sp. Strain ADP1: BenM-mediated synergistic induction in response to benzoate and *cis,cis*-muconate. Ph.D. Thesis. In *Department of Microbiology*. Athens, GA: University of Georgia.

Bundy, B. M., Collier, L. S., Hoover, T. A. & Neidle, E. L. (2002). Synergistic transcriptional activation by one regulatory protein in response to two metabolites. *Proc. Natl. Acad. Sci.* **99**, 7693-7698.

Cebolla, A., Sousa, C. & de Lorenzo, V. (1997). Effector specificity mutants of the transcriptional activator NahR of naphthalene degrading *Pseudomonas* define protein sites involved in binding of aromatic inducers. *J. Biol. Chem.* **272**, 3986-3992.

Choi, H., Kim, S., Mukhopadhyay, P., Cho, S., Woo, J., Storz, G. & Ryu, S. (2001). Structural basis of the redox switch in the OxyR transcription factor. *Cell* **105**, 103-113.

Clark, T. J. & Phillips, R. S. (2002). Unpublished data.

Coco, W. M., Rothmel, R. K., Henikoff, S. & Chakrabarty, A. M. (1993). Nucleotide sequence and initial functional characterization of the *clcR* gene encoding a LysR family activator of the *clcABD* chlorocatechol operon in *Pseudomonas putida*. *J. Bacteriol.* **175**, 417-427.

- Collier, L. S., Gaines, G. L., III & Neidle, E. L. (1998).** Regulation of benzoate degradation in *Acinetobacter* sp. strain ADP1 by BenM, a LysR-type transcriptional activator. *J. Bacteriol.* **180**, 2493-2501.
- Freifelder, D. (1982).** *Physical biochemistry: applications to biochemistry and molecular biology*, second edn. New York, NY, USA: W. H. Freeman and company.
- Gaines, G. L., III, Smith, L. & Neidle, E. L. (1996).** Novel nuclear magnetic resonance spectroscopy methods demonstrate preferential carbon source utilization by *Acinetobacter calcoaceticus*. *J. Bacteriol.* **178**, 6833-6841.
- Ishihama, A. (1993).** Protein-protein communication within the transcriptional apparatus. *J. Bacteriol.* **175**, 2483-2489.
- Jones, R. M., Pagmantidis, V. & Williams, P. A. (2000).** *sal* Genes determining the catabolism of salicylate esters are part of a supraoperonic cluster of catabolic genes in *Acinetobacter* sp. Strain ADP1. *J. Bacteriol.* **182**, 2018-2025.
- Jorgenson, C. & Dandanell, G. (1999).** Isolation and characterization of mutations in the *Escherichia coli* regulatory protein XapR. *J. Bacteriol.* **181**, 4397-4403.
- Kaphammer, B., Kukor, J. J. & Olsen, R. H. (1990).** Regulation of *tfdCDEF* by *tfdR* of the 2,4-dichlorophenoxyacetic acid degradation plasmid pJP4. *J. Bacteriol.* **172**, 2280-2286.
- Kim, S. I., Leem, S.-H., Choi, J.-S. & Ha, K.-S. (1998).** Organization and transcriptional characterization of the *catI* gene cluster in *Acinetobacter lwoffii* K24. *Biochem. Biophys. Res. Commun.* **243**, 289-294.

Kullik, I., Toledano, M. B., Tartaglia, L. A. & Storz, G. (1995). Mutational analysis of the redox-sensitive transcriptional regulator OxyR: regions important for oxidation and transcriptional activation. *J. Bacteriol.* **177**, 1275-1284.

Ladbury, J. E. & Chowdhry, B. Z. (1998). *Biocalorimetry: applications of calorimetry in the biological sciences*. West Sussex, England, UK: Wiley.

Lakowicz, J. R. (1999). *Principles of fluorescence spectroscopy*, second edn. New York, NY, USA: Kluwer Academic.

Lochowska, A., Iwanicka-Nowicka, R., Plochocka, D. & Hryniewicz, M. M. (2001). Functional dissection of the LysR-type CysB transcriptional regulator. *J. Biol. Chem.* **276**, 2098-2107.

Lynch, A. S., Tyrrell, R., Smerdon, S. J., Briggs, G. S. & Wilkinson, A. J. (1994). Characterization of the CysB protein of *Klebsiella aerogenes*: direct evidence that *N*-acetylserine rather than *O*-acetylserine serves as the inducer of the cysteine regulon. *Biochem. J.* **299**, 129-136.

Matheson, I. B. C. (1990). A critical comparison of least absolute deviation fitting (robust) and least-squares fitting - the importance of error distribution. *Comput. Chem.* **14**, 49-57.

Ogawa, N. & Miyashita, K. (1999). The chlorocatechol-catabolic transposon Tn5707 of *Alcaligenes eutrophus* NH9, carrying a gene cluster highly homologous to that in the 1,2,4-trichlorobenzene-degrading bacterium *Pseudomonas* sp. Strain P51, confers the ability to grow on 3-chlorobenzoate. *Appl. Environ. Microbiol.* **65**, 724-731.

- Perez-Rueda, E. & Collado-Vides, J. (2001).** Common history at the origin of the position-function correlation in transcriptional regulators in archea and bacteria. *J. Mol. Evol.* **53**, 172-9.
- Romero-Arroyo, C. E., Schell, M. A., Gaines III, G. L. & Neidle, E. L. (1995).** *catM* encodes a LysR-type transcriptional activator regulating catechol degradation in *Acinetobacter calcoaceticus*. *J. Bacteriol.* **177**, 5891-5898.
- Rothmel, R. K., Aldrich, T. L., Houghton, J. E., Coco, W. M., Ornston, L. N. & Chakrabarty, A. M. (1990).** Nucleotide sequencing and characterization of *Pseudomonas putida catR*: a positive regulator of the *catBC* operon is a member of the LysR family. *J. Bacteriol.* **172**, 922-931.
- Sambrook, J., Fritsch, E. F. & Maniatis, T. (1989).** *Molecular cloning: a laboratory manual, 2nd ed.* Cold Spring Harbor, N. Y.: Cold Spring Harbor Laboratory Press.
- Schell, M. A. (1993).** Molecular biology of the LysR family of transcriptional regulators. *Annu. Rev. Microbiol.* **47**, 597-626.
- Thompson, J. D., Gibson, T. J., Plewniak, F., Jeanmougin, F. & Higgins, D. G. (1997).** The CLUSTAL_X windows interface: flexible strategies for multiple sequence alignment aided by quality analysis tools. *Nucleic Acids Res* **25**, 4876-4882.
- Tyrrell, R., Verschueren, K. H. G., Dobson, E. J., Murshudov, G. N., Abby, C. & Wilkinson, A. J. (1997).** The structure of the cofactor-binding fragment of the LysR family member, CysB: a familiar fold with a surprising subunit arrangement. *Structure* **5**, 1017-1032.
- van der Meer, J. R., Frijters, A. C. J., Leveau, J. H. J., Eggen, R. I. L., Zehnder, A. J. B. & de Vos, W. M. (1991).** Characterization of the *Pseudomonas* sp. Strain P51 gene

tcbR, a LysR-type transcriptional activator of the *tcbCDEF* chlorocatechol oxidative operon, and analysis of the regulatory region. *J. Bacteriol.* **173**, 3700-3708.

CHAPTER 4

CRYSTALLIZATION AND STRUCTURAL DETERMINATION OF THE EFFECTOR-BINDING DOMAIN OF BENM

¹Clark, T. J., E. L. Neidle, and C. Momany. 2002. To be submitted to
Acta. Cryst.

ABSTRACT

The BenM regulator can activate gene expression in response to benzoate, *cis,cis*-muconate, or both compounds. Fluorescence studies described in this dissertation indicated that each compound binds to the same site in BenM. However, the fluorescence investigations suggested that the structural conformation of BenM was different when bound to benzoate compared to *cis,cis*-muconate. In an effort to characterize these structural differences, we have crystallized the effector-binding domain of BenM (BenM-EBD-His) and a selenomethionyl derivative of this protein. Using synchrotron generated X-rays, in collaboration with Dr. Cory Momany, we were able to generate a high-resolution diffraction pattern. From these data, we were able to determine the structure of the BenM effector-binding domain to a resolution of 2.0 Å. This study represents the first successful structural characterization of a protein from the subclass of LysR-type regulators that responds to *cis,cis*-muconate. This regulatory subclass plays a major role in the bacterial degradation of environmental aromatic compounds that arise from natural sources and from industrial pollution.

INTRODUCTION

Tryptophan fluorescence studies described in chapter 3 of this dissertation were initiated to investigate the biochemical mechanisms controlling BenM-mediated synergistic transcriptional activation. These studies demonstrated that BenM binds to both *cis,cis*-muconate (CCM) and benzoate at a common binding site in the protein. Of particular significance was the observation that interactions between BenM and benzoate were different than those with CCM. The presence of benzoate caused BenM to undergo a conformational change affecting the C-terminal region of protein. Such a change was not evident with the addition of CCM. In an effort to test a regulatory model based on these observations, we have undertaken crystallographic studies aimed at solving the structure of the effector-binding domain of BenM (BenM-EBD-His).

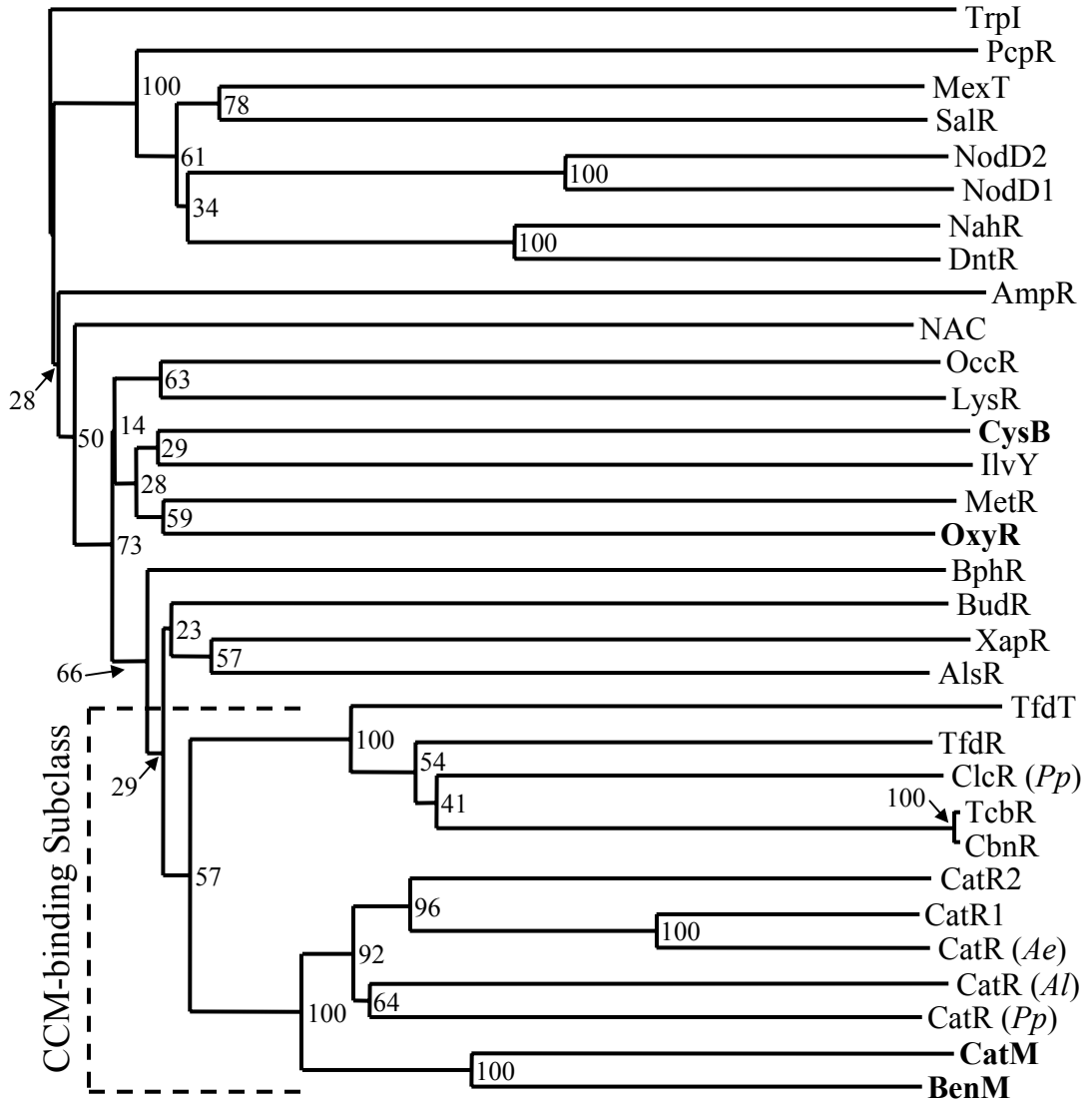
BenM belongs to an important subclass of the LysR-type family of transcriptional regulators (LTTRs) that activate genes necessary for the degradation of aromatic compounds in response to CCM or halogenated derivatives of CCM. As shown by phylogenetic analysis (Fig. 4.1), members of this subclass include proteins that regulate pathways used to degrade many chlorinated-aromatic pollutants such as TfdR (Kaphammer *et al.*, 1990), ClcR (Coco *et al.*, 1993), TcbR (van der Meer *et al.*, 1991), and CbnR (Ogawa & Miyashita, 1999). At present, no structural data are available describing any of these closely related proteins.

The structural determination of a complete LTTR has yet to be accomplished. LTTRs tend to have limited solubility that make these proteins difficult to purify and characterize (Verschueren *et al.*, 2001). This insolubility may be due to the flexible and hydrophobic nature of the N-terminal protein domain (residues 1-66) that is involved in

Fig. 4.1. Unrooted phylogenetic tree based on the amino acid sequences of the putative effector-binding domains of several LTTRs. The bootstrap values were calculated using the CLUSTALX software (Thompson *et al.*, 1997). The tree was constructed using the NJplot software (Perriere & Gouy, 1996). Bootstrap values are shown for each node out of 100 bootstrap resamplings (values below 50 are shown, but not significant). The scale bar represents the evolutionary distance between the proteins at 0.05 substitutions per residue position. The putative effector-binding domain of each protein was determined by aligning the full-length protein sequences with BenM using the CLUSTALX software (data not shown). Regions of each protein corresponding to the DNA-binding domain of BenM were deleted. The proteins used in the tree are listed along with the appropriate Genbank accession numbers (top to bottom): TrpI (P11720) from *Pseudomonas aeruginosa* (Chang *et al.*, 1989), PcpR (P52679) from *Flavobacterium* sp. strain ATCC 39723 (Orser & Lange, 1994), MexT (O87785) from *Pseudomonas aeruginosa* (Kohler *et al.*, 1999), SalR (Q9RBI3) from *Acinetobacter* sp. strain ADP1 (Jones *et al.*, 2000), NodD2 (P12233) from *Bradyrhizobium japonicum* (Applebaum *et al.*, 1988), NodD1 (P12232) from *Bradyrhizobium japonicum* (Applebaum, *et al.*, 1988), NahR (P10183) from *Pseudomonas putida* (You *et al.*, 1988), DntR (Q8VUD7) from *Burkholderia cepacia* (Johnson *et al.*, 2000), AmpR (P12529) from *Citrobacter freundii* (Lindquist *et al.*, 1989), NAC (Q08597) from *Klebsiella aerogenes* (Schwacha & Bender, 1993), OccR (Q00679) from *Agrobacterium tumefaciens* (Habeeb *et al.*, 1991), LysR (P03030) from *Escherichia coli* (Stragier & Patte, 1983), CysB (P45600) from *Klebsiella aerogenes* (Lynch *et al.*, 1994), IlvY (P05827) from *Escherichia coli* (Wek & Hatfield, 1986), MetR (P19797) from *Escherichia coli* (Maxon *et al.*, 1989), OxyR (P11721) from *Escherichia*

coli (Christman *et al.*, 1989), BphR (Q9L4R4) from *Alcaligenes eutrophus* (Mouz *et al.*, 1999), BudR (P52666) from *Klebsiella terrigena* (Mayer *et al.*, 1995), XapR (P23841) from *Escherichia coli* (Seeger *et al.*, 1995), AlsR (Q04778) from *Bacillus subtilis* (Renna *et al.*, 1993), TfdT (P42427) from *Alcaligenes eutrophus* (Leveau & van der Meer, 1996), TfdR (P10086) from *Alcaligenes eutrophus* (Matrubutham & Harker, 1994), ClcR (Q05840) from *Pseudomonas putida* (Coco, *et al.*, 1993), TcbR (P27102) from *Pseudomonas* sp. strain P51 (van der Meer, *et al.*, 1991), CbnR (Q9WXC7) from *Alcaligenes eutrophus* (Ogawa and Miyashita, 1999), CatR2 (AB035325) from *Burkholderia* sp strain TH2 (Suzuki *et al.*, 2002), CatR1 (AB035483) from *Burkholderia* sp strain TH2 (Suzuki, *et al.*, 2002), CatR (*Ae*) (Q9EV43) from *Alcaligenes eutrophus* (Hinner *et al.*, 1998), CatR (*Al*) (O33945) from *Acinetobacter lwolfii* (Kim *et al.*, 1998), CatR (*Pp*) (P20667) from *Pseudomonas putida* (Rothmel *et al.*, 1990), CatM (P07774) from *Acinetobacter* sp. strain ADP1 (Romero-Arroyo *et al.*, 1995), BenM (O68014) from *Acinetobacter* sp. strain ADP1 (Collier *et al.*, 1998). CysB, OxyR, CatM, and BenM are indicated in bold.

Effector-Binding Domain



DNA recognition and binding (Schell, 1993). Removal of the DNA binding domain of two LTTRs distantly related to BenM allowed their effector-binding domain structures to be solved. The dimeric structures of truncated versions of CysB (residues 88-324), which regulates cysteine biosynthesis in *Klebsiella aerogenes*, and OxyR (residues 80-305) a regulator of oxidative stress response in *Escherichia coli*, have been determined at 1.8 Å and 2.3 Å, respectively (Choi *et al.*, 2001; Tyrrell *et al.*, 1997). As shown in the primary sequence alignment (Fig. 4.2), the residues corresponding to the effector-binding domains of CysB and OxyR show relatively little similarity with the corresponding regions of BenM and its homolog CatM. Dissimilarity in the effector-binding domains may not be surprising considering that CysB and OxyR recognize the effectors N-acetylserine and hydrogen peroxide, respectively. These effectors are structurally dissimilar from CCM and benzoate.

We describe here the results of crystallization and diffraction experiments done with Dr. Cory Momany, concluding with the successful solution of the BenM-EBD-His crystal structure. The crystal structure presented here has been refined to a resolution of 2.0 Å, and is approximately 98% complete. Although this protein structure was determined in the absence of effectors, current structural investigations are aimed at determining the conformational changes that result from binding CCM, benzoate, and both effectors.

Fig. 4.2. Multiple sequence alignment of the full-length sequence of BenM, CatM, CysB, and OxyR. The alignment was generated with the CLUSTALX software using the default parameters (Thompson, et al., 1997). The Genbank accession numbers and references for the protein sequences used to generate the alignment are listed in the figure legend of Fig 4.2. The characters above the alignments designate the position of strongly conserved positions based on the Gonnet PAM250 scoring matrix used to estimate the evolutionary conservation between proteins (Gonnet *et al.*, 1992). The asterisk (*) indicates the position of single, fully conserved residues. Conserved residues with a PAM250 matrix score >0.5, are designated with a colon (:). Conserved residues with a matrix score <=0.5 are designated with a period (.). Conserved and structurally related amino acid groups are denoted by the color scheme: Hydrophobic (A, V, F, M, I, L), blue; Polar (S, T, C, N, Q), green; Polar-Aromatic (H, Y, W), gray; Basic (D, E), purple; and Acidic (K, R), red. Glycine (orange) and proline (yellow) residues are colored individually. The boxed region denotes residues that comprise the putative helix-turn-helix DNA-binding motif. The black arrows indicate the position of the N-terminal residues of BenM-EBD-His and the OxyR regulatory domain proteins. The N-terminal residue of CysB(88-324) is a histidine residue located 5 amino acids away from the arrows. The black underlined residues correspond to regions of CysB necessary for effector binding (Lochowska *et al.*, 2001; Tyrrell, et al., 1997). The residues circled in purple denote the cysteine residues that form the active site disulfide bond of OxyR (Kullik *et al.*, 1995). The residues outlined by the red boxes indicate residues corresponding to effector-binding mutants of CatM. The numbers below the alignment correspond to the residue numbers of BenM.

```

*:::.*:* *::: . : * : * * : * : * : * : * : *
BenM MELRHLRYFVAVVEE-QSFTKAADKLCIAQPPLSRQIQNLEEFELGIQLLER-GSRPVKTT
CatM MELRHLRYFVTVVEE-QSISKAAEKLCIAQPPLSRQIQKLEEFELGIQLFER-GFRPAKVT
OxyR MNIRDLEYLVALAEH-RHFRAADSCHVSQPTLSGQIRKLEDELGVMLLER-TSRKVLFT
CysB MKLQQLRYIVEVNVHNLNVSSTAEGLYTSQPGISKQVRMLEDELGIQIFARSGKHLTQVT
1.....10.....19.....29.....39.....49.....59

```

```

* : * : * .. ↓ : : . . . : : : : : * * : * : *
BenM PEGHFFYQYAIKLLSNVDQMVSMITKR-IASVEKTIIRIGFVGSLLFGLLPRIIHLYRQAHF
CatM EAGMFFYQHAVQILITHAQASSMAKR-IATVSQTLRIGYVSSLLYGLLPEIYLFROQNP
OxyR QAGMLLVDQARTVLREVKVLKEMASQQGETMSGPLHIGLIPTVGPYLLPHIIPMLHQTFP
CysB PAGQEIIRIAREVLSKVDAIKSVAGEHTWDPKGSLYVATTHTQARYALPGVIKGFIERYP
.....68.....78.↑.....87.....97.....107.....117

```

```

. : : : . . : * . * : : . . : : *
BenM NLRIELYEMGTKAQTEALKEGRIDAGFGRKISD-PAIKRSLRNERLMVAVHASHPLNQ
CatM EIHIELIECGTKDQINALKQKIDLGFGRLKITD-PAIRRIVLHKEQLKLAIHKHHHLNQ
OxyR KLEMYLHEAQTHOLLAQLDSGKLD CVILALVKES-EAFIEVPLFDEPMLLAIYEDHPWAN
CysB RVSLMHMQGSPQTQIAEAVSKGNADFAIATEALHLYDDL VMLPCYHWNRSIVVTPEHPLAT
.....127.....137.....147.....156.....166.....176

```

```

* : : : : . : * : *
BenM MKDKGVHLNDLIDKILLYPS SPKPNFSTHVMNIFSDHGLEPTKINEVREVQALGLVAA
CatM FAATGVHLSQIIDEPMLLYPVSQKPNFATFIQSLFTELGLVPSKLTEIREIQALGLVAA
OxyR R--ECVPMADLAGEKLLMLEDG--HCLRDAQMGFCFEAGADETHFRATSLETLRNMVAA
CysB KG--SVSIEELAQYPLVITYTFG--FTGRSELDIAFNRAGLTPRIVFTATDADVIKTYVRL
.....186.....196.....206.....216.....226.....236

```

```

* * : : : : : : : *
BenM GEGISLVPASTQSIQLFN--LSYVPLLDPDAITPIYIAVRNMEEST-----Y
CatM GEGVCIVPASAMDIGVKN--LLYIPILDDAYSPISLAVRNMDHSN-----Y
OxyR GSGITLLPALAVPPERKRDGVVYLPCIKPEPRRTIGLVYRPGSPLR-----S
CysB GLGVGVIASMAVDPVSDPD-LVKLDANGIFSHSTTKIGFRRSIFLRSYMYDFIQRFAPHL
.....246.....255.....264.....274.....281

```

```

. : :
BenM IYSLYETIRQIYAYEGFTEPPNW-----
CatM IPKILACVQEVFATHHIRPLIE-----
OxyR RYEQLAEAIRARMDGHFDKVLKQAV---
CysB TRDVVDIAVALRSNEDIAMFKDIKLPEK
.....291.....301.....

```

METHODS

Purification of BenM-EBD-His

BenM-EBD-His was purified as described (Chapter 3, Methods). Fractions containing purified BenM-EBD-His were pooled and dialyzed (twice) for 4 h at 4 °C in 1.0 l of buffer (20 mM Tris-HCl, pH 7.9, 500 mM NaCl, and 10% [v/v] glycerol) using 10,000 Da molecular weight cut-off snakeskin dialysis tubing (Pierce). Protein for crystallization trials was concentrated using an Ultrafree S-10 centrifuge concentrator (Millipore) and stored at 4 °C.

Expression and purification of a selenomethionyl BenM-EBD-His derivative

BenM-EBD-His was expressed from plasmid pBAC435 (Methods, Chapter 3) in the methionine auxotrophic strain *E. coli* 834(DE3) in the presence of selenomethionine. Media and growth conditions for protein expression were as previously described (Ramakrishnan *et al.*, 1993). Protein expression was induced with the addition of 0.2 mM isopropyl- β -D-thiogalactoside (IPTG). Selenomethionyl BenM-EBD-His was purified, dialyzed, and concentrated using identical methods as described for BenM-EBD-His. To prevent oxidation of the selenium during final storage, 0.5 mM tricarboxyethyl phosphine (TCEP) was added to the final selenomethionyl BenM-EBD-His solution. Purified protein was stored at 4 °C.

Gel Filtration analysis

The molecular weight of BenM-EBD-His was determined using a HiPrep sephacryl S-200 gel filtration column (26 X 60 cm) (Amersham-Pharmacia) equilibrated

with 3 column volumes of 20 mM Tris-HCl, pH 7.9 containing 500 mM NaCl and 10% [v/v] glycerol at 25 °C. Purified BenM-EBD-His (0.5 ml at 1 mg/ml) was eluted from the column at a flow rate of 1 ml/min. The following proteins from the Molecular Weight-Gel Filtration-200 kit (Sigma) were used as standards: cytochrome C, 12.4 -kDa; carbonic anhydrase, 29 -kDa; bovine serum albumin, 66 -kDa; alcohol dehydrogenase, 150 -kDa; and β -amylase, 200 -kDa. The data were plotted and fitted using the Sigmaplot 2000 software (SPSS Inc.).

Analysis of selenomethionyl BenM-EBD-His by Liquid Chromatography Mass Spectrometry (LC-MS)

Molecular mass determinations of BenM-EBD-His and selenomethionyl BenM-EBD-His were performed at the Chemical and Biological Sciences Mass Spectrometry facility at the University of Georgia. 20 pmoles of each protein were used for mass determinations.

Crystallization of BenM-EBD-His and selenomethionyl BenM-EBD-His

Initial high-throughput crystallization screenings (HTS) were performed at the Hauptman-Woodward Institute in Buffalo, N. Y. Samples were screened as microbatches under oil at 25 °C using a high-throughput sitting drop method (Luft *et al.*, 2001). A total of 1536 conditions per sample were screened combining 0.2 μ l of BenM-EBD-His (6 mg/ml in 20 mM Tris-HCl, pH 7.9, 0.5M NaCl, 10% glycerol) and 0.2 μ l of precipitating solution per well. Crystallizations were monitored by digital photography at 1-, 4-, 7-, and 14-day intervals. A subset of the conditions that resulted in the formation of crystals

were repeated in-house using 3-6 μ l total volume drops. Temperature and precipitant/protein ratios were optimized to produce data-collection quality crystals. Crystals suitable for high-resolution data collection were generated at 15 °C in sitting drops under paraffin oil (Chayen, 1997) using 4 μ l of BenM-EBD-His (\geq 6 mg ml⁻¹) and 1 μ l of the Crystal Screen™ I condition 20 solution (Hampton Research) (0.2 M ammonium sulfate, 0.1 M sodium acetate trihydrate, pH 4.6, and 25% w/v polyethylene glycol (PEG) 4000) Additional samples of BenM-EBD-His were screened by HTS as before but in the presence of the effectors benzoate (3 mM initial), CCM (2.5 mM), and a combination of CCM and benzoate (2.5 mM & 3 mM).

X-ray Analysis and Data Collection of BenM-EBD-His crystals

Prior to X-ray exposure, BenM-EBD-His crystals were briefly transferred to a cryoprotectant solution containing 35% [v/v] glycerol, 50 mM ammonium sulfate, 25 mM sodium acetate trihydrate, pH 4.6, 6.25% [w/v] PEG 4000, 9mM Tris-HCl, and 225 mM NaCl. Crystals were mounted in a cryoloop and flash frozen in a 100 K nitrogen stream generated by an Oxford Cryojet. Native data was collected on a Bruker Nonius KappaCCD detector mounted on a FR591 rotating-anode generator equipped with a graphite monochromator and miracol optics operated at 45 kV and 100 mA (Cu $K\alpha$ radiation). The X-ray diffraction scheme was defined to collect a complete data set (99%) to 2.4 Å with high redundancy (2113 frames). Each frame was exposed for 300 s with a 0.3° oscillation at crystal-to-detector distance of 90 mm and processed with the DENZO-SMN software package (Otwinowski & Minor, 1997).

Synchrotron Data Collection

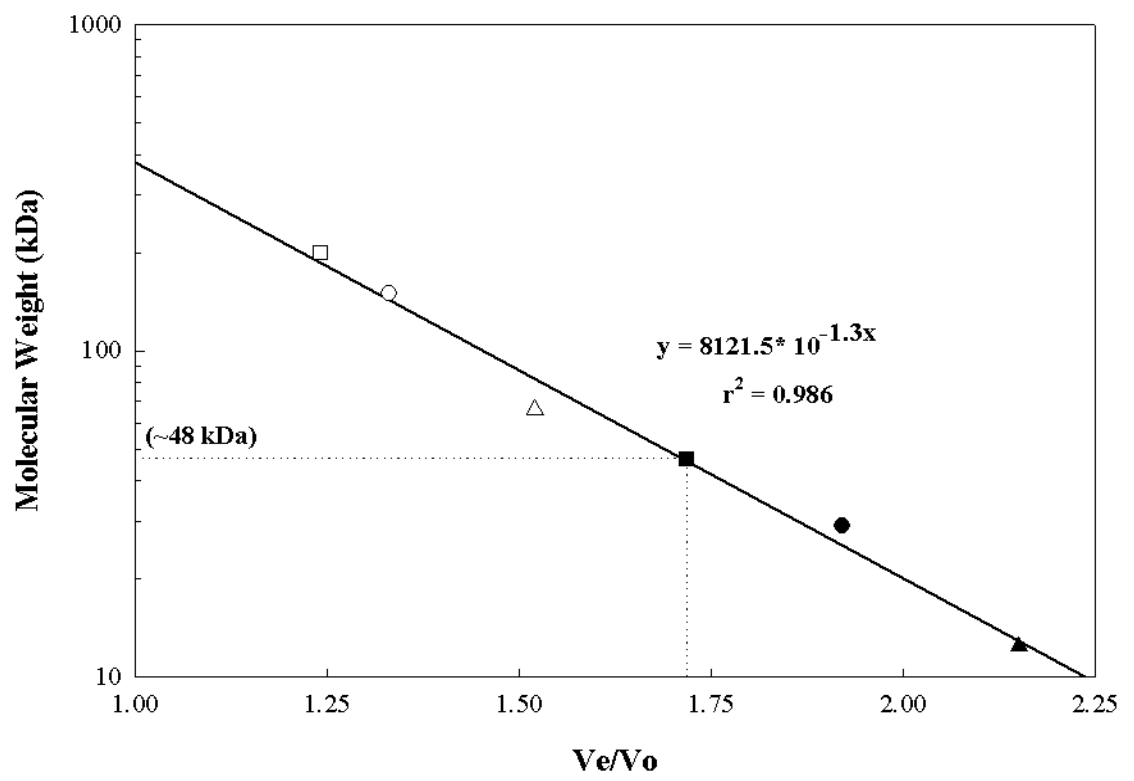
X-ray diffraction data from a selenomethionyl BenM-EBD-His crystal was collected by Dr. Cory Momany at the Southeast Regional Collaborative Access Team (SER-CAT) beamline 17-ID facilities of the Argonne National advanced photon source laboratory (Momany, 2002). Diffraction data was processed using the HKL 2000 software package (Otwinowski and Minor, 1997). An electron density map was generated using the SOLVE and RESOLVE software (Terwilliger, 2001; Terwilliger, 2001). Missing residues were modeled using the program O (Jones *et al.*, 1991) and refined using REFMAC (Murshudov *et al.*, 1999).

RESULTS

Gel-filtration analysis of BenM-EBD-His

The molecular weight and oligomeric state of BenM-EBD-His were determined using gel-filtration chromatography as a preliminary step for structural determinations. BenM-EBD-His and five proteins of known molecular weight were eluted from a gel-filtration column under identical buffering and temperature conditions. The elution volume of each protein (V_e) was converted to a ratio over the column void volume (V_o) and plotted versus the molecular weight of each protein (Fig. 4.3). Amino acid sequence analysis predicted the monomeric weight of BenM-EBD-His to be 26,372 Da. An approximate molecular weight of 48 kDa was estimated for BenM-EBD-His, suggesting that the protein exists as a homodimer in solution. This is in contrast to gel-filtration studies done with full-length BenM that determined that the protein exists as a

Fig. 4.3. Gel-filtration analysis of BenM-EBD-His. The graph depicts a standard curve generated by plotting the molecular weight of known standard proteins versus the ratio of the elution volume (V_e) over the total column void volume (V_o). The proteins used as standards were: β -amylase, 200 -kDa (\square); alcohol dehydrogenase, 150 -kDa (\circ); bovine serum albumin, 66 -kDa (Δ); carbonic anhydrase, 29 -kDa (\bullet); and cytochrome C, 12.4 kDa (\blacktriangle). The molecular mass of BenM-EBD-His (indicated by the \blacksquare symbol and the dashed lines) was estimated to be 48 -kDa. The equation for the slope of the line and the r^2 statistical value is shown.



homotetramer in solution (Bundy *et al.*, 2002). Similar results were obtained with the CysB protein that exists as a homotetrameric full-length protein but a homodimeric protein when the 88-amino acid residue N-terminal DNA binding domain is removed (Miller & Kredich, 1987; Tyrrell, et al., 1997).

Protein purification of a selenomethionyl BenM-EBD-His derivative following expression in *E. coli*.

To generate high-resolution diffraction data using a synchrotron X-ray source, we expressed and purified a derivative of BenM-EBD-His with selenomethionine incorporated in place of methionine. Selenium has a substantial molecular mass that is readily apparent in the electron density maps constructed from synchrotron generated, X-ray diffraction patterns (Hendrickson *et al.*, 1990). This allows the localization of methionine residues to be inferred from the selenomethionine contributions to the electron density map.

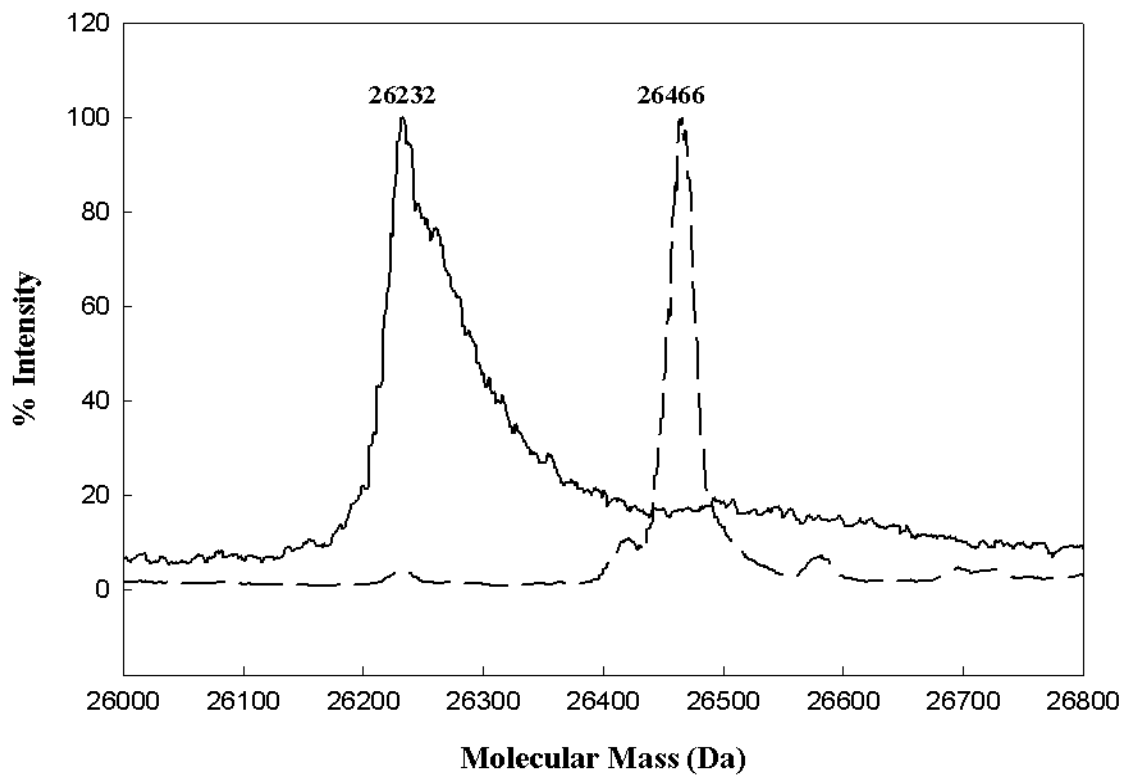
BenM-EBD-His was expressed from plasmid pBAC435 in a methionine auxotrophic strain of *E. coli* in the presence of selenomethionine. Nickel-affinity chromatography was used to purify the protein after it was expressed in *E. coli* with a hexahistidine tag. Following induction, selenomethionyl BenM-EBD-His was estimated to comprise approximately 25% of the total cellular protein in the *E. coli* cells (data not shown). Selenomethionyl BenM-EBD-His was purified to homogeneity from a nickel-chelating column. The protein eluted as a broad peak over a gradient range of 140- 190 mM imidazole (data not shown). The purified protein was estimated to be approximately 26,000 -Da on Coomassie-stained SDS-PAGE gels and similar in size to non-

selenomethionyl-labeled BenM-EBD-His. Approximately 5 mg of protein was obtained per 0.5 L of culture, at $\geq 95\%$ purity.

Verification of selenomethionine incorporation in BenM-EBD-His.

Selenomethionyl protein derivatives are only useful for structure determinations provided that a significant levels of selenomethionine substitution for methionine is achieved. To verify the extent of selenomethionine incorporation in BenM-EBD-His, we compared the mass of selenomethionyl BenM-EBD-His to that of BenM-EBD-His using liquid chromatography mass-spectrometry (LC-MS). Selenomethionine differs from methionine by 47 atomic mass units (amu). BenM-EBD-His contains 6 methionine residues, including the N-terminal, translational initiation residue. We predicted that complete incorporation of selenomethionine would result in a 282 amu increase in the molecular weight of selenomethionyl-BenM-EBD-His. LC-MS analysis determined molecular weights of 26,232 and 26,466 amu for BenM-EBD-His and selenomethionyl BenM-EBD-His, respectively (Fig. 4.4). This increase of 234 amu in the selenomethionyl BenM-EBD-His suggested that only 5 selenomethionine residues were incorporated into the protein. Moreover, the molecular mass determined for BenM-EBD-His differed from that predicted by 141 amu, approximately the weight of a single methionine residue (133.2 amu). This result suggested that the initial methionine residue of BenM-EBD-His was cleaved from the protein most likely as a result of post-translational modification. Taken collectively, we concluded that 5 selenomethionines were incorporated within the protein, completely labeling the selenomethionyl BenM-EBD-His derivative.

Fig. 4.4. Verification of selenomethionyl incorporation in BenM-EBD-His. The mass spectrum of BenM-EBD-His (solid lines) and selenomethionyl BenM-EBD-His (dashed lines) as determined by liquid chromatography mass spectrometry (LC-MS). The numbers denote the molecular mass corresponding to the maximum spectrum peak for each protein.



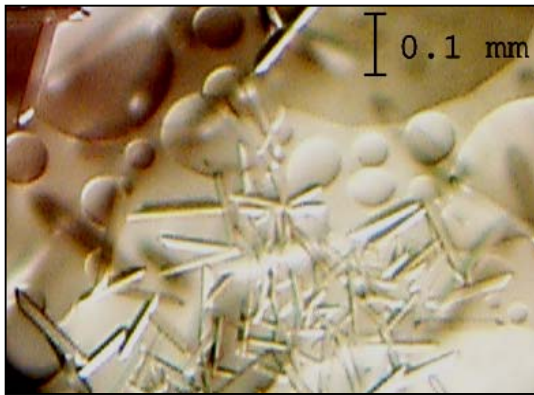
Optimization of conditions for BenM-EBD-His crystallization.

To determine conditions that would yield BenM-EBD-His crystals, we employed the assistance of the Hauptman-Woodward Institute to perform high-throughput screening (HTS) trials. HTS trials were done with BenM-EBD-His in the absence of effectors and in the presence of CCM, benzoate, or CCM and benzoate combined. HTS trials identified many conditions that resulted in the formation of BenM-EBD-His crystals of needle and rod-shaped morphologies. Trials with BenM-EBD-His protein alone resulted in the formation of crystals in 83 out of a total of 1536 conditions. In the presence of effectors, the number of conditions resulting in crystal formation decreased to 54 in the presence of CCM, 43 with benzoate, and 12 in the presence of both benzoate and CCM. Initially, we concentrated on optimizing a subset of the conditions resulting in positive BenM-EBD-His crystal formation in the absence of effectors.

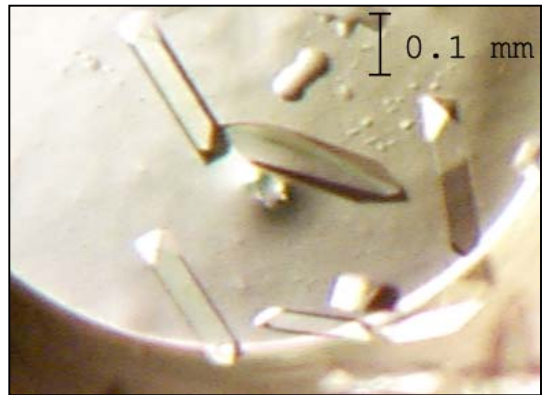
Crystal screens were repeated as microbatches under oil to mimic the initial HTS conditions. The Crystal Screen™ I condition 20 solution resulted in the repeated formation of crystals at room temperature (Fig. 4.5A). Increasing the ratio of protein to precipitant resulted in the formation of larger crystals (Fig. 4.5B and C). Decreasing the incubation temperature to 15 °C further increased the size of the crystals resulting in two slightly different morphologies (Fig. 4.5D and E). These conditions were selected for subsequent BenM-EBD-His crystal growth and contained 4 parts protein (6 mg/ml) added to 1 part precipitant solution, followed by incubation at 15 °C.

Fig. 4.5. Optimization of conditions for the formation of BenM-EBD-His and selenomethionyl BenM-EBD-His crystals. Photographs showing BenM-EBD-His crystals generated at 25 °C from a solution with a protein to precipitant ratio of 1:1 (A), 2:1 (B), and 4:1 (C). Larger BenM-EBD-His crystals were generated at 15 °C using a 4 to 1 ratio of protein to precipitant resulting in two slightly different morphologies (D and E). Selenomethionyl BenM-EBD-His crystals were similarly generated at 15 °C using a 4 to 1 ratio of protein to precipitant (F). A 0.1 mm scale bar is shown in the upper right hand corner of each photograph.

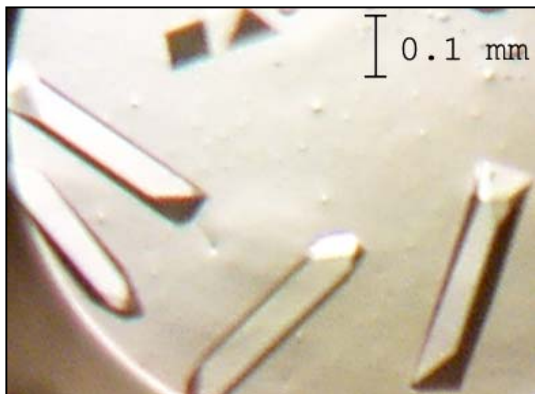
A



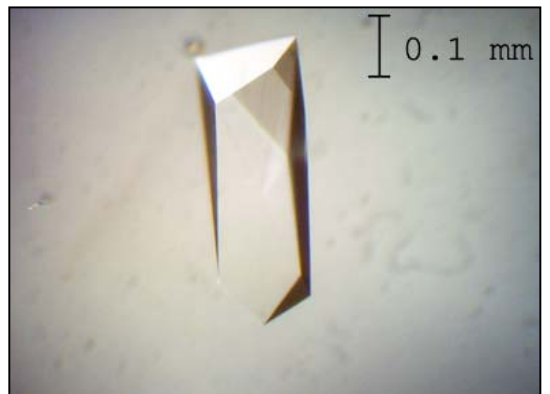
B



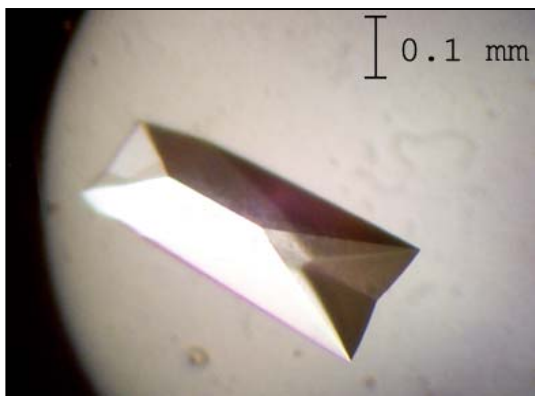
C



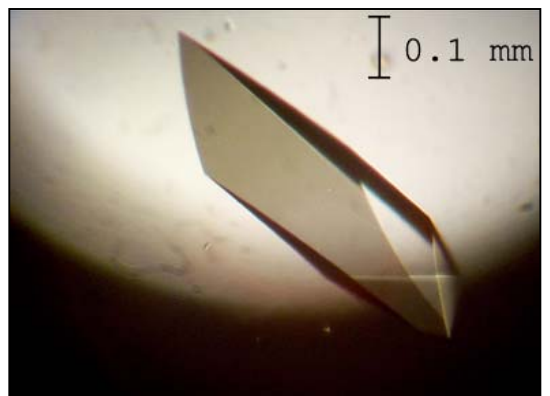
D



E



F



Crystallization of selenomethionyl BenM-EBD-His

Selenomethionyl BenM-EBD-His crystals were formed using the same conditions optimized for non-labeled BenM-EBD-His protein. Crystals of similar shape and size were generated using ≥ 6 mg/ml selenomethionyl BenM-EBD-His (Fig. 4.5F).

This result indicated that the incorporation and presence of the selenomethionyl residues had no detrimental effect on crystal formation.

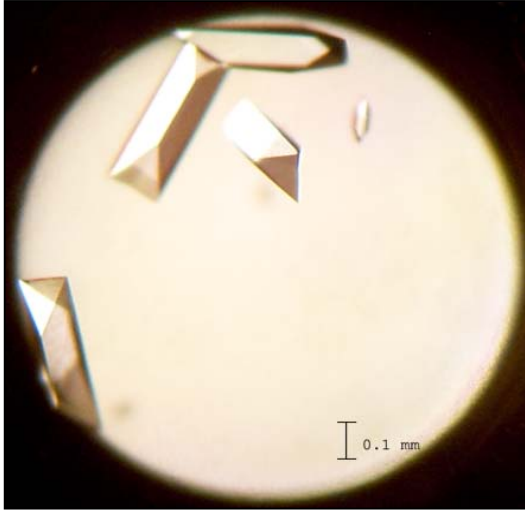
Determination of the influence of effectors on BenM-EBD-His Crystal formation

To determine if the presence of effectors had an effect on BenM-EBD-His crystal formation, crystallization reactions were set up under optimized conditions in the presence of CCM, benzoate, or both CCM and benzoate. The precipitation solution was monitored prior to the addition of protein verifying that the addition of effectors had no effect on the pH of the solution (data not shown).

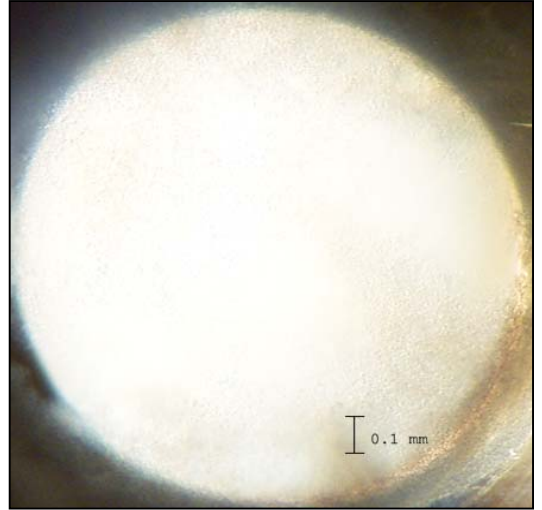
In the presence of CCM, crystals were formed that were comparable to previous BenM-EBD-His crystals formed in the absence of CCM (Fig. 4.6A). In contrast, the presence of benzoate completely hindered crystal formation resulting in a slightly visible precipitation (Fig. 4.6B). The presence of both CCM and benzoate resulted in the formation of BenM-EBD-His crystals of an altered morphology (Fig. 4.3C). These results suggest that the presence of benzoate, or both benzoate and CCM cause BenM-EBD-His to undergo a conformational change that is detrimental to crystal formation.

Fig. 4.6. Photographs showing the influence of effectors on the formation of BenM-EBD-His crystals. BenM-EBD-His protein was combined with precipitant at a ratio of 4 to 1 and incubated at 15 °C in the presence of 3 mM *cis,cis*-muconate (A), 3 mM benzoate (B), and both *cis,cis*-muconate and benzoate at 3 mM each (C). A 0.1 mm scale bar is indicated in the lower right corner of each photograph.

A



B



C



Collection of X-ray diffraction patterns from a BenM-EBD-His crystal and unit cell characterization.

To determine if BenM-EBD-His crystals were suitable for diffraction studies, X-ray diffraction data were collected from a single BenM-EBD-His crystal. Dr. Cory Momany used an in house X-ray generator with the conditions described in the Methods section. Diffraction data collected on an area detector were consistent with the unit cell existing in the space group $P2_12_12_1$. Diffraction spots were observed up to a resolution of 2.2 Å, but final data were processed only to 2.3 Å. Data collection statistics for the BenM-EBD-His crystal are summarized in Table 4.1 (Momany, 2002).

Collection of X-ray diffraction patterns of a selenomethionyl BenM-EBD-His crystal and unit cell characterization.

Attempts to solve the structure of BenM-EBD-His in house using X-ray diffraction and molecular replacement modeling methods were unsuccessful. Alternatively, we explored the possibility that high resolution X-ray diffraction data could be generated from selenomethionyl BenM-EBD-His crystals using high-brilliance X-ray beams. Using the Beamline 17-ID Advanced Photon Source at the Southeast regional collaborative access team (SER-CAT) facilities of the Argonne National laboratory, Dr. Cory Momany collected X-ray data from a single selenomethionyl BenM-EBD crystal (Momany, 2002). Data was collected and processed as described in the Methods section. Using computer-assisted analysis, single-wavelength data corresponding to the selenium peaks of the selenomethionyl residues was used to predict the location of the five internal methionine residues. This analysis allowed a readily

Table 4.1. Data collection statistics for the BenM-EBD crystal.

Wavelength (Å)	1.5418	home source
Space group	P2 ₁ 2 ₁ 2 ₁	
Unit cell (Å)	$a = 65.643$, $b =$ 66.335 , $c =$ 117.463 $V = 511484 \text{ \AA}^3$	
Number of observed reflections (unique)	166,591	(22,112)
Complete resolution range, Å (outer shell)	30.0 – 2.3	(2.37 – 2.30)
Completeness overall, % (outer shell)	93.7	(42.0)
Overall $I/\sigma(I) > 3$, % (outer shell)	91	(89.0)
Overall R_{merge} on I , % (outer shell)	4.7	(12.8)

interpretable electron density map to be generated with 63% of the residues of BenM-EBD-His appropriately assigned. Alteration of the analysis parameters to allow for the introduction of non-crystallographic symmetry resulted in 73% of the total protein residues being properly fitted to the electron density map (Momany, 2002). From this initial model, a relatively complete structural model of BenM-EBD-His was built and refined to 2.0 Å resolution. Refinement statistics for structural data are summarized in Table 4.2. Additional rounds of refinement have resulted in the generation of the current structural model, which is approximately 98% complete.

DISCUSSION

The structure of the BenM-EBD-His monomer

The 224-residue BenM-EBD-His monomer was found to consist of two α/β domains (I and II) connected by two interdomain β -strands. Domain I (Fig. 4.7A, indicated in blue) is mainly comprised of residues 81-161. Domain II (Fig. 4.7A, shown in red) is comprised of residues 162-267. Residues 268-296 loop back away from domain II, forming a β -strand and α -helix that constitutes an edge of domain I. The remaining C-terminal residues, 297-304 (Fig. 4.7A, shown in green), form a loop that runs along the outside edge of domain I.

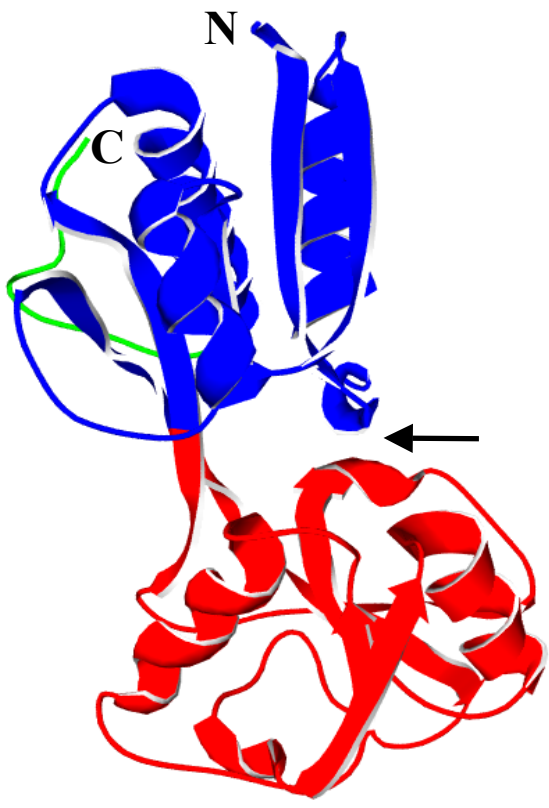
The interfaces of the two α/β domains form a cleft or pocket that is approximately 14 Å deep and 8 Å in diameter (indicated by the black arrow in Fig. 4.7A). The inner surface of the pocket is comprised of mainly hydrophobic residues from both domains. Residues of the interdomain β -strands form the bottom surface or base of the cleft. One side of the cleft opening is partially blocked by an α -helix descending from domain I.

Table 4.2. Refinement statistics for the structure of BenM-EBD-His.

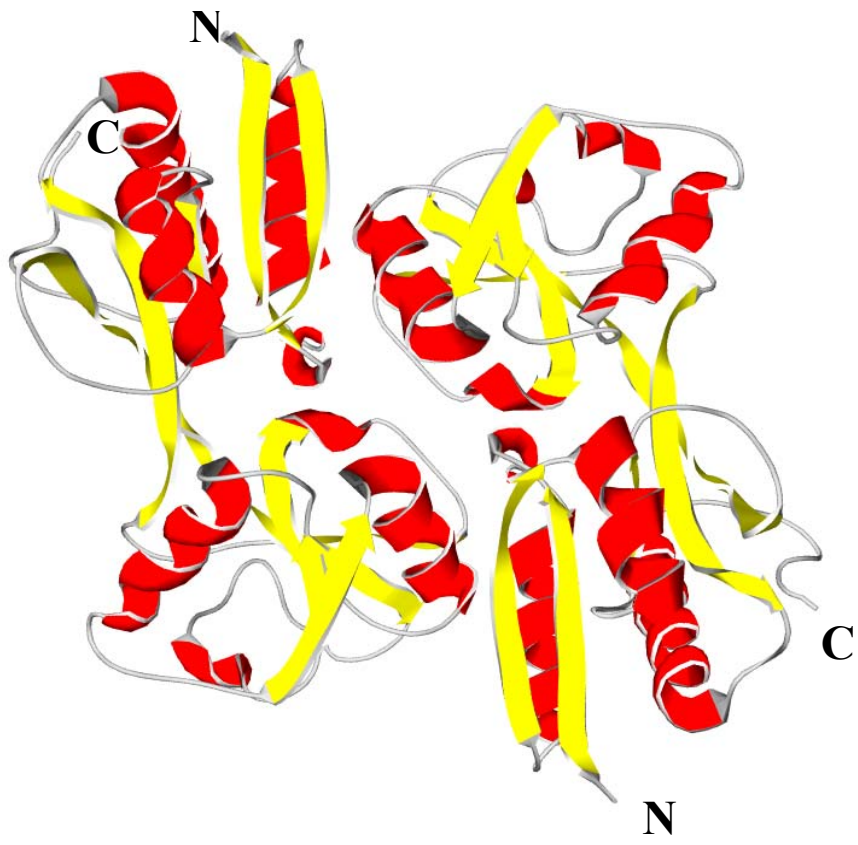
Final Resolution (Å)	2.0
Overall R Factor (%)	20.09
Free R Factor (%)	27.05
Rms deviation from ideality	
Bonds (Å)	0.012
Angles (°)	1.327

Fig. 4.7. Ribbon diagrams depicting BenM-EBD-His. Panel A shows a ribbon diagram of the BenM-EBD-His monomer colored according to domain composition. The residues that make up domain I (residues 81-160, and 269-296) are red. Residues comprising domain II (residues 161-268) are colored blue. C-terminal residues (residues 297-304) are green. Panel B shows the dimer of BenM-EBD-His colored according to secondary structure with α -helices colored red, and β -strands colored yellow. The N and C-terminal ends of the protein are indicated in both panels. The figure was constructed using the Deep View Swiss-PdbViewer (Guex & Peitsch, 1997).

A



B



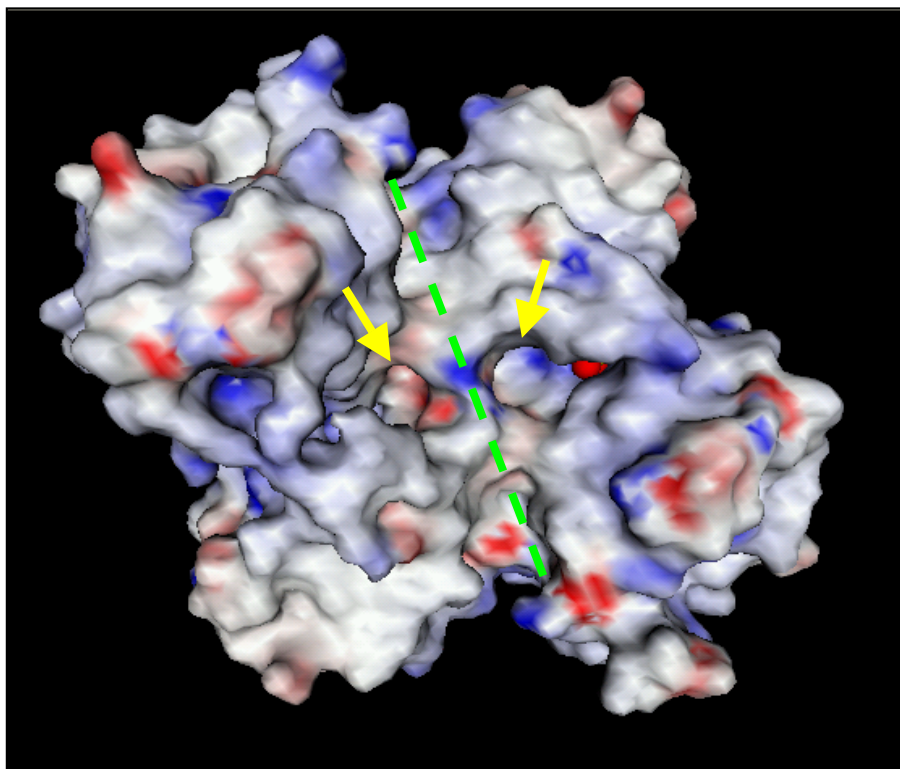
Organization of the BenM-EBD-His dimer

Analysis of the diffraction data showed that two monomers related by a non-crystallographic 2-fold symmetry comprise the asymmetric unit of the protein crystals. The presence of dimers in the crystal is consistent with gel-filtration results indicating that BenM-EBD-His is a dimer in solution. Within the dimer, BenM-EBD-His monomers are arranged in an anti-parallel, side-by-side alignment (Fig. 4.7B). This arrangement allows for a duplicated series of surface interactions to form between each monomer. Hydrogen bonds and hydrophobic interactions between surface residues of domain I of one monomer, and domain II of the second monomer join the two molecules. Additional interactions form between the central regions of each monomer corresponding to domain II. The net result is an extensive set of interactions along a large surface of the monomers creating a compact and stable dimeric complex (Fig. 4.8A and B).

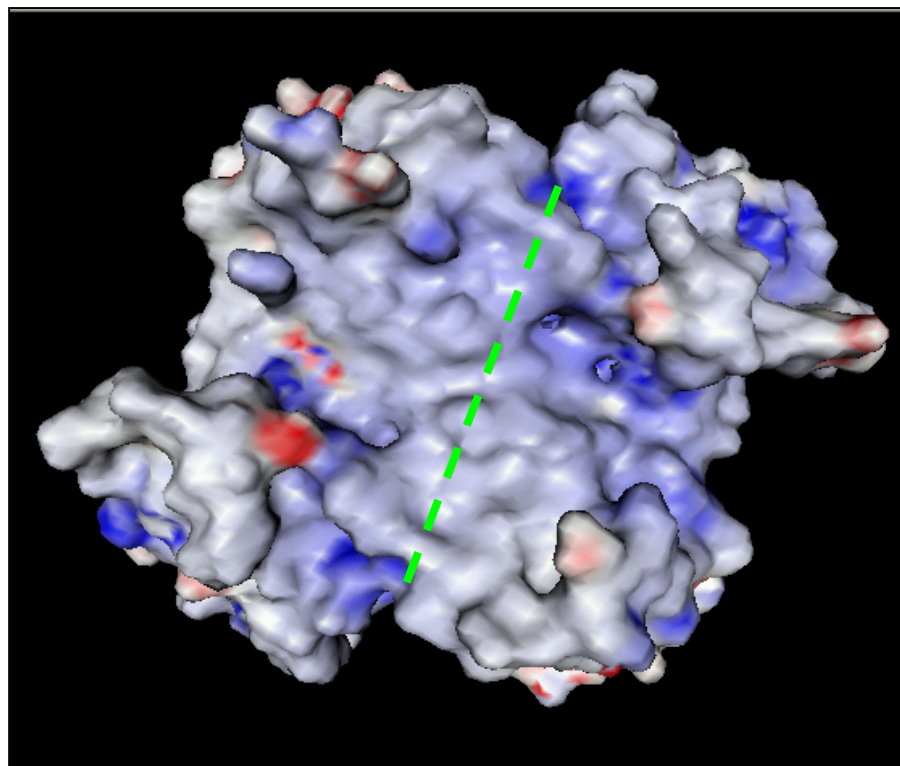
The antiparallel alignment of the BenM-EBD-His monomers places the interdomain clefts of each subunit on the same face of the dimer, with the openings approximately 4 Å from one another (Fig. 4.8A). This face of the dimer, designated as the front face, has an uneven rugged surface. This is in contrast to the opposite, or back face of the dimer (Fig 4.8B), which has a mainly smooth surface in comparison, particularly in the center region of the structure. Several of the residues comprising the flat surface region of the back face are hydrophobic (Fig. 4.8B). This flat region may form other protein interactions with another dimer or with the absent N-terminal DNA binding domain.

Fig. 4.8. Representation of the charge distribution and surface structure of the BenM-EBD-His dimer. The front (A) and rear (B) views of the dimer are shown. Positive and negative electrostatic potentials are shown in blue or red, respectively. Hydrophobic regions in the center of the rear side of the dimer are depicted as the shining, grayish-regions. The green dotted line indicates the interface between the two monomers. The yellow arrows in panel A indicate the location of two pockets that may be the site of effector-binding. The solid red area in the right hand pocket is a glimpse of a sulfate molecule bound within this cleft. Close-up views of the pockets are shown in Fig. 4.10. The model was generated using the GRASS software (Nayal *et al.*, 1999).

A



B



The tertiary structures of CysB(88-324) and the OxyR regulatory domain resemble that of BenM-EBD-His (Fig. 4.9). Structural differences are evident however in the secondary structure organization of some of the domains, particularly in the C-terminal region. Residues within the C-terminal regions of LTTRs have been implicated in protein oligomerization (Jorgenson & Dandanell, 1999; Kullik *et al.*, 1995; Lochowska, et al., 2001). These regions share the least amount of amino acid similarity between individual LTTR members (Schell, 1993). The structural differences seen in the C-terminal region of the proteins may allow native dimers to form the specialized interactions necessary for tetramerization. Full-length BenM, CysB, and OxyR all form tetramers in solution (Bundy, et al., 2002; Colyer & Kredich, 1996; Kullik, et al., 1995).

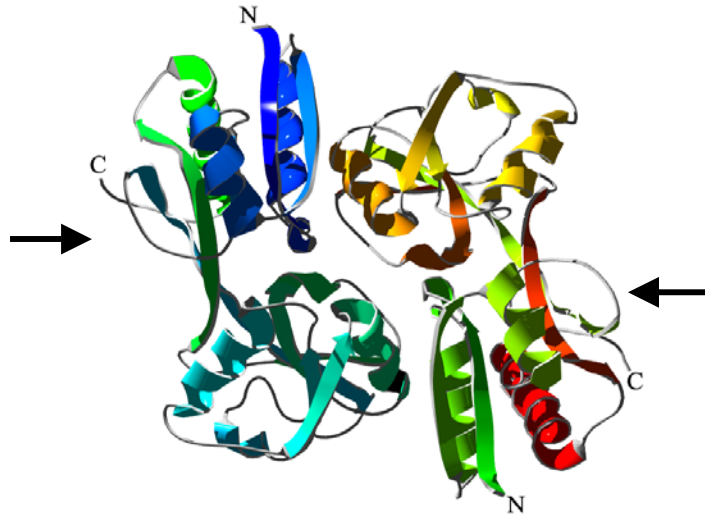
The sulfate-binding site within the BenM-EBD-His interdomain cleft

During model refinement, a significant region of electron density was discovered within the interdomain cleft of one of the BenM-EBD-His monomers that did not correspond to the amino acid residues within this region of the model. After further analysis, it was determined that the density pattern corresponded to a sulfate anion. This molecule likely originated from ammonium sulfate present in the precipitation solution. In the current model, it is unclear whether a second sulfate anion is present in the opposite cleft of the dimer.

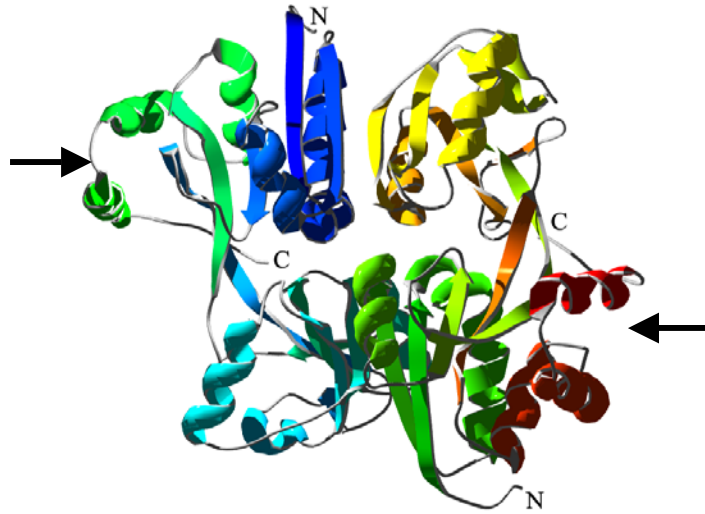
Sulfate anions were similarly reported to be present within both of the cleft regions of the dimeric CysB(88-324) crystal structure (Tyrrell, et al., 1997). Using computer-modeling, Tyrrell and coworkers were able to model a N-acetylserine (NAS) molecule, the effector molecule for CysB, in place of the sulfate molecule without

Fig. 4.9. Ribbon diagrams of dimers of BenM-EBD-His, CysB(88-324), and the OxyR regulatory domain. The diagrams were colored according to secondary structure succession to illustrate the common structural arrangement shared by all three proteins. The black arrows denote the C-terminal domain of each protein where moderate structural variations between the three proteins are evident. Figures were generated with Deep View Swiss-PdbViewer.

BenM-EBD-His



CysB(88-324)



The OxyR Regulatory Domain



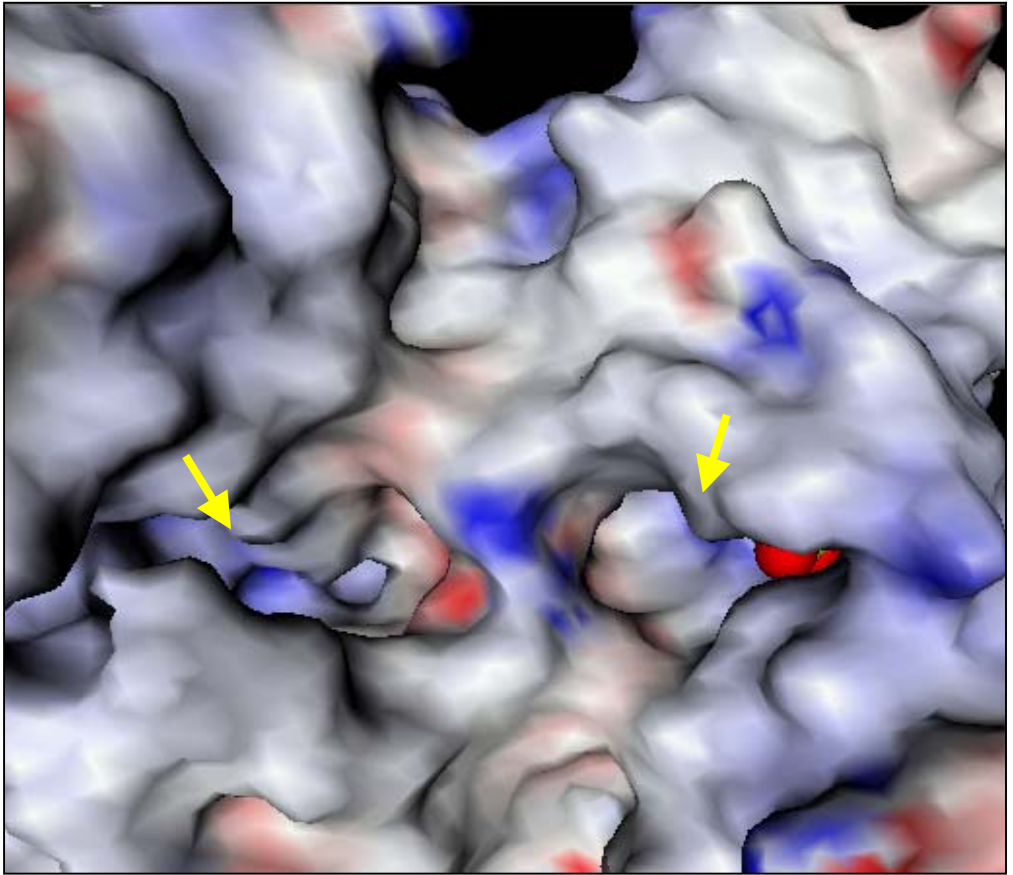
causing dramatic changes to the protein structure (Tyrrell, et al., 1997). The carboxyl group of NAS was able to occupy the approximate site of the sulfate ion and form similar hydrogen-bonding interactions with the residues lining the cleft. Mutational studies of CysB verified that these and several others residues lining the binding cleft are necessary for NAS binding (Colyer and Kredich, 1996; Lochowska, et al., 2001).

Similar mutational studies of OxyR have likewise localized residues necessary for effector recognition within the interdomain cleft region of the OxyR regulatory domain structure (Kullik, et al., 1995). The redox-active Cys199 residue that serves as the active-site hydrogen peroxide sensor is located at the base of the cleft of OxyR (Choi, et al., 2001). Collectively, these results support the notion that the functional effector-binding region of LTTRs is located within the interdomain clefts.

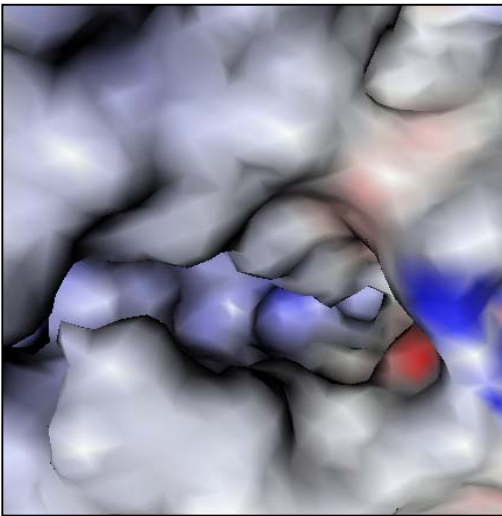
The sulfate anion within BenM-EBD-His was localized near the bottom surface of the cleft. Analysis of the surface structure and the electrostatic charge potential of the residues lining the cleft reveal that the sulfate anion is located near a region of strong positive charge (Fig. 4.10A, B, and C). Computer-aided analysis of the residues within this region predict the formation of a number of hydrogen bonding interactions between the sulfate ion and the main chain and side chain groups of residues lining the inner surface of the cleft (Fig. 4.11). A well-defined set of hydrogen bond interactions form between the sulfate anion and residue Arg146. The sidechain of Arg146 descends directly into the central portion of the cleft base, corresponding to the exact region of the positive charge potential illustrated in Figures 4.10B and 4.10C. This positioning of the arginine residue is ideal for the formation of interactions with negatively charged molecules, like CCM or benzoate, which descend into the cleft.

Fig. 4.10. Close-up views of the pockets on the front surface of the BenM-EBD-His dimer. Panel A shows the view of both pockets (denoted by the yellow arrows). Close-up views of the left, empty pocket (B) and the right pocket containing the sulfate molecule (shown in as red and yellow spheres) (C) are shown. The blue regions within each pocket denote areas of positive electrostatic potential. A small region of negative potential (red) can be seen in the left, empty pocket. These figures were generated using the GRASS software.

A



B



C

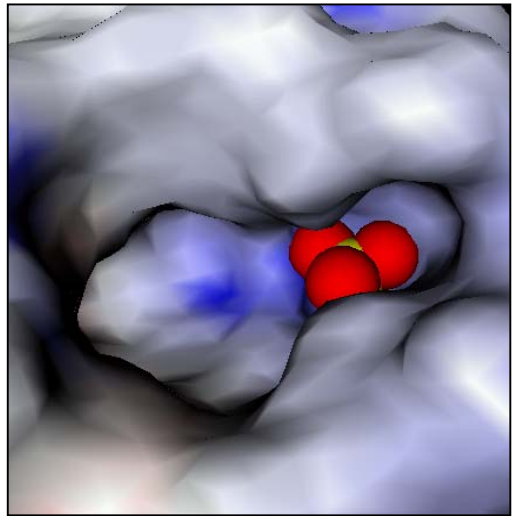
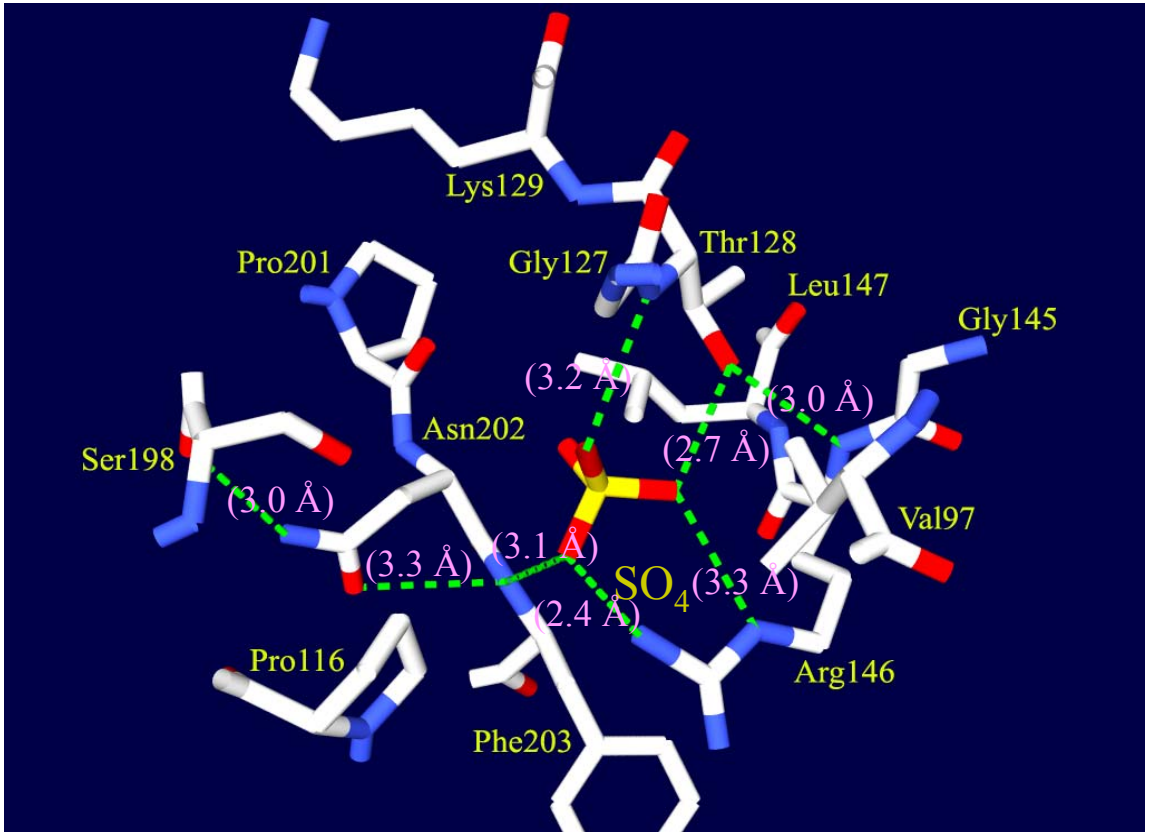


Fig. 4.11. Model of the sulfate binding site. The sulfate ion and the residues of the binding pocket are labeled in gold. The individual atoms are colored as: oxygen atoms are red, nitrogen atoms are blue, carbon atoms are white, and sulfur is yellow. The dashed green lines indicate the predicted hydrogen bond interactions. The distances in angstroms between the polar groups are indicated in parenthesis (purple). The figure was generated using Deep View Swiss-PdbViewer.

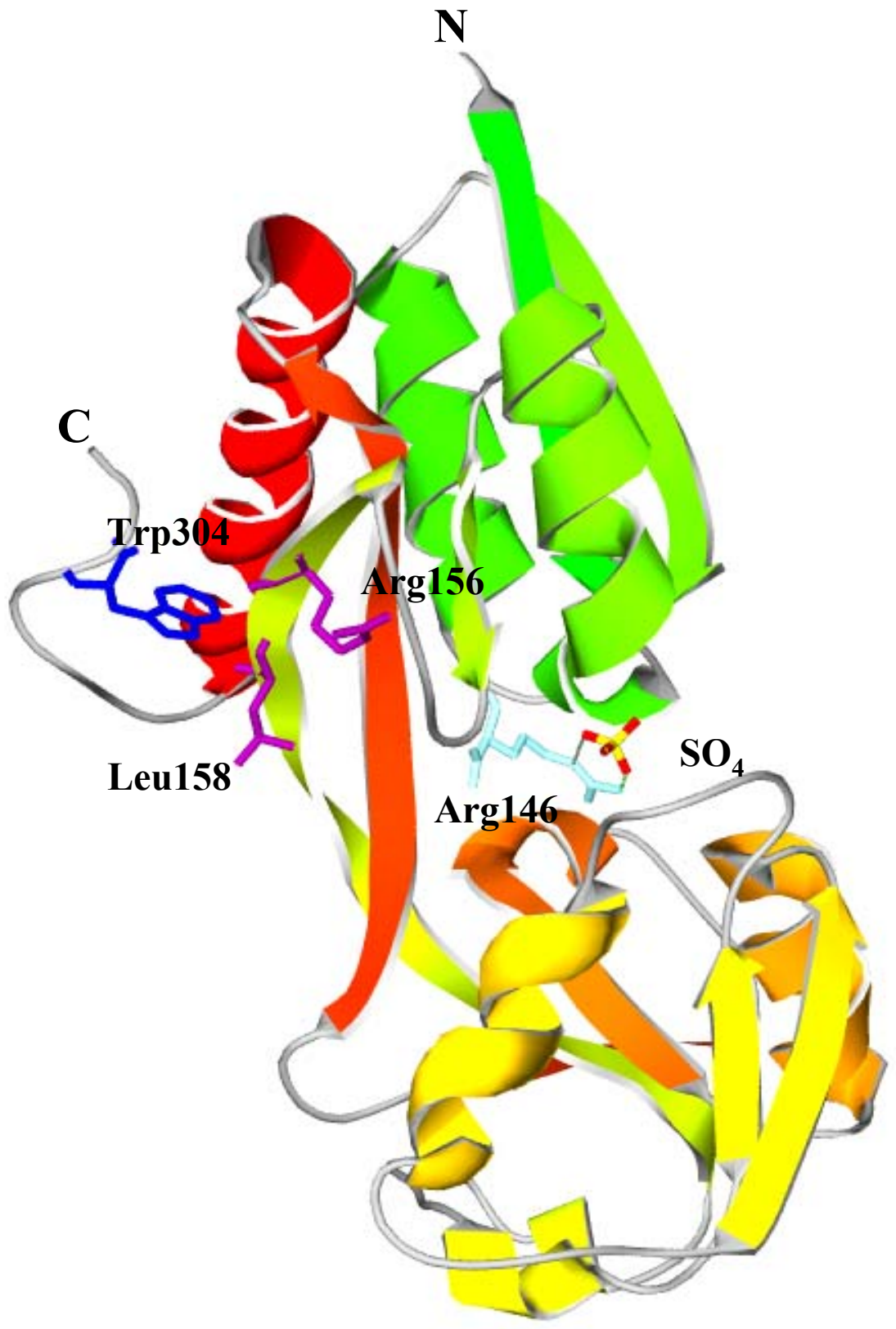


Mutations affecting effector-regulated transcriptional activation

Mutational analysis studies have not been done on BenM. However, two mutations have been characterized that affect the BenM homolog CatM. These amino acid changes generate CatM variant proteins with the substitutions Arg156His or Val158Met. The Arg156His variant activates high-level expression of the *catA* and *catBCIJFD* operons in the absence of CCM (Neidle *et al.*, 1989; Romero-Arroyo, *et al.*, 1995). The Val158Met variant CatM activates high-level expression of *benABCDE* in the presence of CCM (Collier, 2000). This is in contrast to wild-type CatM that is capable of only low-level CCM-induced *benABCDE* gene expression (Bundy, *et al.*, 2002). Collectively, the phenotypes of these mutants imply that Arg156 and Leu158 are located in a region of CatM intimately involved in effector-response.

Alignment of the sequences of BenM and CatM show that Arg156 is conserved in BenM. A leucine residue in BenM occupies the corresponding position of Val158 of CatM (Fig. 4.1). Analysis of the BenM-EBD-His crystal structure shows these residues localize to a β -strand that connects domains I and II of the monomer (Fig. 4.12). Interestingly, this β -strand is attached to a looping region that contains the Arg146 residue discussed earlier that binds sulfate within the cleft. This loop region appears to lay along the surface of domain I. This positioning may allow the loop to be flexible and allow movement along the surface of domain I. If Arg146 were involved in effector binding, it seems likely that binding interactions between this residue and effector could alter the position of this loop. Similarly, it is possible that changes in the position of the loop would alter the position of the connected β -strand containing Arg156 and Leu158.

Fig. 4.12. Ribbon diagram showing a BenM-EBD-His monomer bound sulfate ion. The ribbon diagram is colored according to secondary structure succession. Key residues that may be involved in effector-binding and response are colored and labeled. Trp304 monitored in fluorescence studies described in chapter 3 is colored blue. Residues Arg156 and Leu158 corresponding to the location of residues in two CatM variants are colored purple. Arg146 which was implicated in sulfate binding is colored light blue. Predicted hydrogen bond interactions between Arg146 and the sulfate anion (red and yellow stick figure) are indicated (dashed lines). This figure was generated using the Deep View Swiss-PdbViewer.



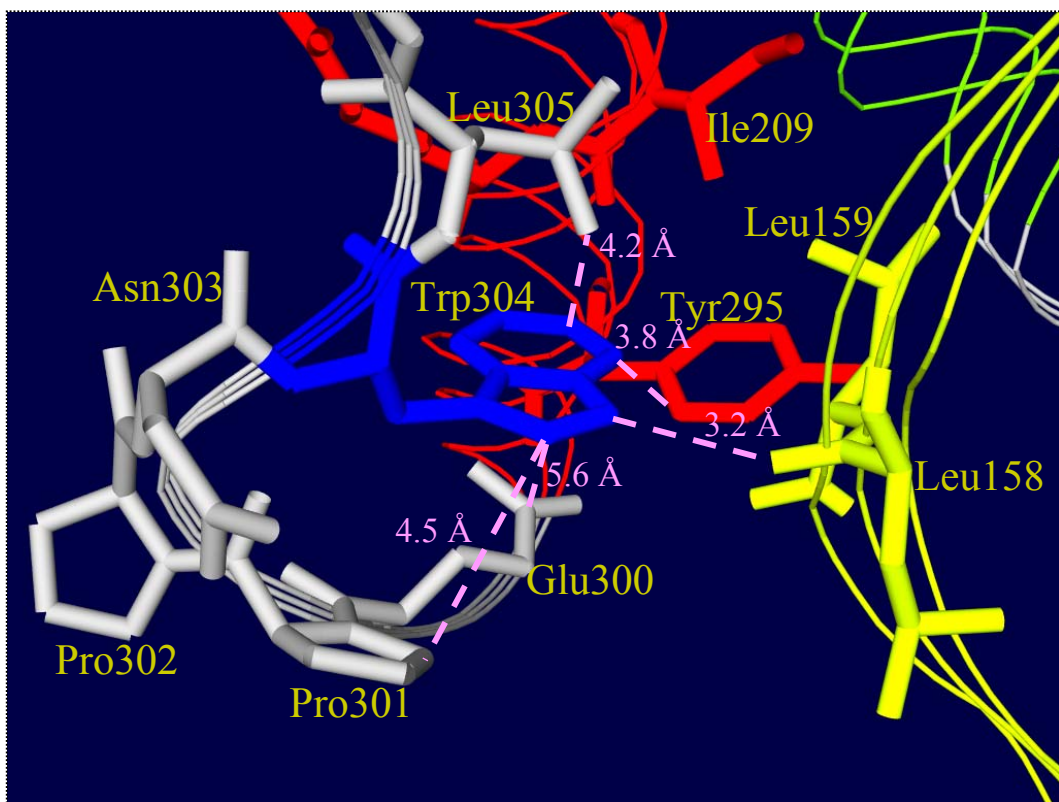
At present no experimental data are available to support this assertion based on the structural data. Nonetheless, it seems likely that these regions could be prone to interdomain movement and thereby play a key structural role in effector-response.

Structural basis for tryptophan fluorescence studies

The binding of CCM or benzoate by BenM resulted in a decrease in the fluorescence signal emitted from Trp304. Benzoate binding additionally caused a conformational change in the C-terminal domain of BenM within the vicinity of Trp304. Assuming that the sulfate-binding region of BenM-EBD-His represents the effector-binding region of BenM, then this site is located approximately 18 Å from Trp304. This distance is too great for the presence of effectors to have a direct influence on fluorescence. Ligand-binding is only able to influence tryptophan fluorescence directly when the residue is located within close proximity (>5 Å) of the binding site (Lakowicz, 1999). Such is the case in CysB, where Trp166 is located approximately 4 Å from the sulfate and putative N-acetylserine binding site (Lynch, et al., 1994; Tyrrell, et al., 1997). Thus, the most likely explanation to account for the change in BenM fluorescence is that effector-binding causes localized changes to occur between the binding site region and the regions adjacent to the tryptophan residue.

Trp304 is located in a pocket formed by an α -helix on the edge of domain I and the β -strand containing the previously described Leu158 and Arg156 residues (Fig. 4.13). Leu158 lies 3.2 Å from Trp304 and hydrogen bond interactions are predicted to form between the two residues. Thus structural changes resulting from effector binding near the position of Leu158 could potentially affect the position or environment of Trp304.

Fig 4.13. Close up view of the residues surrounding Trp304. The distances between the residue groups (purple dotted lines) is denoted in angstroms (Å). This figure was generated with Deep View Swiss-PdbViewer.



Such a mechanism would account for the conformational change caused by benzoate binding. Binding would result in Trp304 being exposed to more hydrophilic conditions consistent with the observed shift in the wavelength of maximum fluorescence emission. This mechanism does not completely explain the decrease in the fluorescence signal seen by CCM or benzoate binding. One possibility is that the side groups of other residues surrounding Trp304 could quench the fluorescence signal. Carboxyl groups like those on the side chain of glutamate and aspartate are capable of quenching the fluorescence signal of the indole group of tryptophan (Lakowicz, 1999). Similar to the presence of effectors, these functional groups have to be within close proximity ($>5 \text{ \AA}$) of the tryptophan residue, specifically the indole group, in order to quench the fluorescence signal. The closest residue to Trp304 fitting these criteria is Glu300. This residue is situated such that its carboxylic group is located approximately 5.6 \AA from the indole ring of Trp304 (Fig. 4.13). It is possible that structural changes resulting from effector binding could force Trp304 closer to the carboxyl group of Glu300 thus accounting for the diminished fluorescence signal.

X-ray diffraction analysis of CCM and benzoate containing BenM-EBD-His crystals is currently in progress. Once obtained, these data should allow for the direct identification of the regions of BenM necessary for effector binding. More importantly, these data will allow the conformational changes resulting from CCM and benzoate binding to be compared. These differences may account for the mechanism of BenM-mediated synergistic transcriptional activation.

REFERENCES

- Applebaum, E. R., Thompson, D. V., Idler, K. & Chartrain, N. (1988).** *Rhizobium japonicum* USDA 191 has two *nodD* genes that differ in primary structure and function. *J. Bacteriol.* **170**, 12-20.
- Bundy, B. M., Collier, L. S., Hoover, T. A. & Neidle, E. L. (2002).** Synergistic transcriptional activation by one regulatory protein in response to two metabolites. *Proc. Natl. Acad. Sci.* **99**, 7693-7698.
- Chang, M., Hadero, A. & Crawford, I. P. (1989).** Sequence of the *Pseudomonas aeruginosa trpI* activator gene and relatedness of *trpI* to other procaryotic regulatory genes. *J. Bacteriol.* **171**, 172-183.
- Chayen, N. E. (1997).** The role of oil in macromolecular crystallization. *Structure* **5**, 1269-1274.
- Choi, H., Kim, S., Mukhopadhyay, P., Cho, S., Woo, J., Storz, G. & Ryu, S. (2001).** Structural basis of the redox switch in the OxyR transcription factor. *Cell* **105**, 103-113.
- Christman, M. F., Storz, G. & Ames, B. N. (1989).** OxyR, a positive regulator of hydrogen peroxide-inducible genes in *Escherichia coli* and *Salmonella typhimurium*, is homologous to a family of bacterial regulatory proteins. *Proc. Natl. Acad. Sci.* **86**, 3484-3488.
- Coco, W. M., Rothmel, R. K., Henikoff, S. & Chakrabarty, A. M. (1993).** Nucleotide sequence and initial functional characterization of the *clcR* gene encoding a LysR family

activator of the *clcABD* chlorocatechol operon in *Pseudomonas putida*. *J. Bacteriol.* **175**, 417-427.

Collier, L. S. (2000). Transcriptional regulation of benzoate degradation by BenM and CatM in *Acinetobacter* sp. Strain ADP1. Ph.D. Thesis. In *Department of Microbiology*. Athens, GA: University of Georgia.

Collier, L. S., Gaines, G. L., III & Neidle, E. L. (1998). Regulation of benzoate degradation in *Acinetobacter* sp. strain ADP1 by BenM, a LysR-type transcriptional activator. *J. Bacteriol.* **180**, 2493-2501.

Colyer, T. E. & Kredich, N. M. (1996). In vitro characterization of constitutive CysB proteins from *Salmonella typhimurium*. *Mol. Microbiol.* **21**, 247-246.

Gonnet, G. H., Cohen, M. A. & Brenner, S. A. (1992). Exhaustive matching of the entire protein sequence database. *Science* **256**, 1443-1445.

Guex, N. & Peitsch, M. C. (1997). SWISS-MODEL and Swiss-PdbViewer: An environment for comparative protein modeling. *Electrophoresis* **18**, 2714-2723.

Habeeb, L. F., Wang, L. & Winans, S. C. (1991). Transcription of the octopine catabolism operon of the *Agrobacterium* tumor-inducing plasmid pTiA6 is activated by a LysR-type regulatory protein. *Mol. Plant Microbe Interact.* **4**, 379-385.

Hendrickson, W. A., Horton, J. R. & LeMaster, D. M. (1990). Selenomethionyl proteins produced for analysis by multiwavelength anomalous diffraction (MAD): a vehicle for direct determination of three-dimensional structure. *EMBO J.* **9**, 1665-1672.

Hinner, I. S., Lohmann, M. & Schloemann, M. (1998). Characterization of gene clusters coding for enzymes of catechol catabolism in *Ralstonia eutropha* 335: *catA*, *R*, *B*, *Cl*, and *Dl*. . Submitted to the EMBL/GenBank/DDBJ databases.

Johnson, G. R., Jain, R. K. & Spain, J. C. (2000). Properties of the trihydroxytoluene oxygenase from Burkholderia cepacia R34: an extradiol dioxygenase from the 2,4-dinitrotoluene pathway. *Arch. Microbiol.* **173**, 86-90.

Jones, R. M., Pagmantidis, V. & Williams, P. A. (2000). *sal* Genes determining the catabolism of salicylate esters are part of a supraoperonic cluster of catabolic genes in *Acinetobacter* sp. Strain ADP1. *J. Bacteriol.* **182**, 2018-2025.

Jones, T. A., Zou, J. Y., Cowan, S. W. & Kjeldgaard, M. (1991). Improved methods for building protein models in electron density maps and the location of errors in these models. *Acta. Cryst.* **A47**, 110-119.

Jorgenson, C. & Dandanell, G. (1999). Isolation and characterization of mutations in the *Escherichia coli* regulatory protein XapR. *J. Bacteriol.* **181**, 4397-4403.

Kaphammer, B., Kukor, J. J. & Olsen, R. H. (1990). Regulation of *tfdCDEF* by *tfdR* of the 2,4-dichlorophenoxyacetic acid degradation plasmid pJP4. *J. Bacteriol.* **172**, 2280-2286.

Kim, S. I., Leem, S.-H., Choi, J.-S. & Ha, K.-S. (1998). Organization and transcriptional characterization of the *catI* gene cluster in *Acinetobacter lwoffii* K24. *Biochem. Biophys. Res. Commun.* **243**, 289-294.

Kohler, T., Epp, S. F., Kocjancic Curty, L. & Pechere, J. C. (1999). Characterization of MexT, the regulator of the MexE-MexF-OprN multidrug efflux system of *Pseudomonas aeruginosa*. *J. Bacteriol.* **181**, 6300-6305.

Kullik, I., Stevens, J., Toledano, M. B. & Storz, G. (1995). Mutational analysis of the redox-sensitive transcriptional regulator OxyR: Residues important for DNA binding and multimerization. *J. Bacteriol.* **177**, 1285-1291.

Kullik, I., Toledano, M. B., Tartaglia, L. A. & Storz, G. (1995). Mutational analysis of the redox-sensitive transcriptional regulator OxyR: regions important for oxidation and transcriptional activation. *J. Bacteriol.* **177**, 1275-1284.

Lakowicz, J. R. (1999). *Principles of fluorescence spectroscopy*, second edn. New York, NY, USA: Kluwer Academic.

Leveau, J. H. & van der Meer, J. R. (1996). The *tfdR* gene product can successfully take over the role of the insertion element-inactivated TfdT protein as a transcriptional activator of the *tfdCDEF* gene cluster, which encodes chlorocatechol degradation in *Ralstonia eutropha* JMP134(pJP4). *J. Bacteriol.* **178**, 6824-6832.

Lindquist, S., Lindberg, F. & Normark, S. (1989). Binding of the *Citrobacter freundii* AmpR regulator to a single DNA site provides both autoregulation and activation of the inducible *ampC* beta-lactamase gene. *J. Bacteriol.* **171**, 3746-3753.

Lochowska, A., Iwanicka-Nowicka, R., Plochocka, D. & Hryniewicz, M. M. (2001). Functional dissection of the LysR-type CysB transcriptional regulator. *J. Biol. Chem.* **276**, 2098-2107.

- Luft, J. R., Wolfley, J., Jusrisica, I., Glasgow, J., Fortier, S. & DeTitta, G. T. (2001).** Macromolecular crystallization in a high throughput laboratory - The search phase. *J. Crystal Growth* **232**, 591-595.
- Lynch, A. S., Tyrrell, R., Smerdon, S. J., Briggs, G. S. & Wilkinson, A. J. (1994).** Characterization of the CysB protein of *Klebsiella aerogenes*: direct evidence that *N*-acetylserine rather than *O*-acetylserine serves as the inducer of the cysteine regulon. *Biochem. J.* **299**, 129-136.
- Matrubutham, U. & Harker, A. R. (1994).** Analysis of duplicated gene sequences associated with *tfdR* and *tfdS* in *Alcaligenes eutrophus* JMP134. *J. Bacteriol.* **176**, 2348-2353.
- Maxon, M. E., Redfield, B., Cai, X. Y., Shoeman, R., Fujita, K., Fisher, W., Stauffer, G., Weissbach, H. & Brot, N. (1989).** Regulation of methionine synthesis in *Escherichia coli*: effect of the MetR protein on the expression of the *metE* and *metR* genes. *Proc. Natl. Acad. Sci.* **86**.
- Mayer, D., Schlenzog, V. & Bock, A. (1995).** Identification of the transcriptional activator controlling the butanediol fermentation pathway in *Klebsiella terrigena*. *J. Bacteriol.* **177**, 5261-69.
- Miller, B. E. & Kredich, N. M. (1987).** Purification of the *cysB* protein from *Salmonella typhimurium*. *J. Biol. Chem.* **262**, 6006-6009.
- Momany, C. (2002).** Unpublished data.

Mouz, S., Merlin, C., Springael, D. & Toussaint, A. (1999). A GntR-like negative regulator of the biphenyl degradation genes of the transposon Tn4371. *Mol. Gen. Genet.* **262**, 790-799.

Murshudov, G. N., Lebedev, A., Vagin, A. A., Wilson, K. S. & Dobson, E. J. (1999). Efficient anisotropic refinement of macromolecular structures using FFT. *Acta Cryst* **D55**, 247-255.

Nayal, M., Hitz, B. C. & Honig, B. (1999). GRASS: A server for the graphical representation and analysis of structures. *Protein Sci.* **8**, 676-679.

Neidle, E. L., Hartnett, C. & Ornston, L. N. (1989). Characterization of *Acinetobacter calcoaceticus catM*, a repressor gene homologous in sequence to transcriptional activator genes. *J. Bacteriol.* **171**, 5410-5421.

Ogawa, N. & Miyashita, K. (1999). The chlorocatechol-catabolic transposon Tn5707 of *Alcaligenes eutrophus* NH9, carrying a gene cluster highly homologous to that in the 1,2,4-trichlorobenzene-degrading bacterium *Pseudomonas* sp. Strain P51, confers the ability to grow on 3-chlorobenzoate. *Appl. Environ. Microbiol.* **65**, 724-731.

Orser, C. S. & Lange, C. C. (1994). Molecular analysis of pentachlorophenol degradation. *Biodegradation* **5**, 277-88.

Otwinowski, Z. & Minor, W. (1997). Processing of X-ray diffraction data collected in oscillation mode. In *Methods Enzymol.*, pp. 307-326. Edited by C. W. Carter & R. M. Sweets. New York: Academic Press.

- Perriere, G. & Gouy, M. (1996).** WWW-Query: An on-line retrieval system for biological sequence banks. *Biochimie* **78**, 364-369.
- Ramakrishnan, V., Finch, J. T., Graziano, V., Lee, P. L. & Sweet, R. M. (1993).** Crystal structure of globular domain of histone H5 and its implications for nucleosome binding. *Nature* **362**, 219-23.
- Renna, M. C., Najimudin, N., Winik, L. R. & Zahler, S. A. (1993).** Regulation of the *Bacillus subtilis* *alsS*, *alsD*, and *alsR* genes involved in post-exponential-phase production of acetoin. *J. Bacteriol.* **175**, 3863-3875.
- Romero-Arroyo, C. E., Schell, M. A., Gaines III, G. L. & Neidle, E. L. (1995).** *catM* encodes a LysR-type transcriptional activator regulating catechol degradation in *Acinetobacter calcoaceticus*. *J. Bacteriol.* **177**, 5891-5898.
- Rothmel, R. K., Aldrich, T. L., Houghton, J. E., Coco, W. M., Ornston, L. N. & Chakrabarty, A. M. (1990).** Nucleotide sequencing and characterization of *Pseudomonas putida* *catR*: a positive regulator of the *catBC* operon is a member of the LysR family. *J. Bacteriol.* **172**, 922-931.
- Schell, M. A. (1993).** Molecular biology of the LysR family of transcriptional regulators. *Annu. Rev. Microbiol.* **47**, 597-626.
- Schwacha, A. & Bender, R. A. (1993).** The *nac* (nitrogen assimilation control) gene from *Klebsiella aerogenes*. *J. Bacteriol.* **175**, 2107-2115.

Seeger, C., Poulsen, C. & Dandanell, G. (1995). Identification and characterization of genes (*xapA*, *xapB*, and *xapR*) involved in xanthosine catabolism in *Escherichia coli*. *J. Bacteriol.* **177**, 5506-5516.

Stragier, P. & Patte, J. C. (1983). Regulation of diaminopimelate decarboxylase synthesis in *Escherichia coli* III. Nucleotide sequence and regulation of the *lysR* gene. *J. Mol. Biol.* **168**, 333-350.

Suzuki, K., Ichimura, A., Ogawa, N., Hasebe, A. & Miyashita, K. (2002). Differential expression of two catechol 1,2-dioxygenases in Burkholderia sp. Strain TH2. *J. Bacteriol.* **184**, 5805-5809.

Terwilliger, T. C. (2001). Map-likelihood phasing. *Acta Cryst.* **D57**.

Terwilliger, T. C. (2001). Maximum-likelihood density modification with pattern recognition of structural motifs. *Acta Cryst.* **D57**, 1755-1762.

Thompson, J. D., Gibson, T. J., Plewniak, F., Jeanmougin, F. & Higgins, D. G. (1997). The CLUSTAL_X windows interface: flexible strategies for multiple sequence alignment aided by quality analysis tools. *Nucleic Acids Res* **25**, 4876-4882.

Tyrrell, R., Verschueren, K. H. G., Dobson, E. J., Murshudov, G. N., Abby, C. & Wilkinson, A. J. (1997). The structure of the cofactor-binding fragment of the LysR family member, CysB: a familiar fold with a surprising subunit arrangement. *Structure* **5**, 1017-1032.

van der Meer, J. R., Frijters, A. C. J., Leveau, J. H. J., Eggen, R. I. L., Zehnder, A. J. B. & de Vos, W. M. (1991). Characterization of the *Pseudomonas* sp. strain P51 gene *tcbR*, a LysR-type transcriptional activator of the *tcbCDEF* chlorocatechol oxidative operon, and analysis of the regulatory region. *J. Bacteriol.* **173**, 3700-3708.

Verschueren, K. H. G., Addy, C., Dobson, E. J. & Wilkinson, A. J. (2001). Crystallization of full-length CysB of *Klebsiella aerogenes*, a LysR-type transcriptional regulator. *Acta Cryst.* **D57**, 260-262.

Wek, R. C. & Hatfield, G. W. (1986). Nucleotide sequence and in vivo expression of the *ilvY* and *ilvC* genes in *Escherichia coli* K12. Transcription from divergent overlapping promoters. *J. Biol. Chem.* **261**, 2441-2450.

You, I. S., Ghosal, D. & Gunsalus, I. C. (1988). Nucleotide sequence of plasmid NAH7 gene *nahR* and DNA binding of the *nahR* product. *J. Bacteriol.* **170**, 5409-5415.

CHAPTER 5

CONCLUSIONS

The studies contained within this dissertation were aimed at characterizing the structure and function of the LysR-type transcriptional activator protein BenM. As described in Chapter 2, BenM and a second LysR-type regulator CatM were purified to homogeneity and shown to regulate the expression of genes involved in the transport of aromatic compounds in the bacterium *Acinetobacter* sp. strain ADP1. Expression of these genes was demonstrated to be in response to the effector compound *cis,cis*-muconate.

In Chapter 3, tryptophan fluorescence studies are described that characterized the interactions of BenM with *cis,cis*-muconate and a second, distinct effector molecule, benzoate. BenM was able to bind to benzoate and to *cis,cis*-muconate, and the affinity for each effector was determined. Further, benzoate and *cis,cis*-muconate were demonstrated to compete for a common BenM binding site. Conformation changes in BenM caused by benzoate were distinct from those caused by *cis,cis*-muconate. From these results, a model was proposed to account for BenM's ability to activate high-level transcription in response to both compounds.

To better understand the structural differences resulting from *cis,cis*-muconate and benzoate binding, the structure of the BenM effector-binding domain was solved. These structural studies, described in Chapter 4, revealed that despite limited sequence identity among corresponding regions, BenM, shares common structural features with

two other LysR-type transcriptional regulators for which crystal structures have been solved. In BenM, specific structural changes appear to underlie the previously observed ability of this protein to activate high-level transcription in response to the two different effectors. Collectively, the studies described in this dissertation clarify the complex role of an important protein in *Acinetobacter* sp. strain ADP1 that may be representative of one of the largest classes of prokaryotic transcriptional regulators.